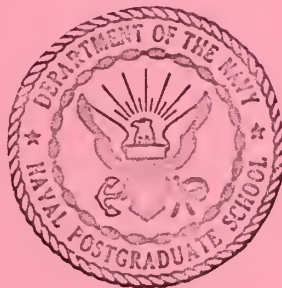


George J. Thaler

BACKLASH IN SECOND ORDER FEEDBACK  
CONTROL SYSTEMS

Library  
U. S. Naval Postgraduate School  
Monterey, Calif. 94034

# UNITED STATES NAVAL POSTGRADUATE SCHOOL



## BACKLASH IN SECOND ORDER FEEDBACK CONTROL SYSTEMS

by

Geo. J. Thaler, Dr. Eng.  
Professor of Electrical Engineering  
N.O. Anderson, Jr., Lt., USN  
C.E. Andrews, Lt., USN  
R. A. Kelley, Lt., USN  
T.W. Lockett, Lt., USN

Supported in Part by the Office of Naval Research

September, 1961

Technical Report No. 19





BACKLASH IN SECOND ORDER  
FEEDBACK CONTROL SYSTEMS

by

GEORGE J. THALER, DR. ENG.  
Professor of Electrical Engineering

N. O. ANDERSON, JR., Lt., USN

C. E. ANDREWS, Lt., USN

R. A. KELLEY, Lt., USN

T. W. LUCKETT, Lt., USN

TECHNICAL REPORT NO. 19

UNITED STATES NAVAL POSTGRADUATE SCHOOL

MONTEREY, CALIFORNIA

SEPTEMBER, 1961

TA7  
.U64  
no. 19

TABLE OF CONTENTS

<u>Section</u>	<u>Page</u>
1. Introduction	1
2. The No Load Case	5
2.1 A Stability Criterion for the No Load Case	11
3. Phase Plane Analysis of Backlash in a Second Order System with Divided Load and Plastic Impact	16
4. Computation by Digital Computer	
4.1 Introduction	27
4.2 Development of Equations	30
4.3 Computer Program Development	41
4.4 Methods and Scope of Examination	45
5. Analysis of Results	48
6. Application of Results	82
7. Transient Response Characteristics; Plastic Impact	
7.1 Maximum Overshoot; Plastic Impact Case	86
7.2 Maximum Overshoot; Elastic Impact Case	107
7.3 Settling Time	108
Tables	110
7.4 Time of Maximum Overshoot	113
7.5 Other System Characteristics	114
8. Conclusions	118
References	119
Appendix	120



## BACKLASH IN SECOND ORDER FEEDBACK CONTROL SYSTEMS

### 1. Introduction

Whenever components are mechanically connected by a linkage or a gear train, there exists the basic problem of providing smooth operation without looseness in the connecting parts of the mechanical system. In general this basic problem is not completely solved, and the connecting parts are free to move independently over a limited range. This phenomenon is commonly called backlash and its effects are usually, but not always, undesirable. In particular, when backlash occurs in a feedback control system it often causes a small amplitude "dither" or limit cycle, and when the system reaches static steady state without a limit cycle the accuracy of the system is affected by the backlash.

In the usual feedback control system, the backlash occurs in two places: in the power drive gear train between motor and load, and in the gear train between load and output measuring device. It is not difficult to establish the pertinent differential equations for either of these cases, nor is there any conceptual difficulty in the solution of these equations, but considerable labor is required for the solution of even the simplest cases. Furthermore, the solution of one or two specific cases does not provide perspective for generalizations, and the multiplicity of parameters involved makes detailed



analyses unattractive. This report deals with some initial results in a long range project to study the backlash phenomena quantitatively, with the ultimate goal of providing charts which will be useful in the engineering analysis and design of feedback control systems involving backlash.

In general, the simplest linear feedback control system has a second order differential equation, and is commonly referred to as a second order system. Backlash may and does occur in such systems. While it is obvious that most feedback control systems are third order or higher, the study of backlash in this report is restricted to second order systems only, so as to provide a firm foundation for future studies while limiting the variable parameters to a variety which makes numerical calculations feasible. In like manner the mechanical parameters are restricted to inertia (mass) and viscous friction; coulomb friction, though of some practical importance, is not considered quantitatively and is permitted in a qualitative sense in only one special case. It is recognized that the mechanical inertia and viscous friction may be subdivided and appear on both sides of the backlash in varying proportions, such cases are considered in detail. It is also recognized that the gear tooth surfaces must hit each other after the meshing gears have gone through the dead space (backlash), and this impact may be either plastic or elastic; this effect is also studied in detail. The mechanical load on the gear train is considered to be only inertia and





viscous friction. This combination contains only one energy storage device (inertia) and is therefore a first order load. In some cases the mechanical connection, e.g. shaft, may act as a spring, thus providing a second order load which is capable of resonance if excited by periodic motion of the proper frequency. This case is not considered but is reserved for future study.

The two basic tools for studying the nonlinear effects of backlash are the phase plane-phase space technique and the describing function method. The describing function method has been applied to a number of backlash studies, and it is intended to devote some future efforts to an extension of such studies; however, the investigations reported on here are based solely on the phase plane-phase space technique. For second order systems the phase space is two dimensional, that is, it reduces to a phase plane, and nonlinear as well as discontinuous systems can be analyzed using the well known graphical methods of integration (method of isoclines, Lienard's construction, the Delta method) which make the phase plane a powerful tool. This provides a convenient starting point for the analysis, though the graphical methods do not apply to higher order systems.

The phase plane technique with graphical integration was used in initial studies recorded here but was applied to only the simplest cases. The results obtained and the procedures developed provided sufficient insight to permit formulation of a rather comprehensive



digital computer program to study the effects of many parameters on the response of a given system. The majority of the data presented here was obtained using a digital computer program; however, any of the results so obtained could be duplicated by graphical methods.

The digital computer was programmed to provide a complete solution of the differential equations, and sufficient data was computed to provide a complete and very accurate phase trajectory. However, for most of this initial phase the question of primary interest was the development of criteria for the existence of limit cycles. The computer program was therefore provided with a subroutine which printed out only the maximum position per cycle. This was done to decrease the read out and print out times. By a simple auxiliary command, complete data for the phase trajectory was made available; however, the complete phase trajectory was solved for only a restricted number of cases because of the time involved. As a result, the limit cycle studies are detailed and fairly complete (more data would improve the results but should not introduce any startling features); but many questions concerning response during the transient period have not been completely answered. Much of the remaining work (within the restricted scope of this initial phase) is just a matter of data reduction.



## 2. THE NO LOAD CASE

For some systems one may neglect inertia and viscous friction on the output side of the gear train containing the backlash. This is arbitrarily called the No Load Case. Two practical variations are common. First, the most commonly encountered, is the case of the instrument servo which is driving some simple indicating or measuring device such as the wiper arm on a potentiometer. In this case the actual driven load has a negligibly small inertia and viscous friction. There is usually some coulomb friction in this load, but it is often too small to affect the differential equations though large enough to prevent jitter in the low inertia driven load. The second case of interest here is that in some larger systems with driven load of appreciable inertia, the power gear train has negligible backlash, but there is a measuring device geared to the load, and there is backlash in the gear train between load and measuring device. Note that while these two cases arise in systems which are physically different, they are mathematically equivalent and thus one analysis suffices.

The block diagram description of the system is given in Fig. 2-1. If it is assumed that a step displacement input is applied to the system when the gears are in contact and the system is driving linearly, then the basic linear differential equations are:

$$J_M \ddot{\Theta}_C + f_M \dot{\Theta}_C = KE \quad (2-1)$$

$$E = \Theta_R - \Theta_C \quad (2-2)$$



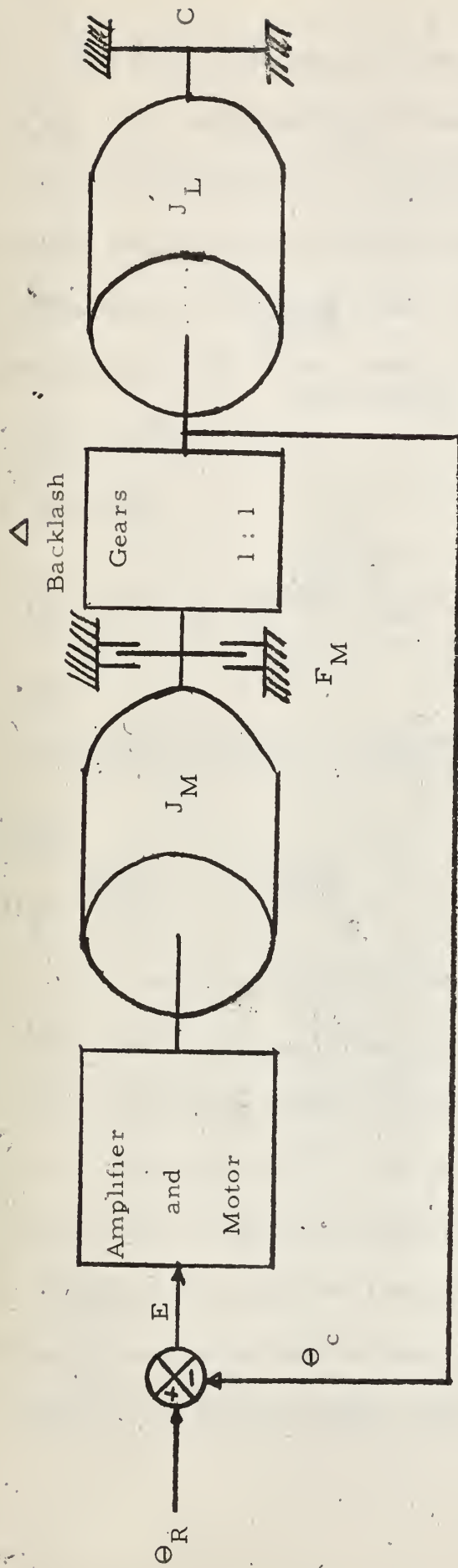


Fig. 2-1 Block Diagram







The dynamic response of the system is shown on the phase portrait of Fig. 2-2, and equations 2-1 and 2-2 describe the first portion of the trajectory from M to N. At point N,  $E = 0$  and  $\Theta_C = 0$ , the motor reverses and runs in the opposite direction, increasing the velocity and displacement of the motor shaft. However the output shaft cannot move and the error,  $E$ , cannot change until the backlash is taken up. The operation during this interval is:

$$J_M \ddot{\Theta}_M + f \dot{\Theta}_M = KE_N \quad (2-3)$$

from which

$$\Theta_M = -KE_N \left[ \frac{t}{f} + \frac{J_M}{f^2} \left( e^{-\frac{ft}{J_M}} - 1 \right) \right] = \frac{-E_N}{4\zeta^2} (-1 + 2\zeta\omega_n t + e^{-2\zeta\omega_n t}) \quad (2-4)$$

where

$$\zeta = f/2\sqrt{KJ_M} \text{ and } \omega_n = \sqrt{K/J_M}$$

Also

$$\dot{\Theta}_M = -\frac{\omega_n E_N}{2\zeta} (1 - e^{-2\zeta\omega_n t}) \quad (2-5)$$

It is readily seen that the horizontal or  $E$ -axis is a locus of points at which the describing differential equation changes discontinuously, and it may then be called a "dividing line." This particular dividing line is a "separation line" i.e. as the state point crosses this line the physical system goes into the backlash region and the drive member is mechanically separated from the load member. During the time interval when equations 2-4 and 2-5 apply, and the backlash is being "taken-up"; the load member does not move,  $E$  and  $\dot{E}$  do not change,



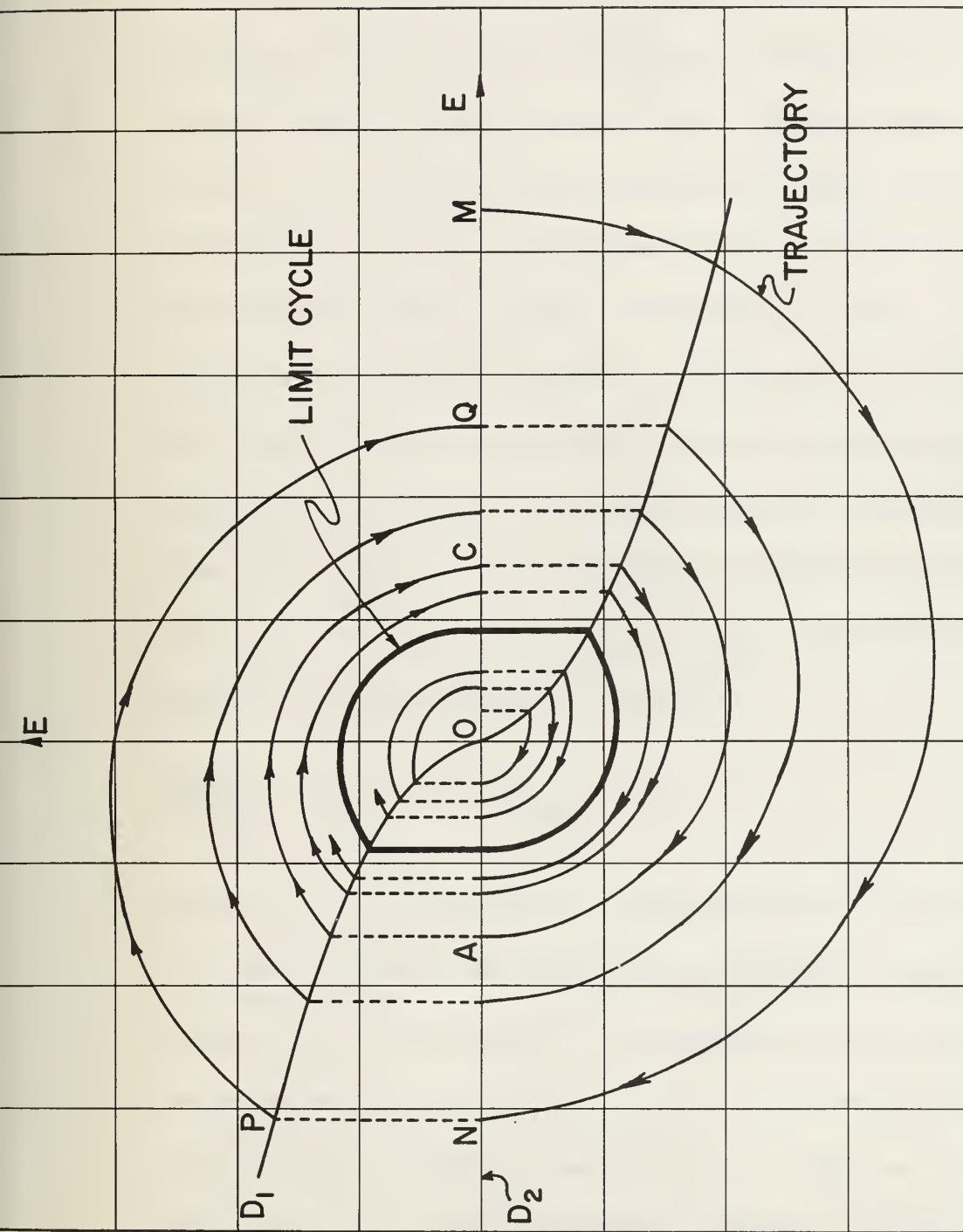


FIG. 2-2 PHASE TRAJECTORIES OF AN INSTRUMENT SERVO-MECHANISM WITH BACKLASH

$D_1$  - DIVIDING LINE FOR RECOMBINATION

$D_2$  - DIVIDING LINE FOR SEPARATION



but  $\Theta_m$  and  $\dot{\Theta}_m$  do change. On the phase plane of Fig. 2-2 the vertical line from N to P indicates the first interval of this type. It can be argued whether this line is or is not validly a segment of the phase trajectory, but the physical interpretation is quite clear:  $E$  and  $\dot{E}$  are constant at point N until the backlash is completely taken up, then as the gear teeth hit (with inelastic impact) the load instantaneously acquires a velocity and the state point jumps discontinuously from N to P. Once the backlash is taken up the system once more operates linearly and the segment of phase trajectory from P to Q is again governed by equations 2-1 and 2-2. The point P is one point on another dividing line, this is the line at which the backlash is taken up and the system physically recombines, i.e., the mechanical connection is restored. Thus the line may be called a backlash "recombination line." This line can be constructed accurately only by a point-by-point calculation. However, equation 2-5 can be rewritten:

$$\frac{\dot{\Theta}_M/\omega_n}{E_N} = \frac{-1}{2\zeta} (1 - e^{-\zeta\omega_n t_\Delta}) \quad (2-6)$$

where  $t_\Delta$  is the time interval required to take up the backlash. For  $t_\Delta \rightarrow \infty$  the slope of the dividing line is  $-1/2\zeta$ . Thus for various values of the backlash,  $\Delta$ , the recombination line may be represented on the phase plane as shown in Fig. 2-3. Only the tangent line is accurate (unless detailed computations are used), but knowledge of this tangent line permits derivation of a stability criterion.



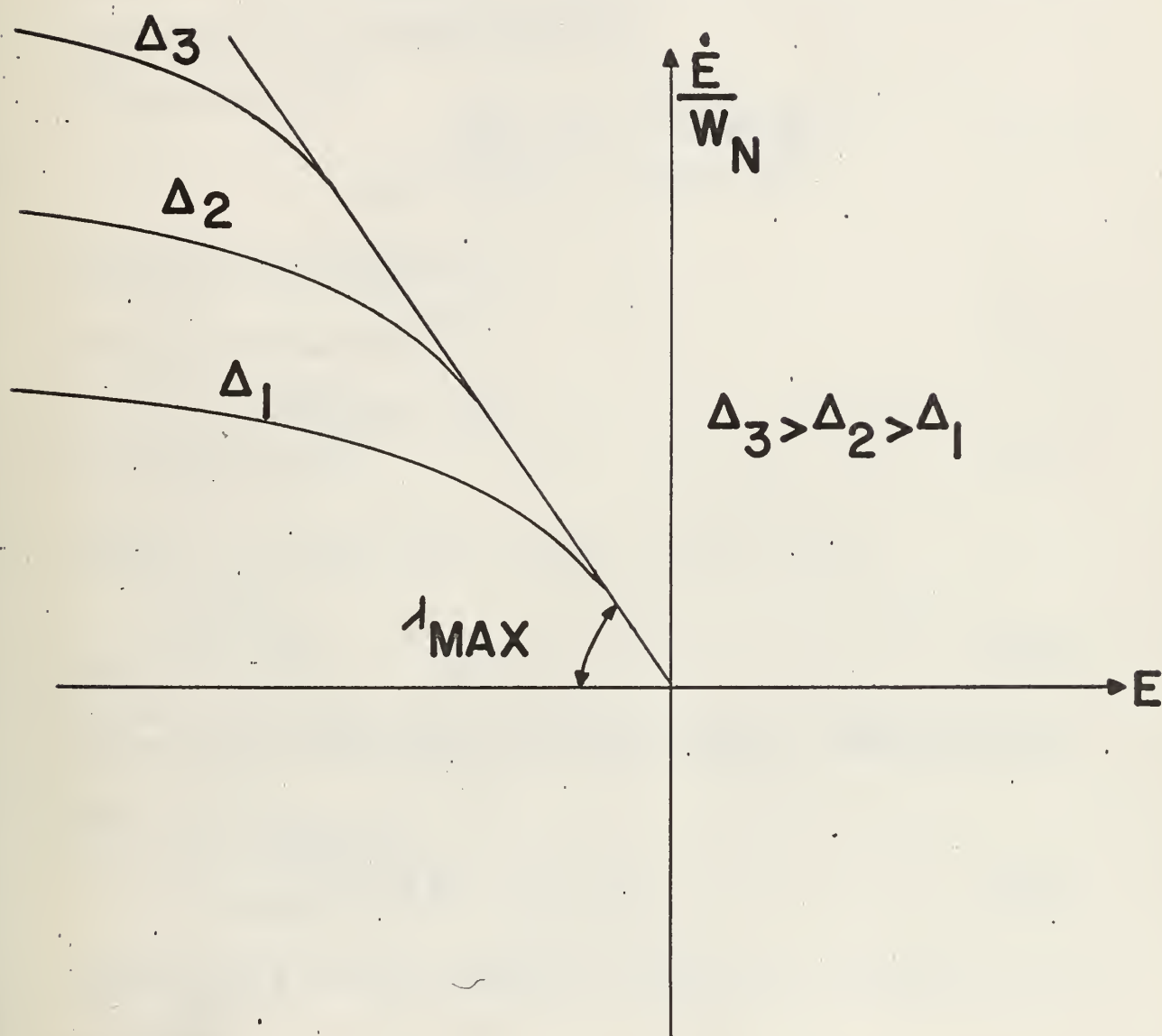


FIG. 2-3 FAMILY OF BACKLASH DIVIDING LINES WITH COMMON TANGENT AT THE ORIGIN.

$$\lambda_{MAX} = \tan^{-1} - 1/2 \zeta$$





## 2.1 A Stability Criterion for the No Load Case

If equations 2-1 and 2-2 are combined and nondimensionalized forming a single equation with error,  $E$ , as the independent variable, this equation can be manipulated and integrated to define the linear phase trajectory on the phase plane as:

$$\begin{aligned} \dot{E}^2 + 2\zeta\omega_n E\dot{E} + \omega_n^2 E^2 \\ = D_e^2 \sqrt{1-\zeta^2} \tan^{-1} \frac{E + \zeta\omega_n E}{\omega_n E \sqrt{1-\zeta^2}} \end{aligned} \quad (2-7)$$

Using the linear transformation

$$Y = \dot{E} + \zeta\omega_n E, X = \omega_n E \sqrt{1-\zeta^2} \quad (2-8)$$

$$X^2 + Y^2 = D_e^2 \sqrt{1-\zeta^2} \tan^{-1} \frac{Y}{X} \quad (2-9)$$

Letting  $Y = \rho \sin \psi$ ,  $X = \rho \cos \psi$ ,  $\psi = \tan^{-1} Y/X$

$$\rho = D_e \sqrt{1-\zeta^2} \quad (2-10)$$

The backlash dividing lines are located on the  $X - Y$  plane by noting that

$$\frac{Y}{X} = \frac{\dot{E} + \zeta\omega_n E}{\omega_n E \sqrt{1-\zeta^2}} \quad (2-11)$$

but the dividing line for separation is the  $E$ -axis, for which  $\dot{E}=0$ , and for this line

$$\frac{Y}{X} = \frac{\zeta}{\sqrt{1-\zeta^2}} = \tan \psi_T \quad (2-12)$$



The backlash dividing line for recombination is not readily determined, but the tangent to this curve  $\lambda_{\max}$  on Fig. 2-3, is easily transferred:

$$\frac{Y}{X} = \frac{\dot{E}/\omega_n}{E} = \frac{1}{\sqrt{1-\zeta^2}} + \frac{\zeta}{\sqrt{1-\zeta^2}} \quad (2-13)$$

$$\text{and for } \lambda_{\max} \quad \dot{E}/E \omega_n = -1/2 \zeta \text{ so } \frac{Y}{X} = \frac{2\zeta^2 - 1}{2\zeta\sqrt{1-\zeta^2}} = \tan \psi_{\max} \quad (2-14)$$

which may be expressed as an acute angle

$$\tan \psi_{\max} = \frac{1 - 2\zeta^2}{2\zeta\sqrt{1-\zeta^2}} \quad (2-15)$$

In Fig. 2-4 the backlash line for recombination is sketched, not calculated, but the basic condition for increasing oscillations is

$$\rho_1 \cos \psi_1 = \rho_2 \cos \psi_t \quad (2-16)$$

Assuming that the angles are measured from the negative real axis in Fig. 2-4 and that  $\rho_1$  and  $Z_1$  are known:

$$D = \rho_1 e^{\frac{\zeta \psi_1}{\sqrt{1-\zeta^2}}} \quad (2-17)$$

$$\rho_2 = D e^{-\frac{\zeta \psi_2}{\sqrt{1-\zeta^2}}} = \rho_1 e^{-\frac{\zeta(\psi_2 - \psi_1)}{\sqrt{1-\zeta^2}}} \quad (2-18)$$

$$\psi_2 = \pi - \psi_T \quad (2-19)$$



$$\text{Substituting, } \frac{-\mathfrak{L}(\pi - \psi_T - \psi_1)}{\sqrt{1 - \mathfrak{L}^2}} \quad (2-20)$$

$$\cos \psi_1 \leq \cos \psi_T e$$

$$\leq \frac{1}{\sqrt{1 - \mathfrak{L}^2}} e^{\frac{-\mathfrak{L}(\pi - \psi_T - \psi_1)}{\sqrt{1 - \mathfrak{L}^2}}} \quad (2-21)$$

The angle  $\psi_1$  may be chosen arbitrarily, and by inspection of Fig. 2-4 it is apparent that if the required inequality exists it must be most pronounced when the point  $(\rho_1, \psi_1)$  is located near the origin on the tangent line, in which case  $\psi_1 = \psi_{\max}$ . Substituting this value for  $\psi_1$ :

$$1 \leq \frac{1}{2\mathfrak{L}} e^{-\frac{\mathfrak{L}}{\sqrt{1 - \mathfrak{L}^2}} \left( \pi - \tan^{-1} \frac{1 - 2\mathfrak{L}^2}{2\mathfrak{L}\sqrt{1 - \mathfrak{L}^2}} - \tan^{-1} \frac{\mathfrak{L}}{\sqrt{1 - \psi^2}} \right)} \quad (2-22)$$

Equation 2-22 has been plotted in Fig. 2-5, and the stability point is marked. This shows that the system with backlash, but no load, will have a limit cycle if  $\mathfrak{L} \leq 0.29$ , and the existence of the limit cycle is independent of the amount of backlash, so long as some backlash is present. Obviously the amplitude of the limit cycle will be determined by the amount of backlash.









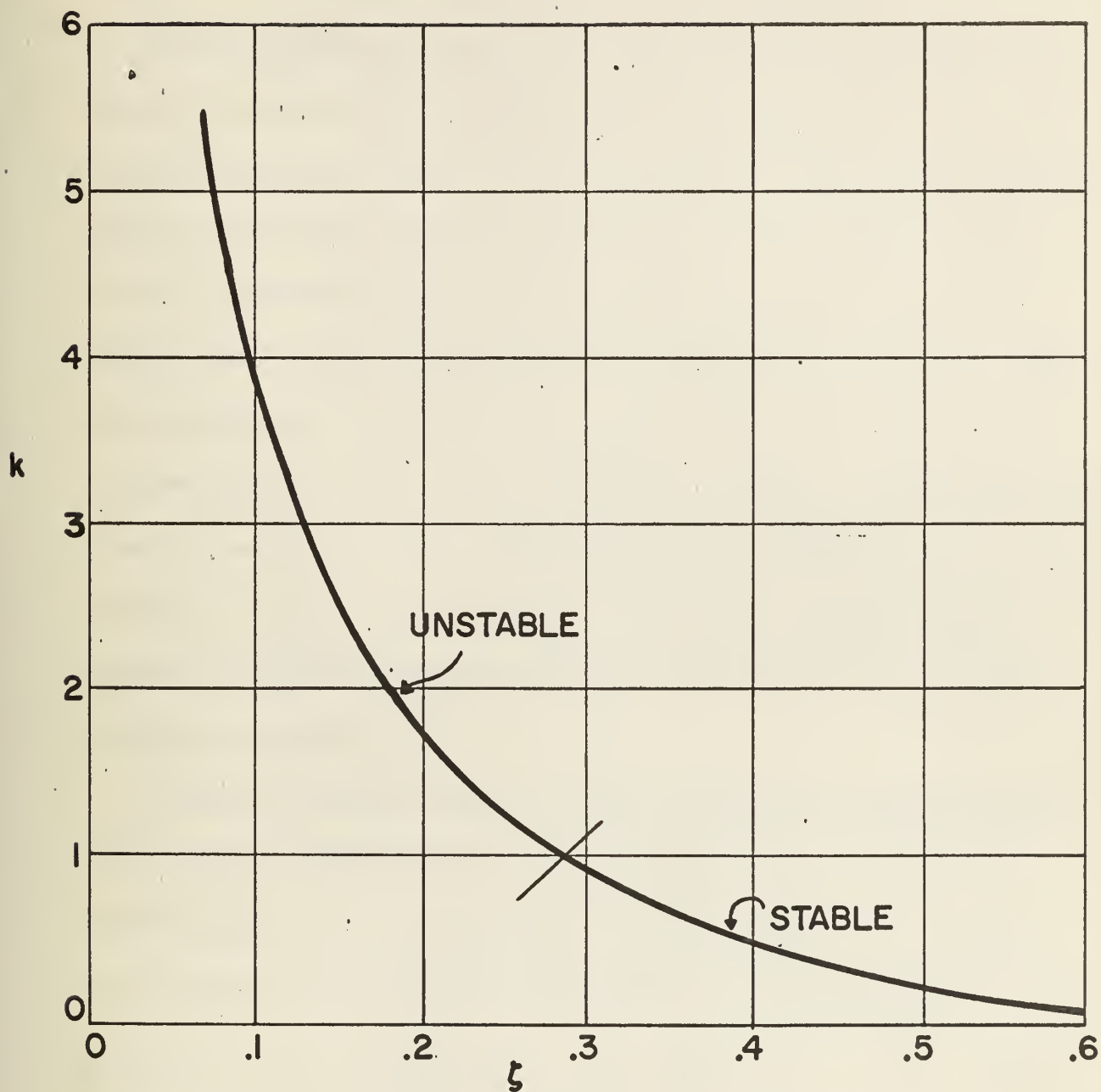


FIG. 2-5 GRAPH OF STABILITY CRITERION FOR BACKLASH.

$$k = \frac{e}{2\zeta} - a(\Pi - \tan^{-1} b - \tan^{-1} a)$$

$$a = \zeta / \sqrt{1 - \zeta^2}$$

$$b = (1 - 2\zeta^2) / 2\zeta \sqrt{1 - \zeta^2}$$



### 3. PHASE PLANE ANALYSIS OF BACKLASH IN A SECOND ORDER SYSTEM WITH DIVIDED LOAD AND PLASTIC IMPACT.

In the more general cases of backlash, the inertia and viscous friction on the output side of the gear train are not negligible. For second order systems, such cases can be analyzed using phase plane techniques. This is true for any subdivision of inertia and friction between drive member and driven member, for any gear ratio, and for plastic or elastic impact at the gear tooth surface. While actual graphical integration to construct the phase trajectories is too laborious to be a tool for generalized analysis, understanding the techniques, and actual analysis of one or two specific cases helps build appreciation for the nature of the problem. Graphical solution points out the physical phenomena and boundary conditions, and leads naturally into the preparation of digital computer programs.

When the backlash is taken up and the system is operating linearly, the equations of motion are exactly the same as for the no load case. Considering here that the motor used is specifically a D. C. armature driven motor, and using a detailed notation, the equations of motion are:

$$\frac{1}{N} (N^2 J_m + J_L) \ddot{\Theta}_c + \frac{1}{N} (N^2 f_m + f_L) \dot{\Theta}_c = T \quad (3-1)$$

$$T = K_1 I \quad (3-2)$$

$$V = R I + K_2 \dot{\Theta}_m \quad (3-3)$$

$$I = \left( \frac{V}{R} - \frac{K_2}{R} N \dot{\Theta}_c \right) \quad (3-4)$$



$$V = K_3 (\Theta_R - \Theta_c) \quad (3-5)$$

$$\begin{aligned} \frac{1}{N} (N^2 J_m + J_L) \ddot{\Theta}_c + \frac{1}{N} (N^2 f_m + f_L + \frac{K_1 K_2 N^2}{R}) \dot{\Theta}_c \\ + \frac{K_1 K_3 \Theta_c}{R} = \frac{K_1 K_3 \Theta_R}{R} \end{aligned} \quad (3-6)$$

Where

- $K_1$  = Motor torque constant
- $K_2$  = Motor generated voltage constant
- $K_3$  = Error measurement constant
- $K = K_1 K_3 / R$
- $R$  = armature resistance
- $N$  = gear ratio
- $J$  = inertia of system without load
- $J_m$  = load inertia
- $f_m$  = viscous friction (mechanical) of system without load
- $f_L$  = viscous friction of load
- $F_m = N f_m + K_1 K_2 N / R$  = viscous damping of system without load but including motor back EMF
- $F_L = f_L / N$
- $\Theta_L$  = commanded displacement
- $\Theta_R$  = displacement of motor
- $\Theta_m$  = displacement of load
- $\Theta_c$  = displacement of combined system.

To permit convenient numerical manipulation, let  $N = 1$  and  $\Theta_R = 1$ , then equation 3-6 becomes:

$$\ddot{\Theta}_c + \left( \frac{F_m + F_L}{J_m + J_L} \right) \dot{\Theta}_c = \left( \frac{K}{J_m + J_L} \right) (1 - \Theta_c) \quad (3-7)$$

Equation 3-7 may be manipulated into the isocline equation in the usual fashion:

$$\Theta_c = 1 - \dot{\Theta}_c \left[ \frac{N_1 + \frac{F_m + F_L}{J_m + J_L}}{\frac{K}{(J_m + J_L)}} \right] \quad (3-8)$$

where  $N_1$  is defined to be  $d\dot{\Theta}_c / d\Theta_c$  and is the slope of the phase trajectory as it crosses the designated isocline.



Equation 3-8 is the normal isocline equation for a linear second order feedback control system. It is expressed in terms of motor inertia and friction and the load inertia and friction because this subdivision becomes important when backlash is considered.

When there is backlash between motor and load, and when this backlash is inside\* the closed loop, the system enters the backlash region (i.e., the gears lose contact) when the slope of the load deceleration trajectory is exactly equal to that of the linear system. In terms of equations, when the load is drifting free:

$$J_L \ddot{\Theta}_L + F_L \dot{\Theta}_L = 0 \quad (3-9)$$

from which

$$\frac{d\dot{\Theta}_L}{d\Theta_L} = N_L = - \frac{F_L}{J_L} \quad (3-10)$$

When the system is operating linearly as described by equation 3-8, and the state point reaches the isocline  $N_1$  which is numerically equal to  $N_L$ , then the gears lose contact, i.e., the backlash separation line is that isocline of the linear system for which  $N_1 = N_L = - F_L / J_L$

When the backlash separation line is crossed the load drifts freely according to the relationship of equation 3-10, which guarantees a phase trajectory that is a straight line. The motor shaft does not remain stationary. It moves, but is driven open loop rather than closed loop,

\*It is possible to have backlash in the gear train between motor and load but so located that it is between the measurement pick off and the load. Then there is no backlash in the closed loop, which operates linearly. This case cannot have a limit cycle and is not considered here.





with a time varying input. The equations for the motor shaft motion is

$$J_m \ddot{\Theta}_m + F_m \dot{\Theta}_m = K (\Theta_R - \Theta_L) \quad (3-11)$$

The phase plane representation of these equations is shown in Fig. 3-1. The separation dividing line is the isocline passing through  $\mathbf{X}$ . Equation 3-11 cannot be represented by an isocline relationship, so first the analysis requires a time solution of equations 3-9 and 3-11. The backlash is completely taken up in the reverse direction when the difference between the displacement of the load and the displacement of the motor is exactly  $\Delta$ , the magnitude of the backlash. In the solution of equations 3-9 and 3-11 the initial conditions are determined at the separation dividing line and are as shown on Fig. 3-2. Transforming equation 3-9:

$$J_L \left[ s^2 \Theta_L(s) - s \Theta_{L_1} - \dot{\Theta}_{L_1} \right] + F_L \left[ s \Theta_L(s) - \Theta_{L_1} \right] = 0 \quad (3-12)$$

from which

$$\Theta_L(s) = \frac{\dot{\Theta}_{L_1}}{s(s + F_L/J_L)} + \frac{\Theta_{L_1}}{s} \quad (3-13)$$

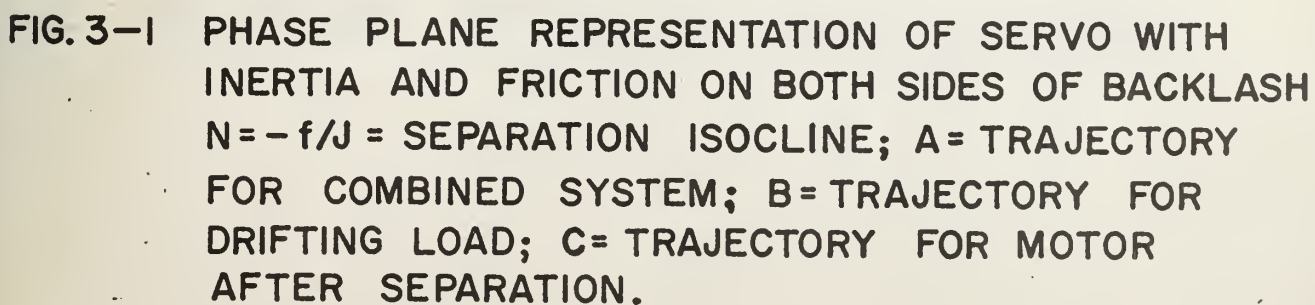
Taking the inverse transform

$$\Theta_L(t) = \Theta_{L_1} + \frac{\dot{\Theta}_{L_1}}{F_L/J_L} \left( 1 - e^{-\frac{F_L t}{J_L}} \right) \quad (3-14)$$

Equation 3-11 transforms to

$$\begin{aligned} J_m \left[ s^2 \Theta_m(s) - s \Theta_{m_1} - \dot{\Theta}_{m_1} \right] + F_m \left[ s \Theta_m(s) - \Theta_{m_1} \right] \\ = K \left[ \frac{1}{s} - \Theta_L(s) \right] \end{aligned} \quad (3-15)$$







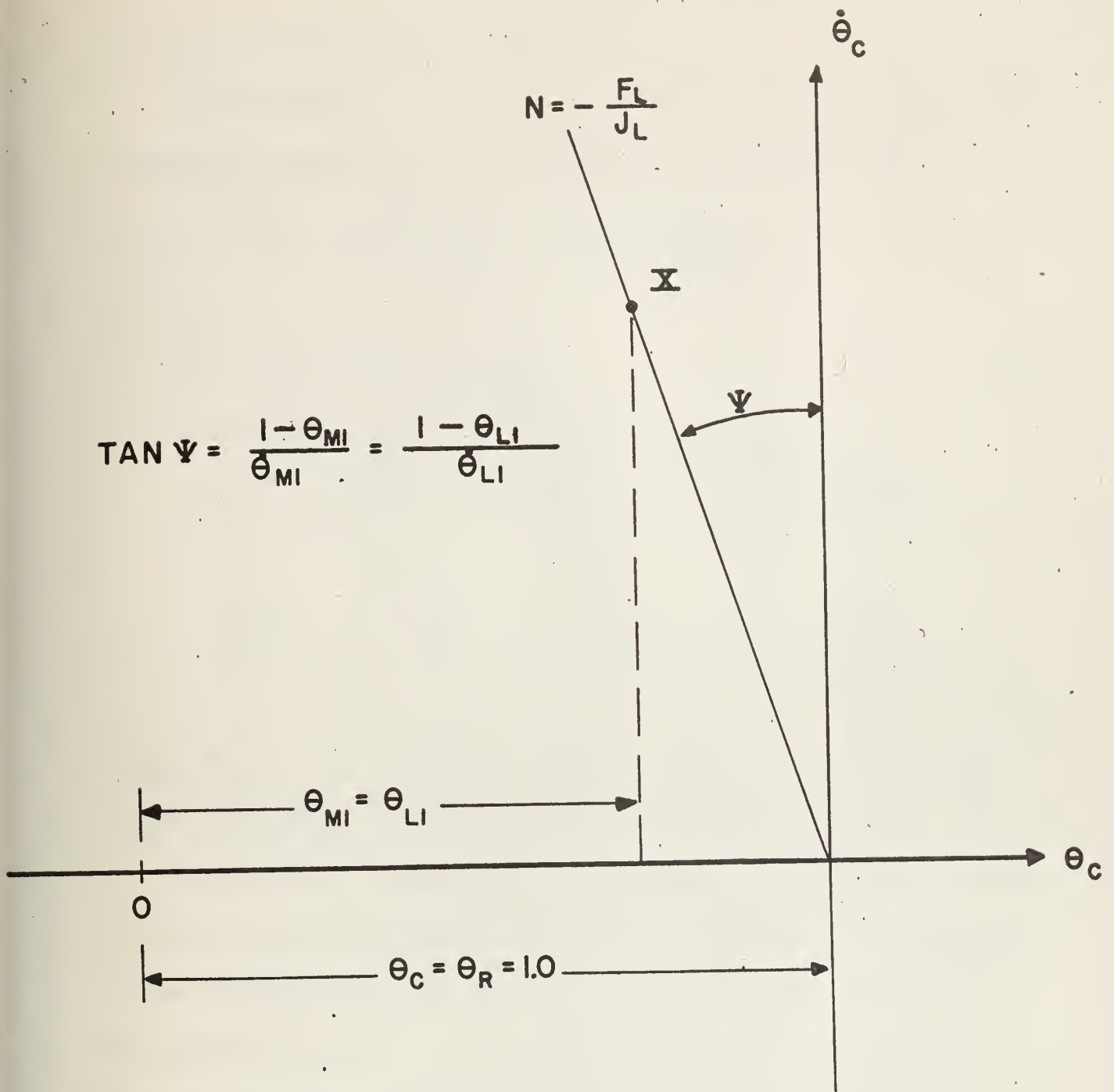


FIG.3-2 RELATIONSHIP BETWEEN  $\theta_{LI}$ ,  $\dot{\theta}_{LI}$  and  $\dot{\theta}_{MI}$



since  $\Theta_R(t) = u(t)$  and  $\Theta_R(s) = 1/s$ .

Substituting equations 3-13 for  $\Theta_L(s)$ , and noting equivalent initial conditions from Fig. 3-2, equation 3-15 may be manipulated to

$$\Theta_m(s) = \frac{\Theta_{m1}}{s} + \frac{\dot{\Theta}_{m1}}{s(s + F_m/J_m)} + \frac{K(1 - \Theta_{m1})}{J_m s^2(s + F_m/J_m)} - \frac{K \dot{\Theta}_{m1}}{J_m s^2(s + F_m/J_m)(s + F_m/J_m)} \quad (3-16)$$

Taking the inverse transform of equation 3-16 gives:

$$\begin{aligned} \Theta_m(t) = & \Theta_{m1} + \frac{J_m \dot{\Theta}_{m1}}{F_m} \left( 1 - e^{-\frac{F_m t}{J_m}} \right) - \frac{K(1 - \Theta_{m1}) J_m}{F_m^2} \\ & \left( 1 - \frac{F_m t}{J_m} - e^{-\frac{F_m t}{J_m}} \right) - \frac{K \dot{\Theta}_{m1} J_L}{F_L F_m} \left[ t - \frac{J_m J_L}{F_m F_L} - \right. \\ & \left. \frac{F_m F_L}{J_L F_m - J_m F_L} \left( \frac{J_m^2}{F_m^2} e^{-\frac{F_m t}{J_m}} - \frac{J_L^2}{F_L^2} e^{-\frac{F_L t}{J_L}} \right) \right] \end{aligned} \quad (3-17)$$

If equations 3-14 and 3-17 are plotted with displacement as ordinate and time as abscissa they may be used as a nomograph to evaluate points on the backlash dividing line for recontacting of the gear teeth. If both are plotted on the same coordinate axes, then at any instant the difference between the ordinate values is the relative displacement  $\Theta_L - \Theta_m$ , and whenever  $\Theta_L - \Theta_m = \Delta$  the backlash is taken up. Since this point also defines values for  $\Theta_L$  and for  $t$ , differentiation of the proper equations permits evaluation of  $\dot{\Theta}_m$  and  $\dot{\Theta}_L$  at that instant.





For repeated cycles these time curves need not be replotted, but may be used as a nomograph by simply adjusting the ordinate scales. This is due to the fact that the only change in the physical situation is a change in the initial conditions, and from Fig. 3-2 there is a fixed relationship

such that

$$\tan \psi = \frac{1 - \Theta_{m_1}}{\dot{\Theta}_{m_1}} = \frac{1 - \Theta_{L_1}}{\dot{\Theta}_{L_1}} \quad (3-18)$$

where  $\tan \psi$  is known number. Then  $1 - \Theta_{m_1} = \dot{\Theta}_{m_1} \tan \psi$  which (3-19) indicates the required adjustment in ordinate scales. A pair of  $\Theta_L$  and  $\Theta_m$  curves is shown on Fig. 3-3.

At the instant backlash is taken up both motor and load have finite velocities. Therefore both the law of conservation of momentum and the law of conservation of energy must be considered. If the impact is defined to be inelastic (plastic) this is equivalent to stating that sufficient deformation occurs to dissipate some energy as heat; then the law of conservation of energy need not apply to the dynamics of the mechanical system, but the law of conservation of momentum still restricts the boundary conditions. It follows that after recontact of the gear teeth, the requirement that momentum must be conserved is

$$J_L \dot{\Theta}_L + J_m \dot{\Theta}_m = (J_m + J_L) \dot{\Theta}_{L_2} \quad (3-20)$$

where  $\dot{\Theta}_{L_2}$  is the instantaneous velocity of the recombined system. Note that the points at which the gear teeth recontact define a dividing line on



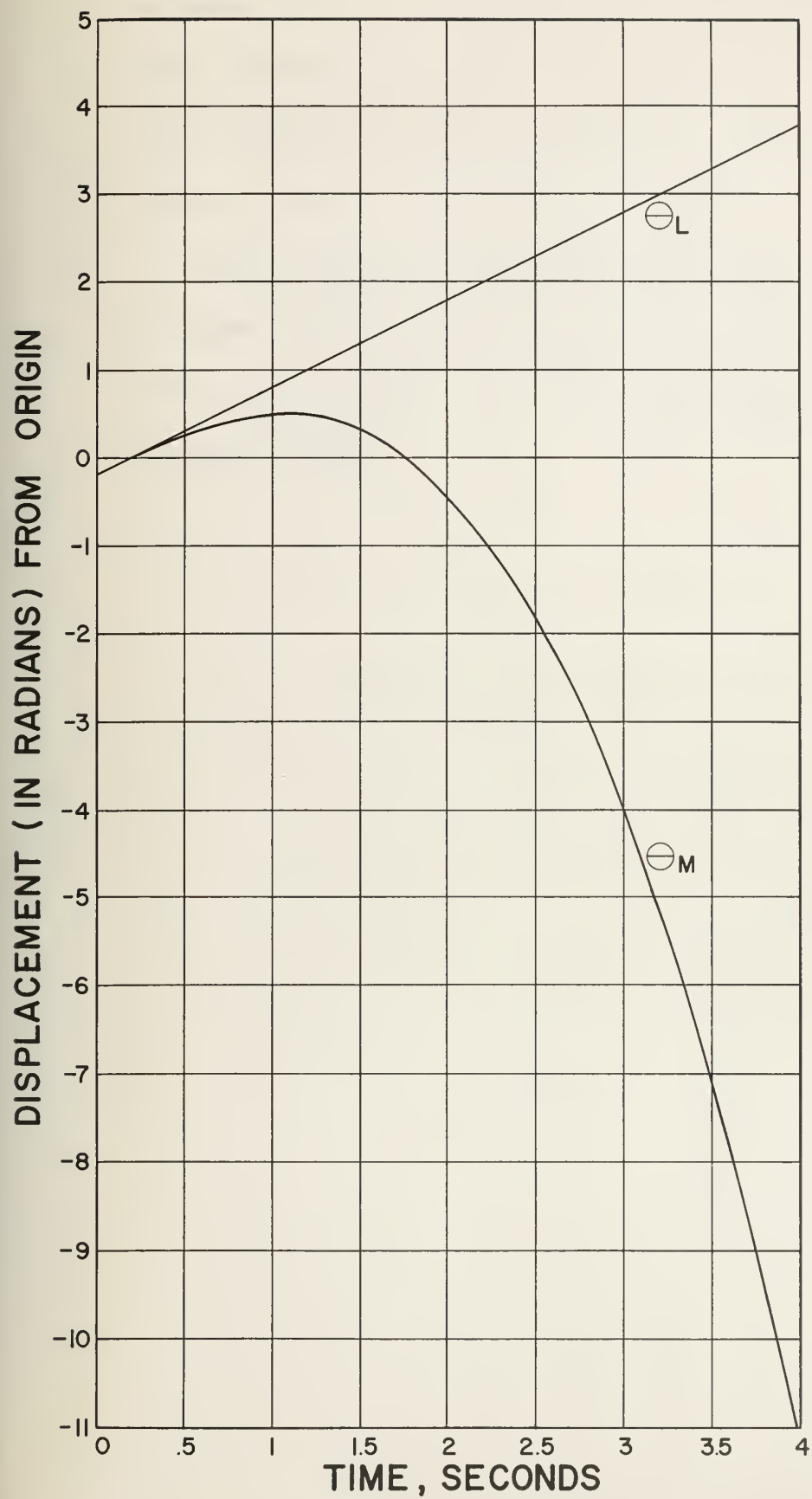


FIG. 3-31 DISPLACEMENT CHARACTERISTICS OF MOTOR AND OF LOAD DURING BACKLASH TAKE-UP.



the phase plane, and the result of the applying the momentum restoration defines another dividing line on the phase plane. These lines may be established point by point in evaluating the phase trajectory, but no simple equation for these lines has been obtained.

A phase plane plot for a particular case is given on Fig. 3-4. This plot shows the three dividing lines, and the nomograph of Fig. 3-3 was used in computing Fig. 3-4. Note that the system goes into a limit cycle along path ABCD.



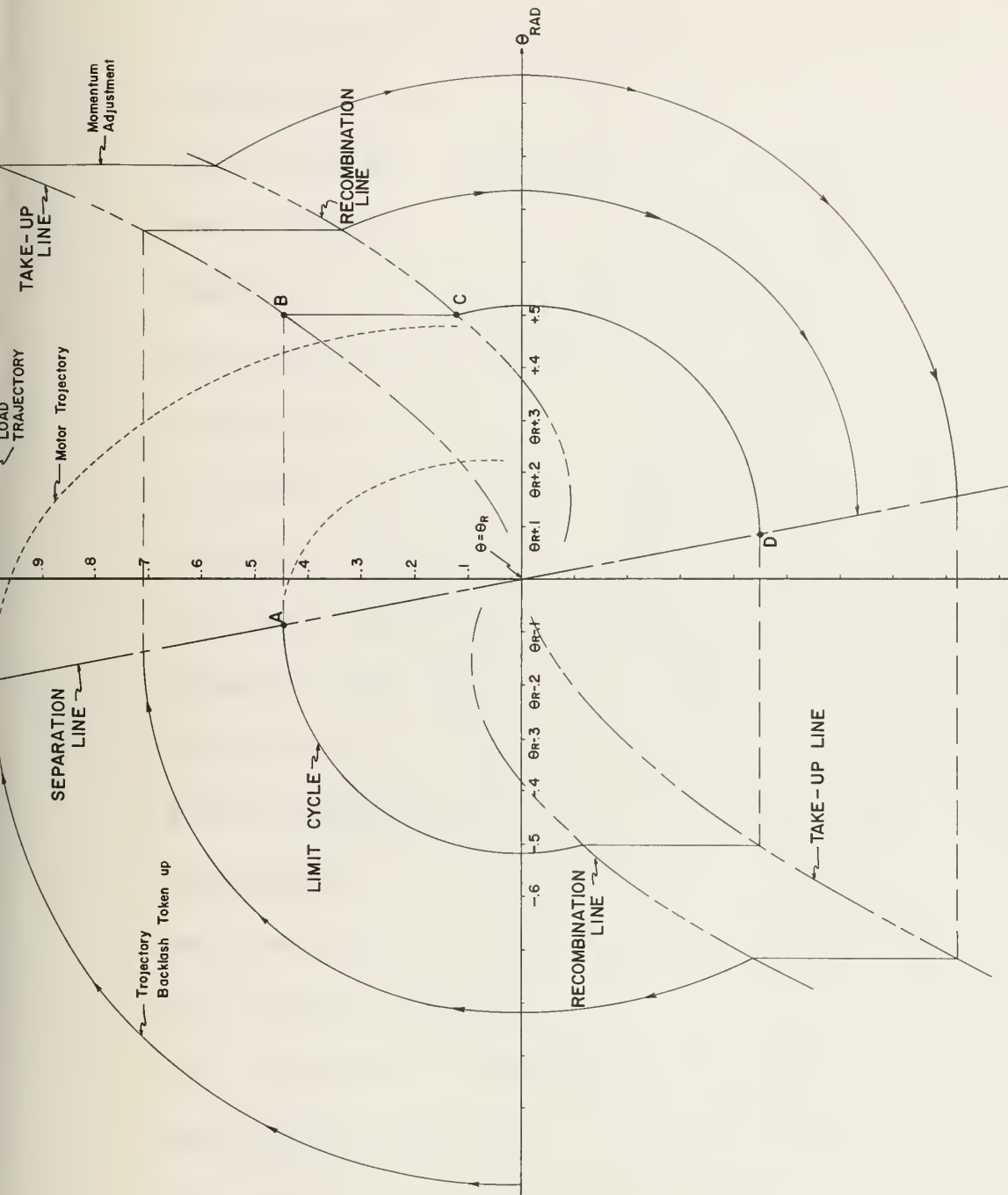


FIGURE 3-4 PHASE TRAJECTORY and LIMIT CYCLE, SERVO WITH BACKLASH

Combined System  $\dot{\theta}_c + 0.2\ddot{\theta}_c + \dot{\theta}_c = \dot{\theta}_R$   
 System with load Separated  $0.5\ddot{\theta}_M + 0.2\dot{\theta}_M = \dot{\theta}_R - \dot{\theta}_L$   
 Load Only  $0.5\ddot{\theta}_L = 0$   
 Backlash = 0.3 RAD





## 4. COMPUTATION BY DIGITAL COMPUTER

### 4.1 Introduction

Use of the phase plane techniques of section 3 is instructive but prohibitively laborious if a large number of cases is to be investigated. Alternatives are analog simulation or digital computation. The individual equations are readily simulated on the analog computer, but instrumentation of the boundary conditions can be difficult. An analysis using analog simulation has been carried out elsewhere\* but was restricted to the inelastic impact case. It was decided to use a digital computer to calculate the desired data, and the computer was to be programmed using phase plane concepts so that all of the data required for phase plane plots would be available when needed. The first program\* was prepared for the inelastic impact case only. It operated successfully as verified by point checks calculated long hand on the phase plane. While the results were accurate, only a limited amount of data was computed due to lack of available time. Upon resumption of the project it was decided to reprogram the computer to handle the general case of elastic \* contact of the gear teeth, including the case of plastic impact as a limiting case. This program was completed and operated satisfactorily. It is given in detail in the appendices. The results reported in the remainder of this text is based on computations made with this program.

\*Knoll & Narud

\*New

\*Anderson & Luckett



TABLE 4-1 SYMBOLS\*

$\Theta_R$	(ONE)**	Angular step input (radians). Desired load displacement at steady state
$\Theta_c$	(THETAL)	Output displacement of load (radians).
$\dot{\Theta}_c$	(THETADL)	Output velocity of load ( $\frac{\text{radians}}{\text{sec}}$ )
$E$		Error in radians. $E = \Theta_R - \Theta_c$
$K$	(KMOTCONST)	Constant of proportionality relating position error to torque developed by the motor.
$T_m$		Developed torque of motor.
$T_L$		Torque of load.
$T_{Lm}$		Torque of load referred to motor.
$\rho$	(RHO)	$\frac{\text{Number of teeth on gear 1}}{\text{Number of teeth on gear 2}}$
$J_m$	(MOINERT)	Inertia of motor measured at motor.
$J_L$	(JLOADVAL)	Inertia of load measured at load.
$J$		Total inertia measured at motor $J = J_m + \rho^2 J_L$
$F_m$	(FMOTOR)	Friction of motor measured at motor.
$F_L$	(FLOAD)	Friction of load measured at load.
$\Delta$	(DELTA)	Backlash of gearbox measured in radians at the output.

$N_s$  Slope of phase trajectory (combined system).

$$N_s = \frac{\Delta}{\frac{d\dot{\Theta}_c}{d\Theta_c}} = \frac{\ddot{\Theta}_c}{\dot{\Theta}_c}$$

\*In this table some of the symbols are redefined and have different meanings than in preceding sections.

\*\* ( ) Terms indicate computer mnemonics referred to in Sec. 3, Computer Program Development.



$N_L$		Slope of phase trajectory (load floating free).
		$N_L \triangleq \frac{d\dot{\Theta}_c}{d\Theta_c} = \frac{\ddot{\Theta}_c}{\dot{\Theta}_c}$
$\dot{\Theta}_m, \dot{\Theta}_c$		Velocities of motor and load after impact.
$e$	(RESTITUT)	Coefficient of restitution.
$\zeta$	(ZETA)	System damping coefficient.
$\omega_n$	(OMEGAN)	System natural frequency.
$\omega_n^2$	(OMEGANSQ)	System natural frequency, squared.
$\frac{f_L}{F_T}$	(FLFTPRIN)	Load friction ratio with respect to friction of the system.
$\frac{J_m}{J_L}$	(INERTRAT)	Inertia ratio.
$\Theta_m$	(THETAM)	Displacement of motor (radians).
$\dot{\Theta}_m$	(THETADM)	Velocity of motor $\left(\frac{\text{radians}}{\text{sec}}\right)$



#### 4.2 Development of Equations

The equations developed were those of a phase plane analysis. Prior to defining the net system equations, the assumptions under which the analysis was made will be stated. When necessary these assumptions will be amplified and referred to later in this work.

It was assumed that:

1. The gear teeth were initially in contact and the initial conditions of the system were all equal to zero. This was later proved to be an unnecessary limitation for the study of steady state response.
2. Plastic deformation of the gear teeth during steady contact and impact and any torsional deformations of driving shafts are negligible.
3. The inertias of the gears and drive shafts are considered as part of the load or motor inertia depending on their attachment in the system.
4. The law of conservation of energy was completely satisfied in only the perfect elastic case by maintaining the total mechanical rotational energy of the system constant at the instant prior to and after impact. The law of conservation of momentum is satisfied in plastic, elastic, and intermediate cases. When the law of conservation of momentum is the only equation required to be satisfied, the energy lost from the





system is dissipated in the heat of infinitesimal deformations of the gear teeth.

5. The gear teeth are in contact only instantaneously during impact for the elastic and intermediate cases (excluding plastic) and that the impulse torques of drive, friction and bearing supports, etc., are zero during impact, e.g.

$$\int_{dt \rightarrow 0} T_m dt = 0 \quad \text{and} \quad \Theta = \Theta^1$$

6. The coefficient of restitution of the two opposing gear teeth is the same or is described by an equivalent coefficient if the two gear teeth are of unequal coefficients.
7. Backlash is assumed to be equal at all points on the gear circumference. Backlash is measured at the output shaft.

A block diagram of the system considered is presented in Fig. 4-1, and symbols have been defined in Table 4-1.

The equations for the motor and load in contact are:

$$E = \Theta_R - \Theta_c \quad (4-1)$$

$$T_m = KE = K (\Theta_R - \Theta_c) \quad (4-2)$$

$$T_L = J_L \ddot{\Theta}_c + f_L \dot{\Theta}_c \quad (4-3)$$

$$T_{Lm} = \rho T_L = \rho (J_L \ddot{\Theta}_c + f_L \dot{\Theta}_c) \quad (4-4)$$

$$\Theta_c = \rho \Theta_m \text{ forward drive} \quad \Theta_c = \rho \Theta_m + \Delta \text{ backward drive} \quad (4-5)$$



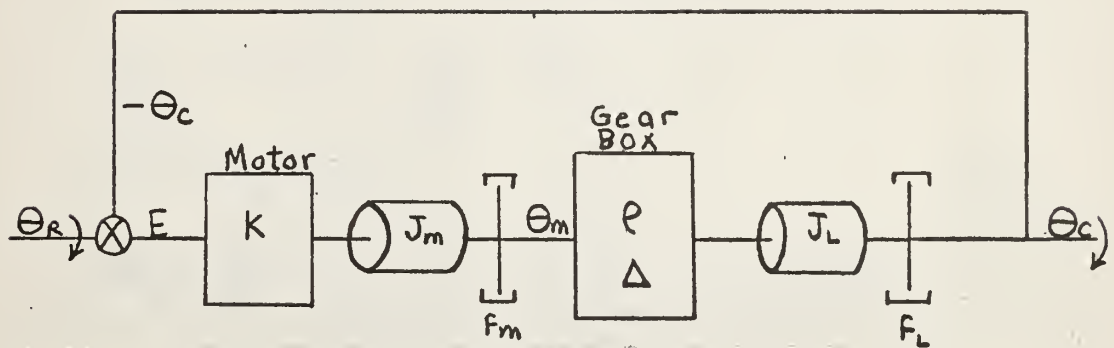


Fig. 4-1 Block diagram of second order servo-mechanism with backlash in the gears between motor and load.



$$\dot{\Theta}_c = \rho \dot{\Theta}_m \text{ forward and backward drive} \quad (4-6)$$

$$\begin{aligned} \text{hence } T_{Lm} &= \rho (J_L \ddot{\Theta}_m + f_L \rho \dot{\Theta}_m) \\ &= \rho^2 (J_L \ddot{\Theta}_m + f_L \dot{\Theta}_m) \end{aligned} \quad (4-7)$$

$$\begin{aligned} T_m &= J_m \ddot{\Theta}_m + f_m \dot{\Theta}_m + T_{Lm} \\ &= J_m \frac{\ddot{\Theta}_c}{\rho} + f_m \frac{\dot{\Theta}_c}{\rho} + \rho^2 (J_L \frac{\ddot{\Theta}_c}{\rho} + f_L \frac{\dot{\Theta}_c}{\rho}) \end{aligned} \quad (4-8)$$

$$\begin{aligned} &= \frac{(J_m + \rho J_L)}{\rho} \ddot{\Theta}_c + \frac{(f_m + \rho f_L)}{\rho} \dot{\Theta}_c \\ T_m &= K (\Theta_R - \Theta_c) \end{aligned} \quad (4-9)$$

$$K \Theta_R = \left( \frac{J_m}{\rho} + \rho J_L \right) \ddot{\Theta}_c + \left( \frac{f_m}{\rho} + \rho f_L \right) \dot{\Theta}_c + K \Theta_c \quad (4-10)$$

$$\ddot{\Theta}_c + \frac{\left( \frac{f_m}{\rho} + \rho f_L \right)}{\left( \frac{J_m}{\rho} + \rho J_L \right)} \dot{\Theta}_c + \frac{K \Theta_c}{\left( \frac{J_m}{\rho} + \rho J_L \right)} = \quad (4-11)$$

$$\begin{aligned} &\frac{K \Theta_R}{\frac{J_m}{\rho} + \rho J_L} \\ \ddot{\Theta}_c + 2 \zeta \omega_n \dot{\Theta}_c + \omega_n^2 \Theta_c &= \omega_n^2 \Theta_R \end{aligned} \quad (4-12)$$

$$\text{where } \omega_n^2 = \frac{\rho K}{J_m + \rho^2 J_L} \quad (4-13)$$

$$2 \zeta \omega_n = \frac{f_m + \rho^2 f_L}{J_m + \rho^2 J_L} \quad (4-14)$$



The equation for load alone with gears not in contact is:

$$J_L \ddot{\Theta}_c + f_L \dot{\Theta}_c = 0 \quad (4-15)$$

or

$$\ddot{\Theta}_c + \frac{f_L}{J_L} \dot{\Theta}_c = 0$$

The equation for the motor alone with the gears not in contact is.

$$J_m \ddot{\Theta}_m + f_m \dot{\Theta}_m = K (\Theta_R - \Theta_c) \quad (4-16)$$

The method of analysis used by New, Ref. e, is used in order to be able to examine the system independently of its  $\omega_n$

Defining first  $\omega_n t \triangleq t^*$

and differentiating  $\omega_n dt = dt^*$

$$\omega_n = \frac{dt^*}{dt} \text{ and } \omega_n^2 = \left( \frac{dt^*}{dt} \right)^2$$

$$\dot{\Theta}_c = \frac{d\Theta_c}{dt} = \frac{d\Theta_c}{dt^*} \frac{dt^*}{dt}, \quad \frac{d\Theta_c}{dt^*} = \dot{\Theta}_c^* \quad (4-17)$$

$$\text{hence } \dot{\Theta}_c = \dot{\Theta}_c^* \omega_n \quad (4-18)$$

similarly

$$\ddot{\Theta}_c = \frac{d^2 \Theta_c}{dt^2} = \frac{d^2 \Theta_c}{(dt^*)^2} \left( \frac{dt^*}{dt} \right)^2 = \frac{d^2 \Theta_c}{(dt^*)^2} \omega_n^2 \quad (4-19)$$

$$\frac{d^2 \Theta_c}{(dt^*)^2} = \ddot{\Theta}_c^* \text{ and } \ddot{\Theta}_c = \ddot{\Theta}_c^* \omega_n^2 \quad (4-20)$$

finally

$$\dot{\Theta}_c = \dot{\Theta}_c^* \omega_n = \dot{\Theta}_c^* \frac{dt^*}{dt} \quad (4-21)$$

$$\int \dot{\Theta}_c dt = \int \dot{\Theta}_c^* dt^* \text{ or } \Theta_c = \Theta_c^* \quad (4-22)$$





Using the equations of the combined system and the load alone,

$$\ddot{\Theta}_c + 2 \int \omega_n \dot{\Theta}_c + \omega_n^2 \Theta_c = \omega_n^2 \Theta_r \quad \text{combined system} \quad (4-23)$$

$$\ddot{\Theta}_c + \frac{f}{J} \frac{L}{L} \dot{\Theta}_c = 0 \quad \text{Load alone} \quad (4-24)$$

and making the indicated substitution to a transformed (\*) coordinate system for the system equation

$$\omega_n^2 \ddot{\Theta}_c^* + 2 \int \omega_n^2 \dot{\Theta}_c^* + \omega_n^2 \Theta_c^* = \omega_n^2 \Theta_R \quad (4-25)$$

$$\ddot{\Theta}_c^* + 2 \int \dot{\Theta}_c^* + \Theta_c^* = \Theta_R \quad (4-26)$$

and introducing the slope equations of the phase plane

$$N_s \dot{\Theta}_c^* + 2 \int \ddot{\Theta}_c^* + \dot{\Theta}_c^* = \Theta_R \quad (4-27)$$

If the load equation is first put in the form for the phase plane

$$N_L \dot{\Theta}_c + \frac{f}{J} \frac{L}{L} \dot{\Theta}_c = 0 \quad (4-28)$$

and then transformed to the (\*) coordinate system where  $\dot{\Theta}_c^* \neq 0$

$$N_L \dot{\Theta}_c^* + \frac{f}{J} \frac{L}{L} \dot{\Theta}_c^* = 0 \quad (4-29)$$

The same result may be obtained by setting  $\omega_n=1$ . The results of such a transformation require inverse scaling for practical application, examples of which given later. It is noted that the slope of the load-free equation is mathematically the same whether in the phase plane or in the transformed phase plane. It is pointed out at this time that the equations later developed to satisfy the laws of conservation of momentum and energy are independent of the system natural frequency.



To establish equations for the law of the conservation of momentum and a relationship satisfying the law of the conservation of energy, the schematic of Fig. 4-2 is used. It is seen that

$$\Theta_c = -p \Theta_1, \dot{\Theta}_c = -p \dot{\Theta}_1 \quad \text{and since } p^1 = 1 \text{ an equivalent}$$

schematic is shown in Fig. 4-2b. By representing the inertia of the load and motor as inertia of the gears figure 4-2c is obtained at the instant of impact. The torque equation may be expressed

$$T = J \ddot{\Theta} = J \frac{d\dot{\Theta}}{dt}$$

Impulse is equal to the time rate of change of momentum. The expressions for the rates of change of momentum of the gears treated separately may be written:

$$-\int \left| F_{1j} \right| r'_1 dt = \int_{\dot{\Theta}_m}^{\dot{\Theta}'_m} J_m \frac{d\dot{\Theta}_m}{dt} dt \quad (4-30)$$

$$-r'_1 \int \left| F_{1j} \right| dt = J_m (\dot{\Theta}'_m - \dot{\Theta}_m) \quad (4-31)$$

$$-\int \left| F_{1j} \right| dt = \frac{J_m}{r'_1} (\dot{\Theta}'_m - \dot{\Theta}_m) \quad (4-32)$$

and

$$\int \left| F_{2j} \right| r'_2 dt = \int_{\dot{\Theta}_1}^{\dot{\Theta}'_1} \overset{\text{for the motor}}{p^2 J_L} \frac{d\dot{\Theta}_1}{dt} dt \quad (4-33)$$

$$\int \left| F_{2j} \right| dt = p^2 \frac{J_L}{r'_2} (\dot{\Theta}'_1 - \dot{\Theta}_1) \quad (4-34)$$



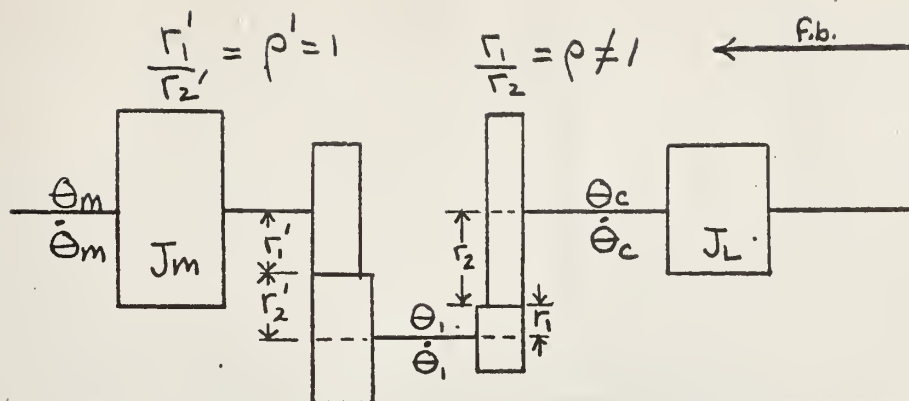


Fig. 4-2a Schematic diagram of motor and load inertias with interconnecting gears.

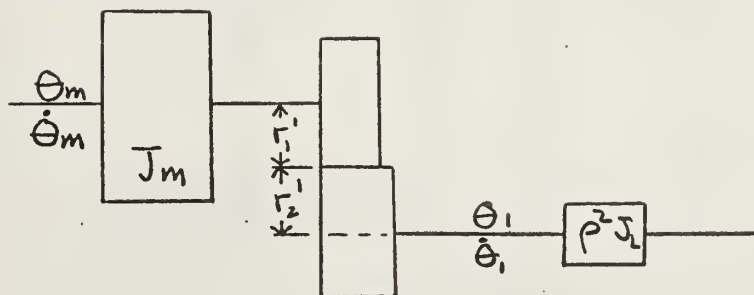


Fig. 4-2b Schematic diagram of mechanical system equivalent to Fig. 4-2a.



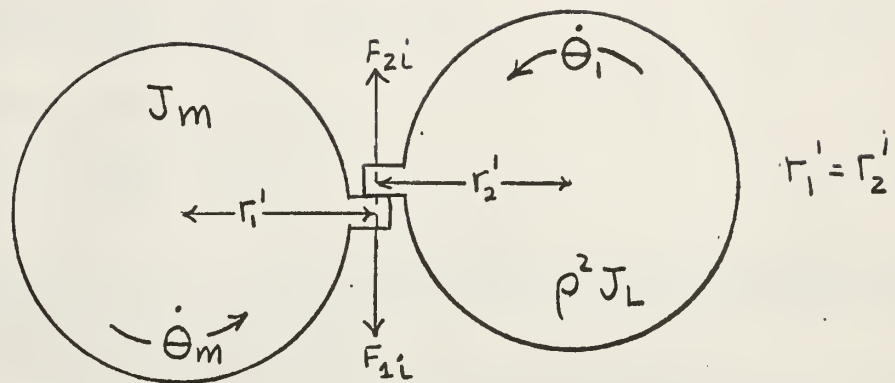


Fig. 4-2c Gear teeth and loads involved at instant of impact.





where the primed velocities are those following impact.

If the momentum is to be conserved in the system the impulse functions are equal and opposite.

$$\frac{J_m}{r_1} (\dot{\theta}'_m - \dot{\theta}_m) = \frac{\rho^2 J_L}{r_2} (\dot{\theta}'_1 - \dot{\theta}_1) \quad (4-35)$$

and

$$\frac{J_m}{J_L} \frac{1}{\rho} (\dot{\theta}'_m - \dot{\theta}_m) = (\dot{\theta}'_c - \dot{\theta}_c) \quad (4-36)$$

from substitution of the equations

$$r_1' = r_2', \quad \dot{\theta}'_c = -\rho \dot{\theta}'_1$$

The assumption that all other impulse functions are zero at the instant of impact is restated at this point.

A definition of the coefficient of restitution will be made for purposes of this work:

$$e \triangleq - \frac{\dot{\theta}'_m + \dot{\theta}'_1}{\dot{\theta}_m + \dot{\theta}_1} = - \frac{(\rho \dot{\theta}'_m - \dot{\theta}'_c)}{\rho \dot{\theta}_m - \dot{\theta}_c} \quad (4-38)$$

It will be shown that this definition of  $e$  will satisfy the law of conservation of energy. Consider the case of  $e=0$ ,

$$0 = -(\rho \dot{\theta}'_m - \dot{\theta}'_c), \quad \rho \dot{\theta}' = \dot{\theta}'_c \quad (4-39)$$

in which case for plastic impact ( $e=0$ ) the gears are moving at the same velocity following impact.

The expression for the coefficient of restitution is examined for the case of perfect elastic contact,  $e=1$ , for which the law of conservation of energy is satisfied.



Solution of the restitution equation for  $e=1$  yields.

$$p \dot{\Theta}_m - \dot{\Theta}_c = -p \dot{\Theta}'_m + \dot{\Theta}'_c \quad (4-40)$$

$$p(\dot{\Theta}_m + \dot{\Theta}'_m) = \dot{\Theta}'_c + \dot{\Theta}_c \quad (4-41)$$

For conservation of energy

$$\frac{1}{2} (J_m \dot{\Theta}_m^2 + J_L \dot{\Theta}_c^2) = \frac{1}{2} (J_m \dot{\Theta}_m'^2 + J_L \dot{\Theta}_c'^2) \quad (4-42)$$

or

$$\frac{J_m}{J_L} (\dot{\Theta}_m^2 - \dot{\Theta}_m'^2) = (\dot{\Theta}_c'^2 - \dot{\Theta}_c^2) \quad (4-43)$$

and factoring

$$\frac{J_m}{J_L} (\dot{\Theta}_m + \dot{\Theta}'_m) (\dot{\Theta}_m - \dot{\Theta}'_m) = (\dot{\Theta}'_c + \dot{\Theta}_c) (\dot{\Theta}'_c - \dot{\Theta}_c) \quad (4-44)$$

The momentum equation which is independent of  $e$  is :

$$\frac{J_m}{p J_L} (\dot{\Theta}'_m - \dot{\Theta}_m) = (\dot{\Theta}_c - \dot{\Theta}'_c) \quad (4-45)$$

$$\text{or rearranging } \frac{J_m}{p J_L} (\dot{\Theta}_m - \dot{\Theta}'_m) = (\dot{\Theta}'_c - \dot{\Theta}_c) \quad (4-46)$$

The factored energy equation is now divided by the momentum equation to yield

$$p(\dot{\Theta}_m + \dot{\Theta}'_m) = (\dot{\Theta}'_c + \dot{\Theta}_c) \quad (4-47)$$

which checks with the definition of the coefficient of restitution

for  $e=1$ .

The momentum equation implied from the impulse approach that  $dt \rightarrow 0$  hence  $\Theta_c = \Theta'_c$  and  $\Theta_m = \Theta'_m$ . The definition of the coefficient of restitution is independent of position. It may be noted that the equations for energy and momentum depend only on the inertia distribution, gear ratio and angular velocities.



In manipulation of these equations it is seen that load inertia may be transferred to the  $\Theta_1$ , shaft by multiplication  $\rho^2$ , the same transfer may be accomplished with load friction. Since  $\Theta_1$ , and  $\dot{\Theta}_1$ , are related to  $\Theta_L$  and  $\dot{\Theta}_L$  it may be reasoned that the results for  $\rho=1$  may be extrapolated to physical systems where  $\rho \neq 1$ .

Since a total energy accounting may be made for the system with the equations used, the rotational energy lost is attributed to the heat of deformation of the gear teeth. This transfer of energy could in fact be determined from the equations used. Thus the conservation of rotational energy  $e=1$  is a special case of a broad interpretation of the law of conservation of energy.



### 4.3 Computer Program Development

The physical equations of the net systems were programmed for solution using the Control Data Corporation 1604 high speed digital computer utilizing paper tape program input and magnetic tape output. An IBM 717 line printer was used to extract data from the magnetic tape. The Control Data Corporation machine library and the U. S. Naval Postgraduate School computer subroutine library were used for assembly, Runge-Kutta-Gill numerical integration, and decimal output.

Several changes were made in the forms of the physical equations of the net system in order to eliminate duplicate computing operations and to fit the equations to a form suited to the variable parameters. In the table of symbols, computer mnemonic (m) terms which are used in the assembly subroutine have been indicated by parentheses and will be defined when encountered.

The equation of the system with motor and load combined

$$\ddot{\theta}_c = \omega_n^2 \theta_R - \omega_n^2 \theta_c - 2 \zeta \omega_n \dot{\theta}_c \quad (4-48)$$

was put in the form

$$\ddot{\theta}_c = \omega_n^2 \theta_R - \omega_n^2 \theta_c - \underline{A} \dot{\theta}_c \quad \text{where} \quad (4-49)$$

$$\underline{A} = 2 \zeta \omega_n \text{ and}$$

$$\underline{\text{THETAL}} = \theta_c$$

$$\underline{\text{ONE}} = \theta_R$$

$$\underline{\text{THETALD}} = \underline{U} = \dot{\theta}_c$$

$$\underline{\text{ZETA}} = \zeta$$

$$\underline{\text{UDOT}} = \ddot{\theta}_c$$

$$\underline{\text{OMEGANSQ}} = \omega_n^2$$





(RUNGE), numerical integration method. The RUNGE subroutine required the definition of synonymous terms for the four iterative cycles used to produce one extrapolated set of variables. The increment of the independent time variable chosen was 0.01 sec. for all  $\zeta > 0.1$  and 0.004 sec. for all  $\zeta \leq 0.1$ .

The load free equation  
was put in the form  $\ddot{\Theta}_c + \frac{f}{J_L} \dot{\Theta}_c = 0$  (4-50)

for the computer  $\ddot{\Theta}_c + \underline{B} \dot{\Theta}_c = 0$  (4-51)

A separate set of RUNGE synonyms was used for the load free equation in order not to destroy the previous computations before they were determined of no further value in computing and also in the making of program decisions.

$\dot{\Theta}_c$  was designated V and  $\ddot{\Theta}_c$  was designated VDOT for the computer program.

The equation for the motor alone

$$\ddot{\Theta}_m + \frac{f}{J_m} \dot{\Theta}_m + \frac{K}{J_m} \Theta_c = \frac{K}{J_m} \Theta_R$$
 (4-52)

was put in the form

$$\ddot{\Theta}_m = -\frac{f}{J_m} \dot{\Theta}_m + \frac{K}{J_m} (\Theta_R - \Theta_c)$$
 (4-53)

$$\ddot{\Theta}_m = -\underline{D} \dot{\Theta}_m + \underline{C} (\Theta_R - \Theta_c)$$
 (4-54)

and for RUNGE, the terms

$$\Theta_m = \underline{\text{THETAM}} \quad \dot{\Theta}_m = \underline{\text{THETADM}} = \underline{W}$$

and  $\ddot{\Theta}_m = \underline{\text{WDOT}}$  were used.



The equation representing the law of conservation of momentum and the definition of coefficient of restitution were combined to the forms

$$\dot{\Theta}'_c = \frac{J_m}{J_m + \rho^2 J_L} \left[ \rho \dot{\Theta}_m (1 + e) + \dot{\Theta}_c \left( \rho^2 \frac{J_L}{J_m} - e \right) \right] \quad (4-55)$$

$$\dot{\Theta}'_m = \frac{\dot{\Theta}'_c - e \rho \dot{\Theta}_m + e \dot{\Theta}_c}{\rho} \quad (4-56)$$

for the computer program. No provision for additional m terms was made to denote the primed values. The additional terms:

$$e = \text{RESTITUT} \quad \rho = \text{RHO} \quad \text{and} \quad \rho^2 = \text{RHOSQ} \quad \text{were used.}$$

Two equations were used to define the boundaries of operation of the load and motor when they were acting separately,

$$\Theta_c = \rho \Theta_m \quad \text{and} \quad \Theta_c = \rho \Theta_m + \Delta \quad (4-57)$$

Two major decisions of the computing cycle were the determination of the point where the motor and load would float free, FLOATEST, and the response of the system to impact of the load and motor gears when the boundary conditions on position were met, COMBTST.

The first decision, the point of float free, is made on the equality or inequality of slopes in the phase plane, i.e., at separation

$N_L = N_S$  Equating the slopes:

$$\frac{\omega_n}{\dot{\Theta}_c} (\Theta_R - \Theta_c) - \underline{A} + \underline{B} = 0 \quad (4-58)$$

The above equation is solved after computing each point in the combined phase trajectory. If  $N_S + N_L > 0$  the system remains combined. If  $N_S + N_L \leq 0$  the system separates, having the response motor alone and load alone immediately thereafter.



The second major decision, that of whether after impact the response should be that of the combined system or the response of the load and motor acting separately, is made on the basis of the resultant velocities after impact and upon which side of the backlash the motor and load positions are found.

The computer program, its flow diagram, a description of the program operation, and an explanation of the readout of information with examples are presented in the Appendix.



#### 4.4 Methods and Scope of Examination

Two modes of operation of the computer program were used. The first mode considered was the phase trajectory. This mode was used to check the operation of the computing cycle. Time, velocity and position of the load were printed when the system was combined. When the system was separated, the values of motor velocity and motor position were also printed. Although the time increment used for computations was either 0.01 sec. or 0.004 sec., printed outputs for the first mode were taken only every 0.1 sec. Additional printed outputs were taken at the time of contact of the gears just prior to and immediately following the solution of the momentum and restitution equations. A typical printout of the phase trajectory mode of operation is shown in the Appendix.

The second mode of operation was used for printing only the maximum computed positive load overshoot position for each cycle, the associated load velocity and the exact problem time of the computation. A sufficient number of print-outs for each problem was obtained to prove limit cycle existence and average size. Since this investigation was concerned primarily with the steady state response, the second mode of operation was the one utilized to obtain the majority of the data. This read-out method markedly decreased the data reduction time for the problem analysis, as opposed to the analysis of steady conditions provided by a full phase trajectory print-out. Since the time required





for computer read-out was several magnitudes greater than the computing time, valuable computer time was saved by this mode of operation. An example of the printed output obtained when only maximum load position overshoot was of interest is given in the Appendix. Approximately 1400 phase trajectories were solved using this mode of operation. Each solution required an average of three minutes of computer time.

For the purpose of general examination of the problem it was assumed that  $\rho = 1$ ,  $K = 1$ ,  $\omega_n = 1$ ,  $J_m + \rho^2 J_L = 1$ . Specific solutions were made with  $\rho \neq 1$ ,  $\omega_n \neq 1$  to determine scaling effects. It was determined that velocities were scaled in direct proportion with  $\omega_n$  and time is scaled in an inverse ratio with  $\omega_n$ . It was also determined that  $\rho^2 \frac{f_L}{F_T}$  and  $\rho^2 \frac{J_L}{J_m}$  were valid parameters and in agreement with the non dimensional parameters used for the investigation.

The program can also be made to solve linear systems by setting  $\Delta = 0$ .

The major variable parameters used in this investigation were:

$$\zeta = 0.1, 0.2, 0.3, 0.4, 0.5, 0.6, 0.8, 1.0$$

$$\rho^2 \frac{f_L}{F_T} = 0, 0.2, 0.4, 0.6, 0.8, 1.0$$

$$\rho^2 \frac{J_L}{J_m} = \frac{0.1}{0.9}, \frac{0.2}{0.8}, \frac{0.5}{0.5}, \frac{0.8}{0.2}, \frac{0.9}{0.1}$$

$$\Delta = 0.3 \text{ radians}$$

$$e = 0, 0.6, 0.8, 1.0$$



Additional parameters of

$\rho^2 \frac{J_L}{F_T} = 0.04, 0.1, 0.9$ ; and  $\Delta = 0.01, 0.03, 0.1, 0.15$  radians were used in certain instances to examine particular characteristics of the response.

The program was limited somewhat in that the value of

$\rho^2 \frac{J_L}{J_m} = \infty$  and zero were excluded due to generation of undefined mathematical quantities.

The value of backlash was made abnormally large,  $\Delta = 0.3$  radians, to allow an easier interpretation of the non-linear response. Since the influence of  $\Delta$  was linear, this caused no inaccuracies. All graphs for limit cycle size were plotted with  $\Delta = 0.3$  radians. The effect of values for  $\Delta$  other than 0.3 is also shown in graphical form.



## 5. ANALYSIS OF RESULTS

The primary purpose of this study was the determination of the conditions for existence of a limit cycle. Due to the nature of the computations an analysis of the results of each numerical case provided an individual "yes" or "no" answer, i.e., a limit cycle existed or did not exist. This information plots conveniently as individual points, and has been recorded on Figs. 5-1 and 5-2 in condensed, semi-quantitative form to give a broad view of limit cycle conditions. On Figs. 5-1 and 5-2 the small circles merely indicate points at which a computation was made, the curved lines were averaged in as accurately as possible with the available data. In general these figures are sufficiently accurate for an engineering check, since parameter values which are close to a boundary obviously lead to a long-duration oscillation even if there is no limit cycle.

The data in Figs. 5-1 and 5-2 can be presented in the form of a three dimensional picture which provides considerable perspective. Such a presentation is given on Fig. 5-3, which is a three dimensional sketch of the limit cycle boundary for the particular case of  $e=1.0$ . The surface of this contour is the limit cycle boundary. For combinations of parameters specifying a point on or below the surface there is no limit cycle. For combinations of parameters specifying a point above the surface a limit cycle is guaranteed, and the





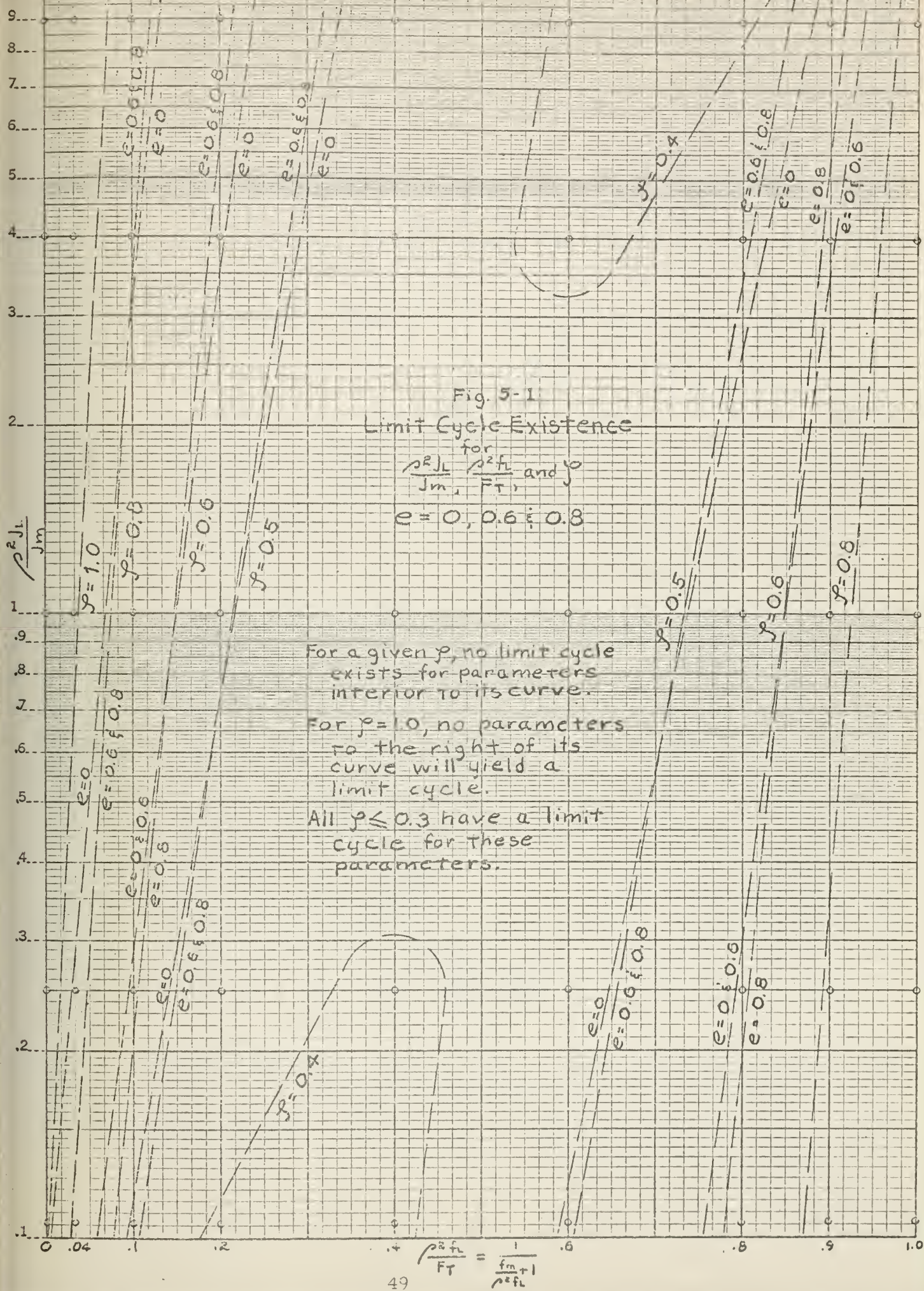


Fig. 5-1  
Limit Cycle Existence

for  
 $\frac{p^2 J_L}{J_m}$ ,  $\frac{p^2 f_L}{F_T}$ , and  $p$   
 $e = 0, 0.6 \text{ \& } 0.8$

For a given  $p$ , no limit cycle exists for parameters interior to its curve.

For  $p = 1.0$ , no parameters to the right of its curve will yield a limit cycle.

All  $p \leq 0.3$  have a limit cycle for these parameters.





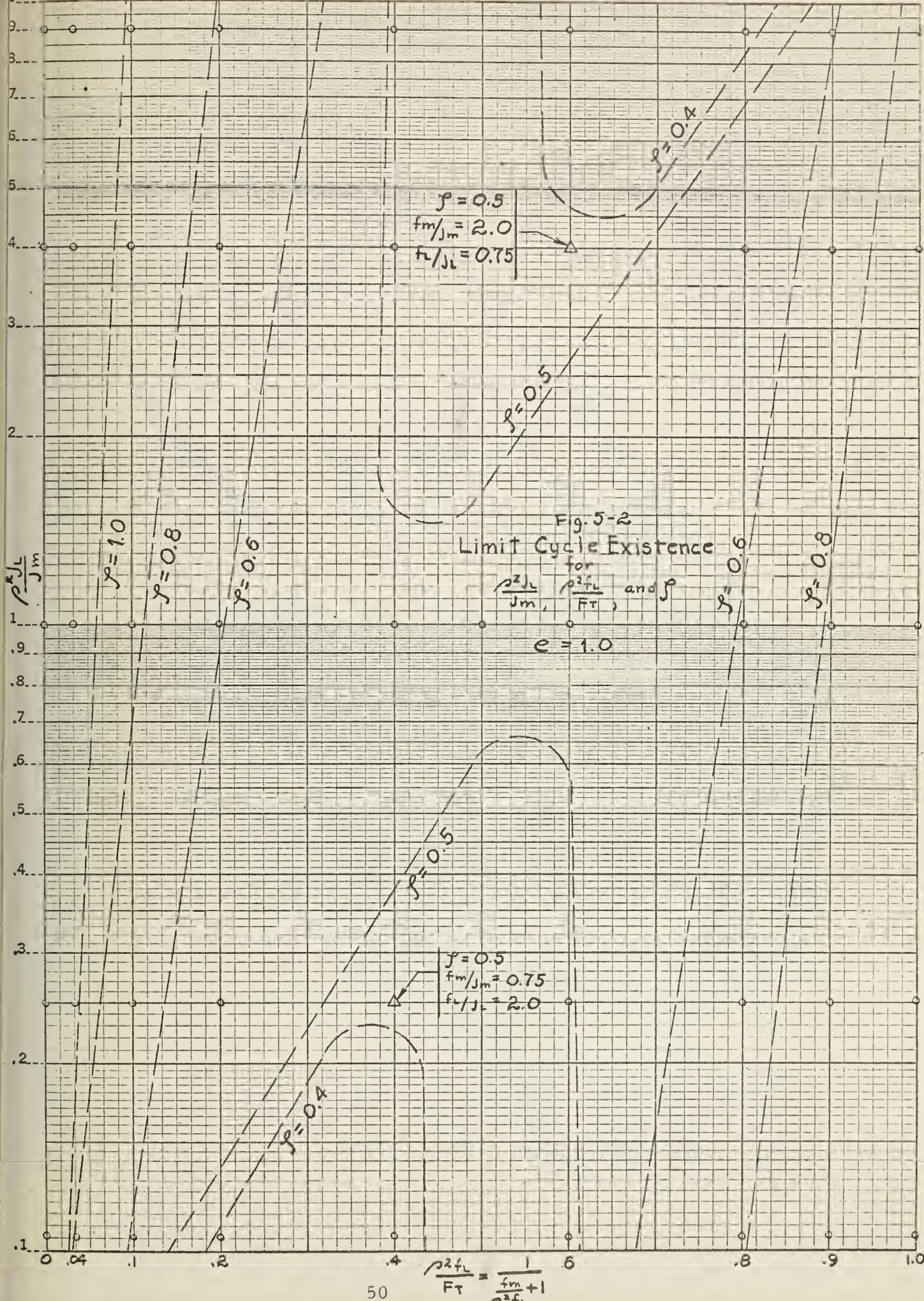


Fig. 5-2  
Limit Cycle Existence

for  $\frac{\rho^2 J_L}{J_m}$ ,  $\frac{\rho^2 f_L}{F_T}$ , and  $\eta$

$e = 1.0$





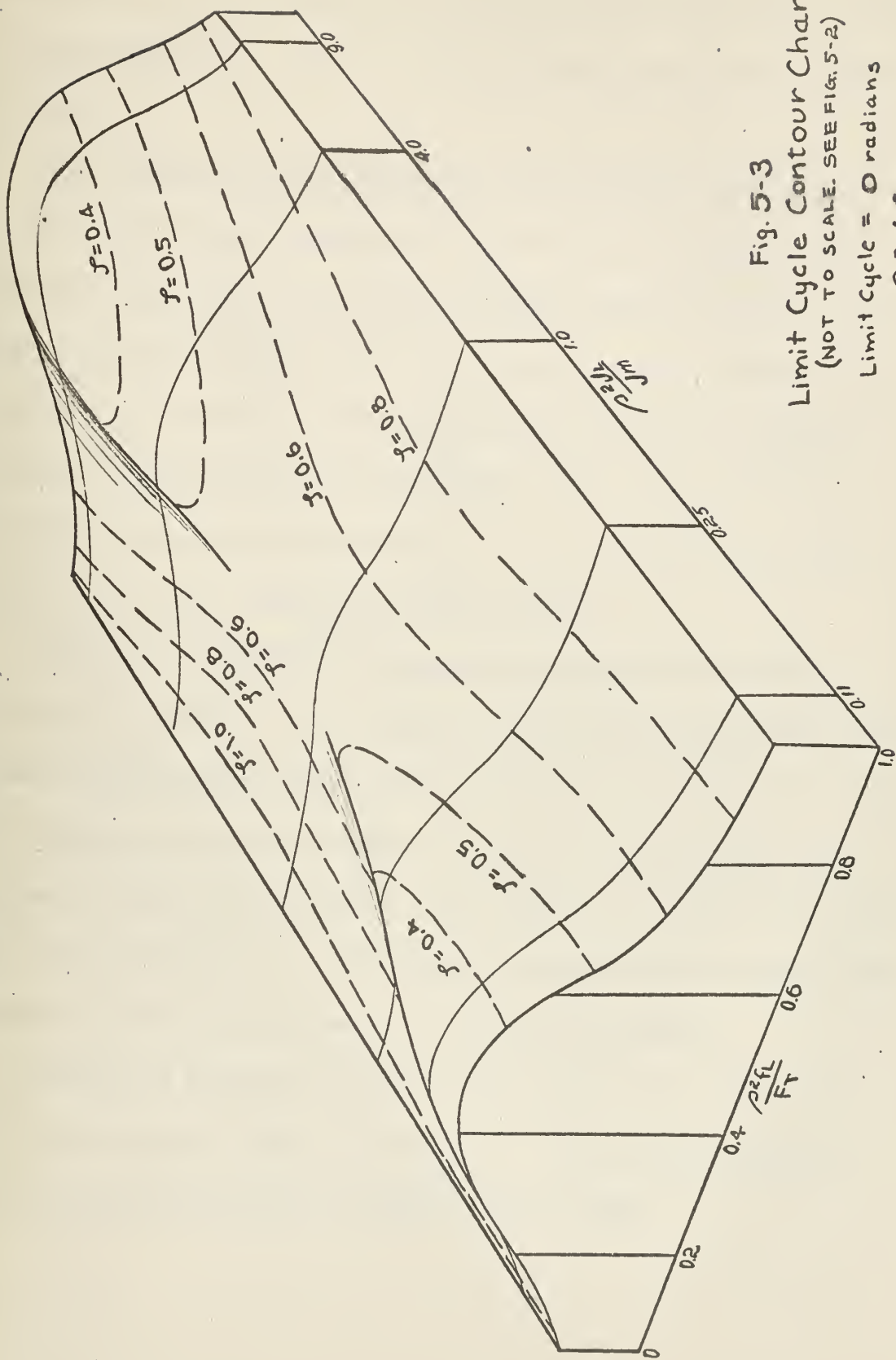


Fig. 5-3

Limit Cycle Contour Chart  
(NOT TO SCALE. SEE FIG. 5-2)

Limit Cycle = 0 radians  
 $e = 1.0$



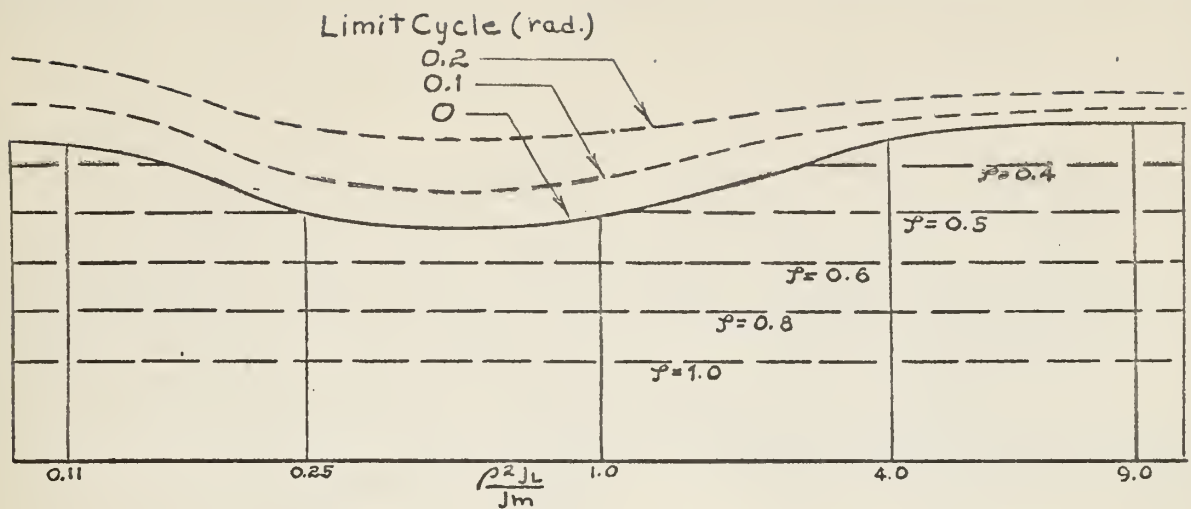
amplitude of the limit cycle is related to the distance from the surface to the pertinent point. This is further elaborated on by the sketches of Fig. 5-4.

For calculation purposes detailed and quantitative curves are desired, and the three dimensional figure is not a convenient tool. Therefore the results of the digital computer study are summarized using a series of families of curves. These are given in Figs. 5-5 through 5-28 to show the effects of parameter variation on both the existence and amplitude of the limit cycle. This is essentially the data which was summarized in Figs. 5-1 and 5-2 (limit cycle existence), but is more complete and more accurate.

In all of the computations reported to this point the backlash was set a  $\Delta = 0.3$  radians. It was tacitly assumed that all amplitude phenomena would be directly proportional to the amount of backlash. Since this condition was easily checked by additional computations it was decided to verify the assumption. The results are shown on Fig. 5-29 and 5-30, from which it is evident that the amplitude of the limit cycle is indeed directly proportional to the amount of backlash.

Included for purposes of general information are two phase trajectory plots shown on Fig. 5-31 and 5-32. These show the type of information available from the digital computer data.

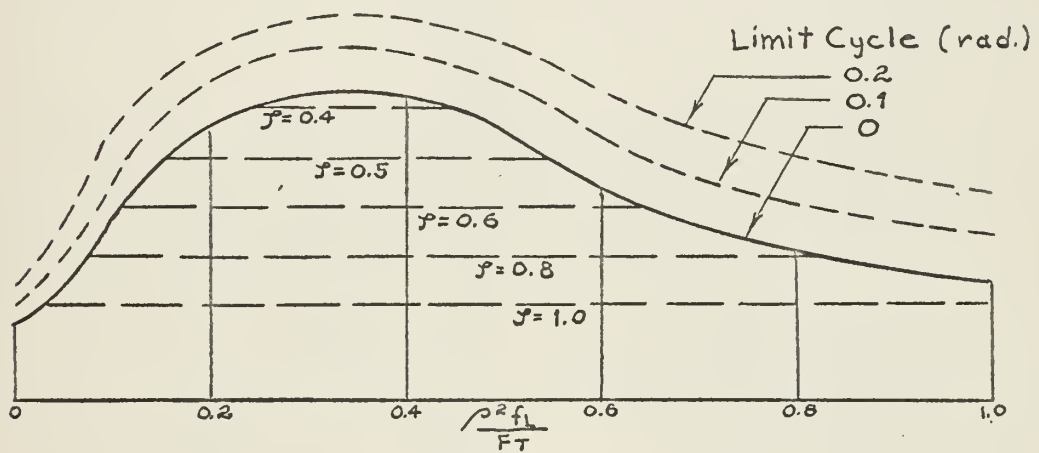




Constant  $\frac{\rho^2 f_L}{F_T}$  Profile

$$\frac{\rho^2 f_L}{F_T} = 0.6$$

(NOT TO SCALE. SEE FIG. 5-26)



Constant  $\frac{\rho^2 J_L}{J_m}$  Profile

$$\frac{\rho^2 J_L}{J_m} = 0.11$$

Fig. 5-4

Limit Cycle Contour Chart  
Profile Views

$$e = 1.0$$

$$\Delta = 0.3$$





Limit Cycle Error (Radians)

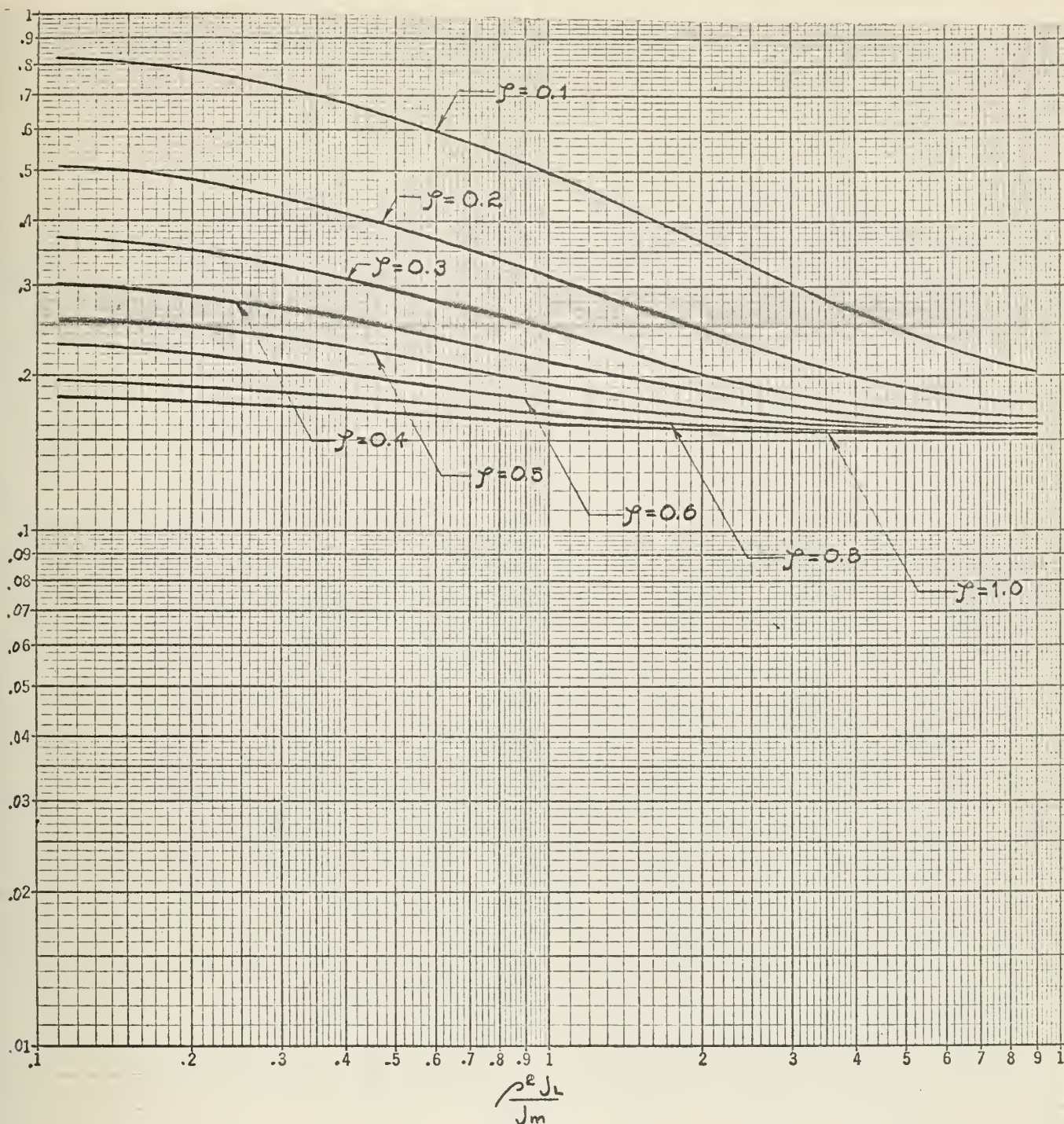


Fig. 5-5

Maximum Error of Limit Cycle from Unit Step Input

Limit Cycle Error (Radians)  $\left( \frac{0.3}{\Delta} \right)$  for  $\frac{\rho^2 J_L}{J_m}$  Variable

$$\frac{\rho^2 f_L}{F_T} = \frac{1}{\frac{f_m}{\rho^2 f_L} + 1} = 0$$

$$e = 0$$



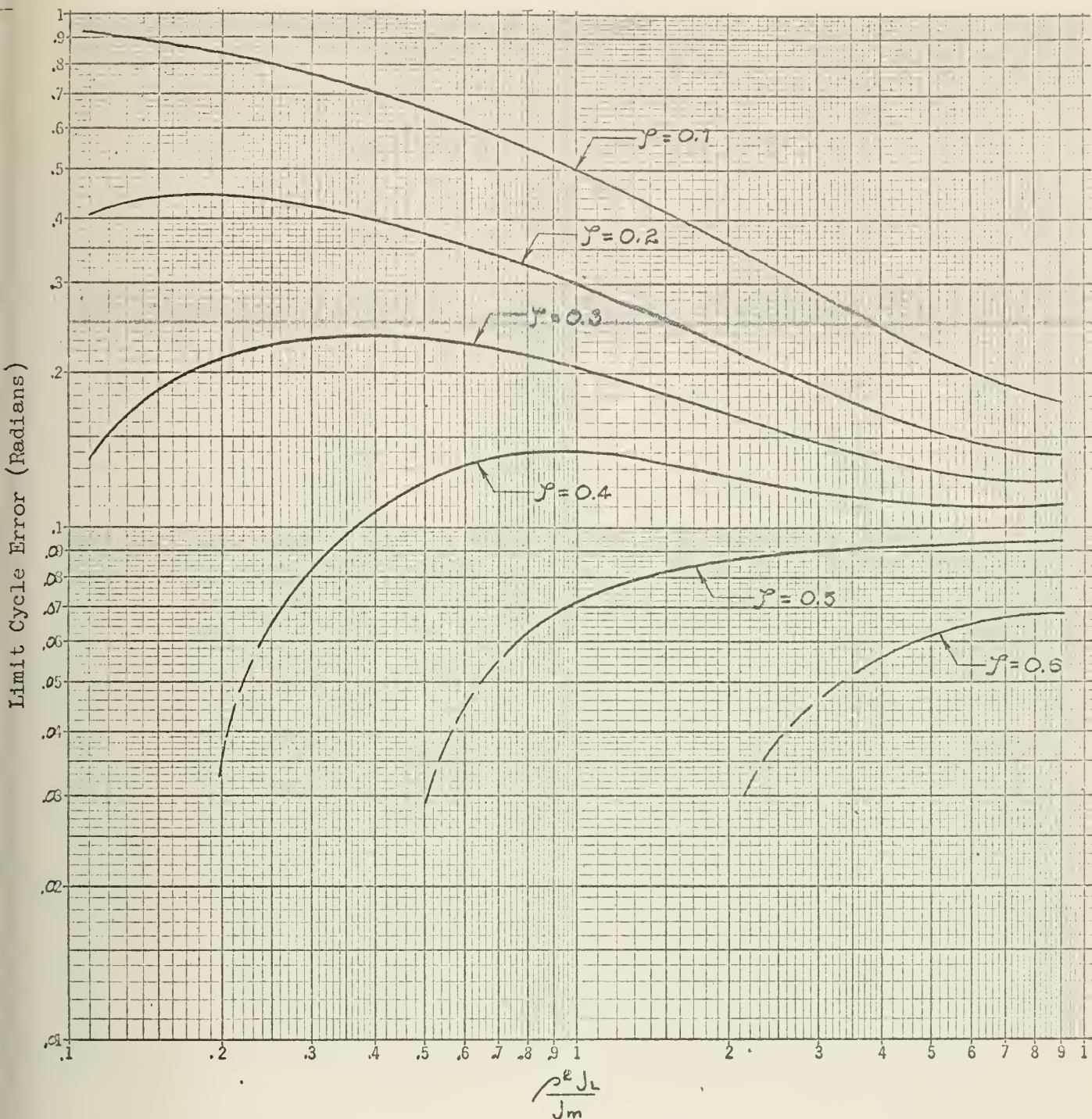


Fig. 5-6

Maximum Error of Limit Cycle from Unit Step Input

Limit Cycle Error (Radians)  $\left( \frac{0.3}{\Delta} \right)$  for  $\frac{\rho^2 J_L}{J_m}$  Variable

$$\frac{\rho^2 f_L}{F_T} = \frac{1}{\frac{f_m}{\rho^2 f_L} + 1} = 0.2$$

$$e = 0$$

No limit cycle exists for  $\gamma \geq 0.8$





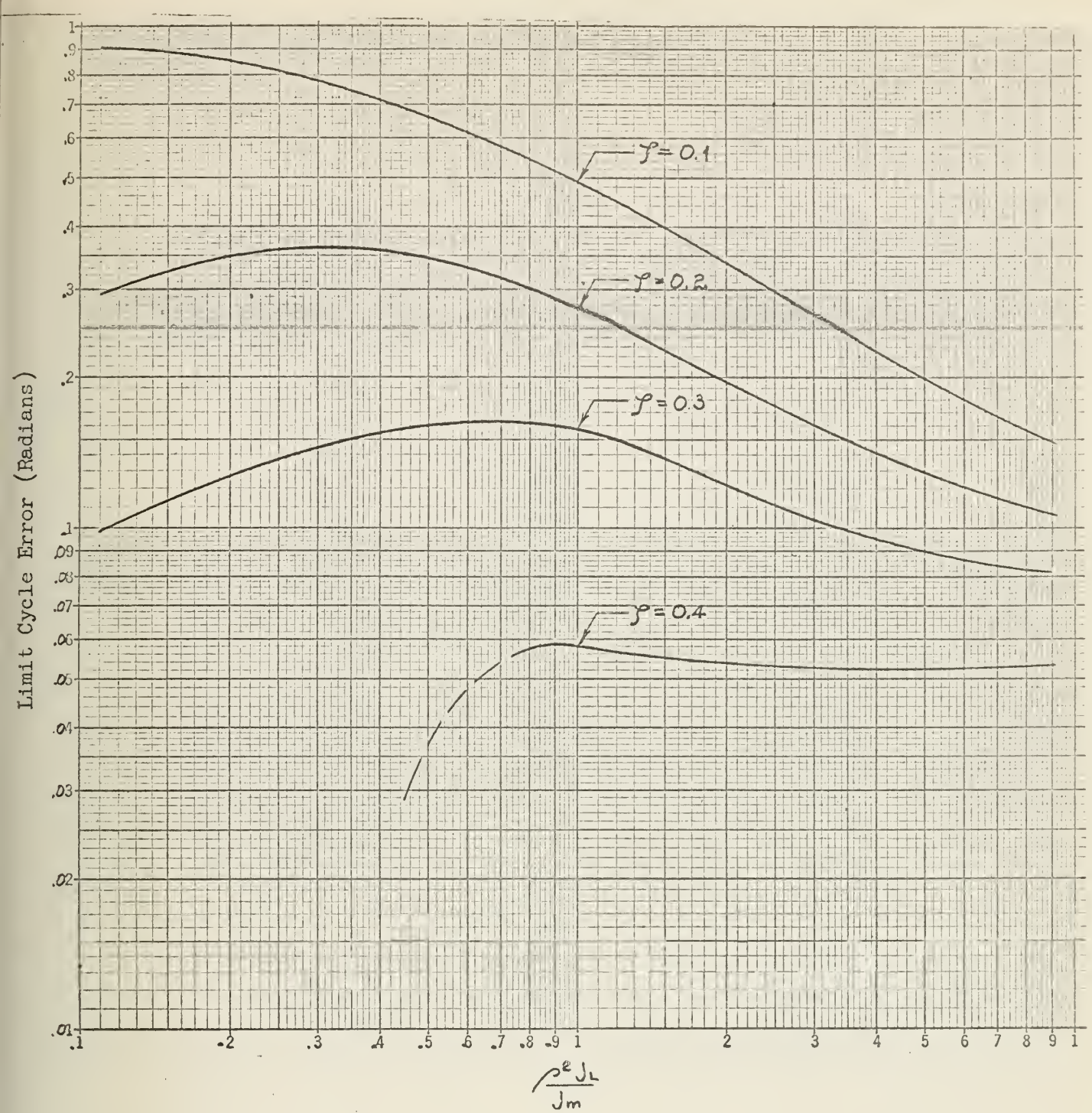


Fig. 5-7

Maximum Error of Limit Cycle from Unit Step Input

Limit Cycle Error (Radians)  $\left( \frac{0.3}{\Delta} \right)$  for  $\frac{\rho^2 J_L}{J_m}$  Variable

$$\frac{\rho^2 f_L}{F r} = \frac{1}{\frac{f_m}{\rho^2 f_L} + 1} = 0.4$$

$$e = 0$$

No limit cycle exists for  $\gamma \geq 0.5$





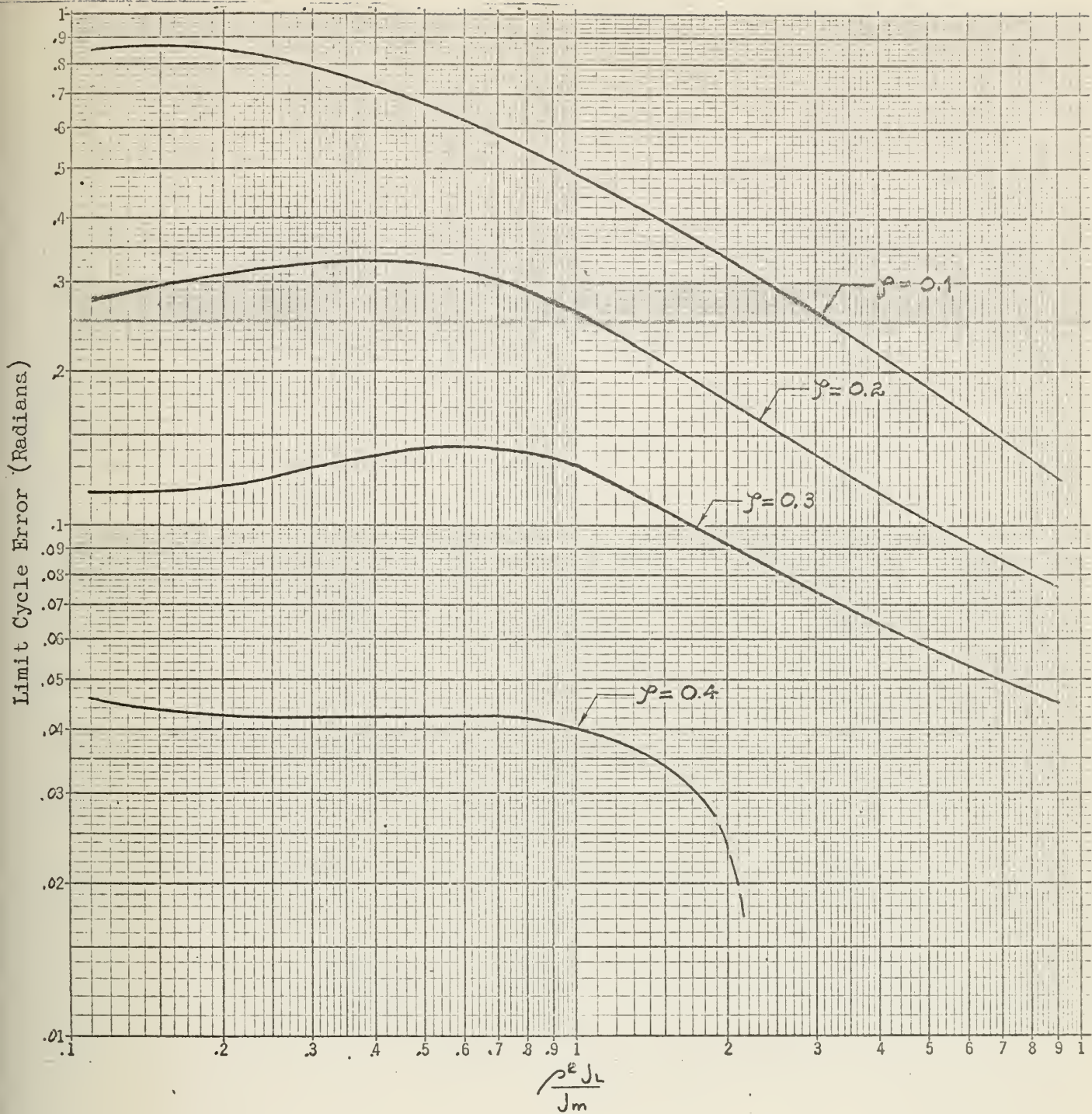


Fig. 5-8

Maximum Error of Limit Cycle from Unit Step Input

Limit Cycle Error (Radians)  $\left( \frac{0.3}{\Delta} \right)$  for  $\frac{\rho^2 J_L}{J_m}$  Variable

$$\frac{\rho^2 f_L}{F\tau} = \frac{1}{\frac{f_m}{\rho^2 f_L} + 1} = 0.6$$

$$e = 0$$

No limit cycle exists for  $\gamma \geq 0.5$





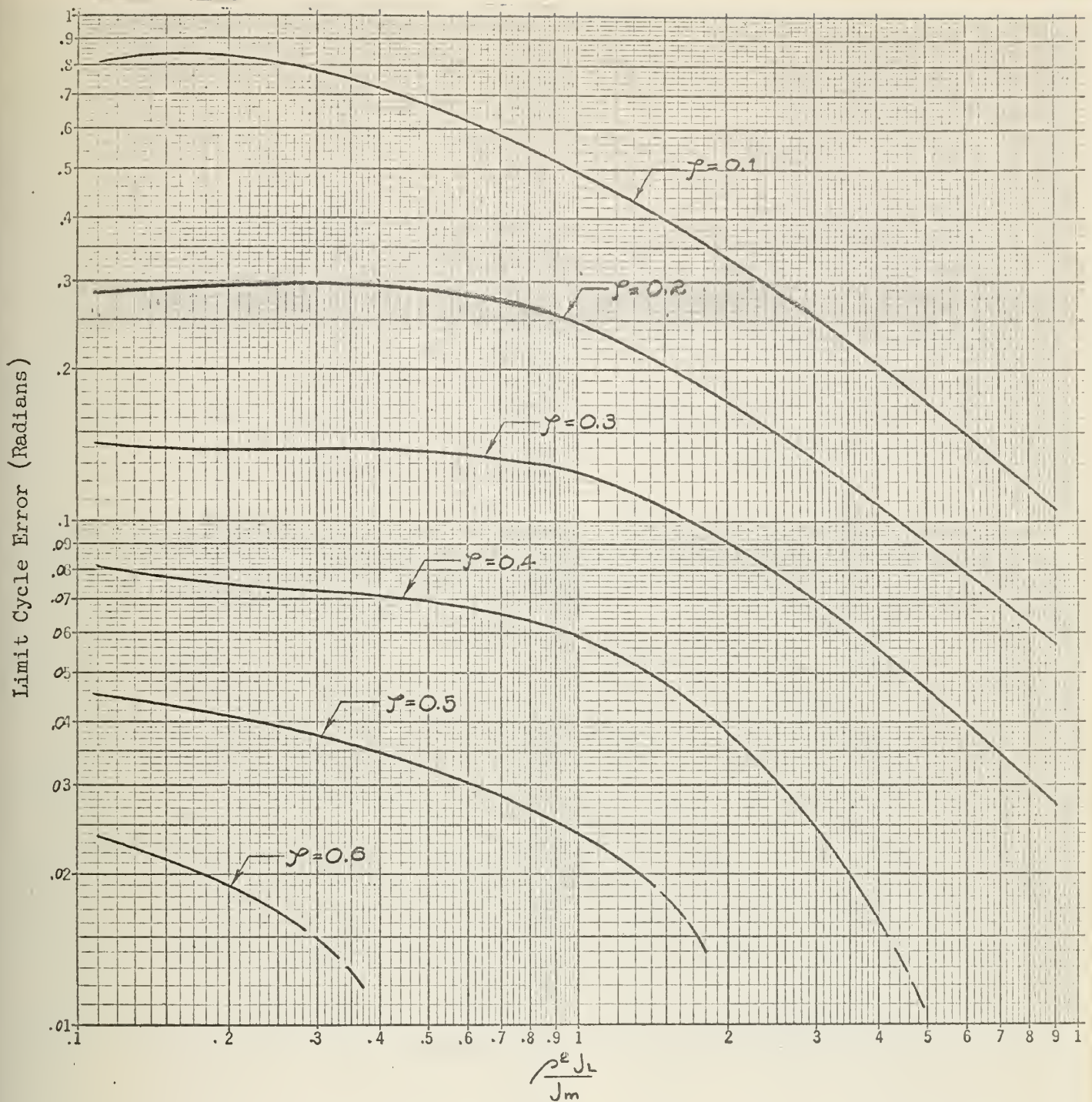


Fig. 5-9

Maximum Error of Limit Cycle from Unit Step Input

Limit Cycle Error (Radians)  $\left( \frac{0.3}{\Delta} \right)$  for  $\frac{\rho^2 J_L}{J_m}$  Variable

$$\frac{\rho^2 f_L}{F_r} = \frac{1}{\frac{f_m}{\rho^2 f_L} + 1} = 0.8$$

$$e = 0$$

No limit cycle exists for  $\gamma \geq 0.8$





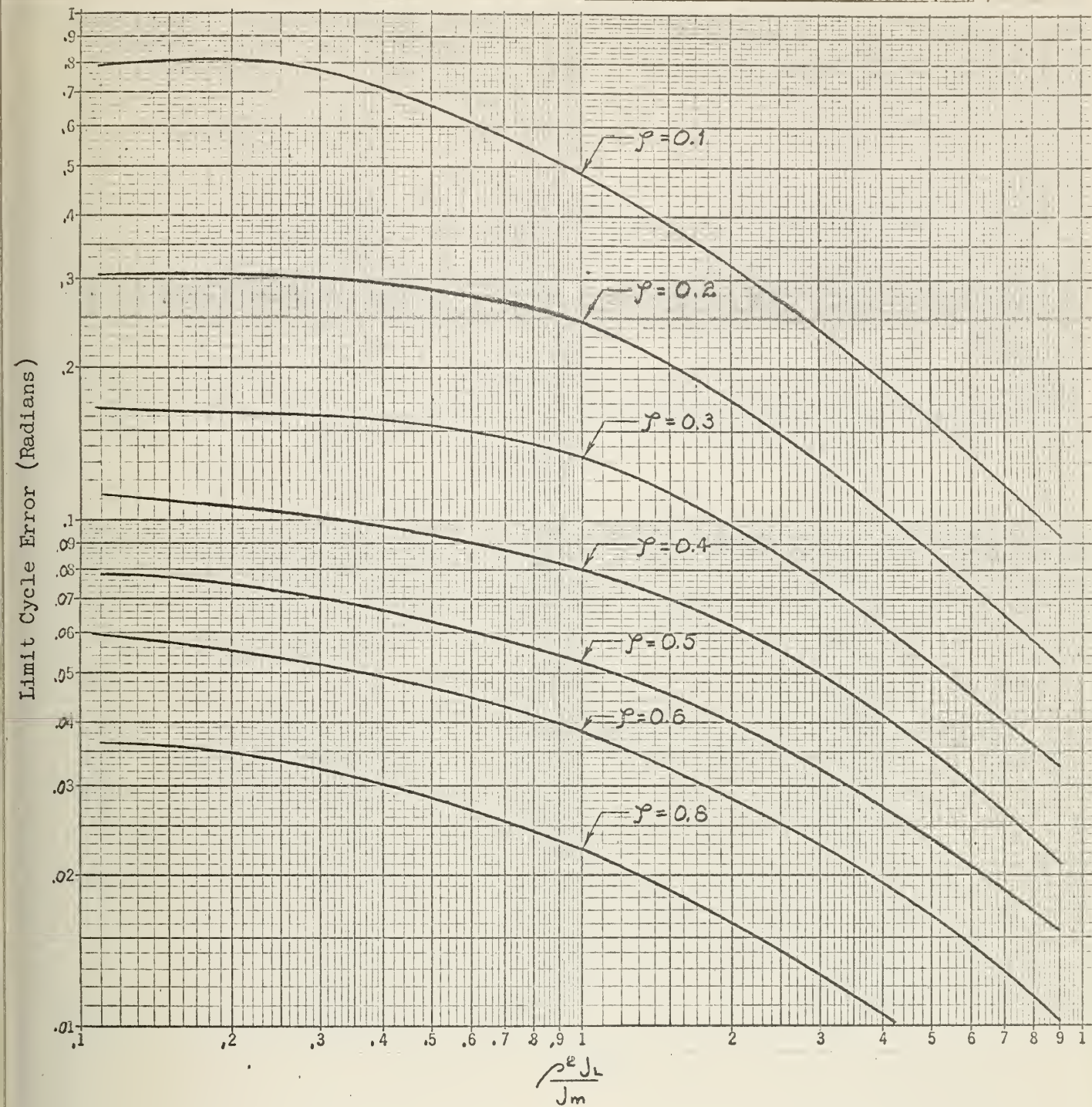


Fig. 5-10

Maximum Error of Limit Cycle from Unit Step Input

Limit Cycle Error (Radians)  $\left( \frac{0.3}{\Delta} \right)$  for  $\frac{\rho^2 J_L}{J_m}$  Variable

$$\frac{\rho^2 f_L}{F_T} = \frac{1}{\frac{f_m}{\rho^2 f_L} + 1} = 1.0$$

$$e = 0$$

No limit cycle exists for  $\gamma \geq 1.0$





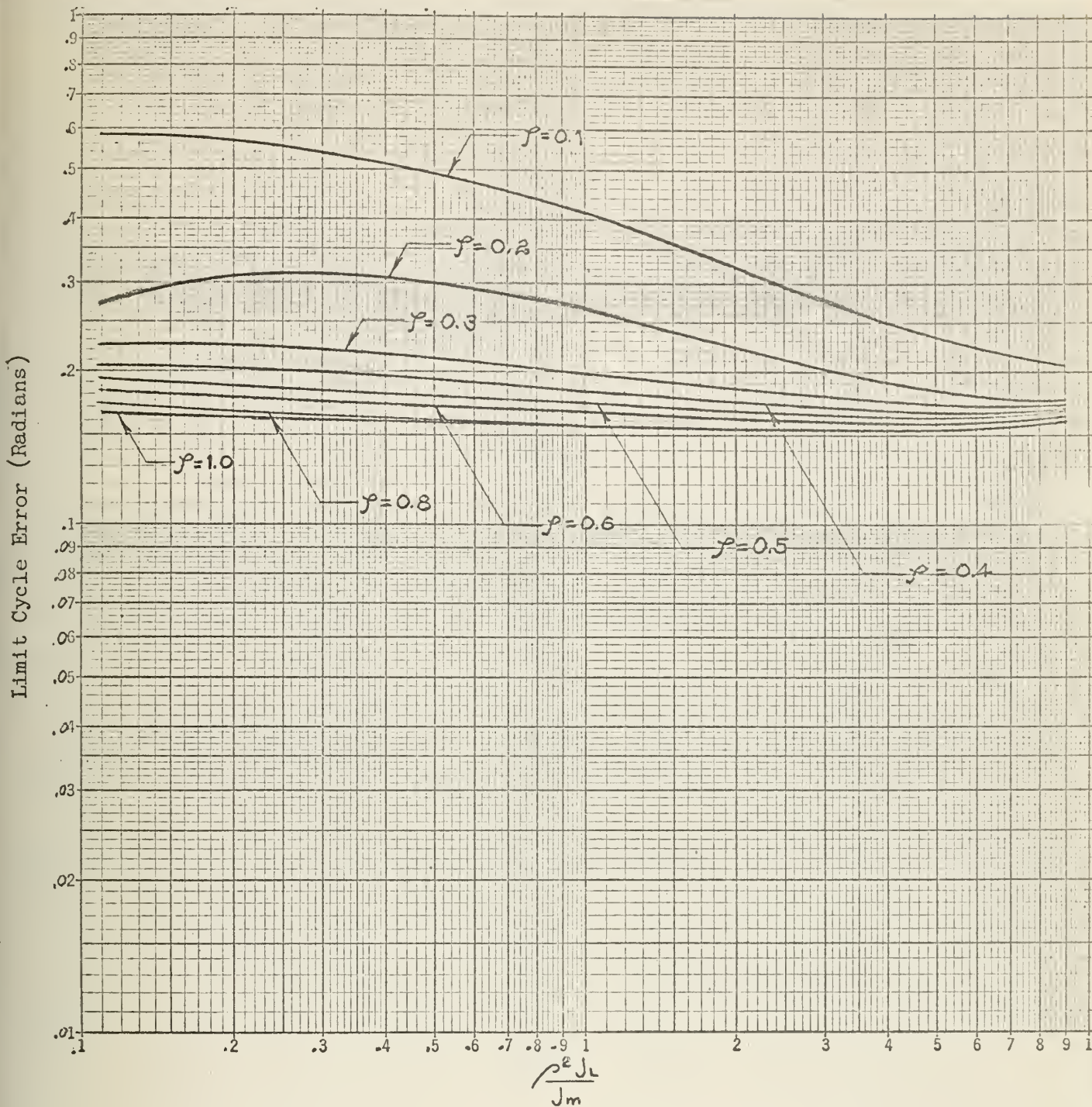


Fig. 5-11

Maximum Error of Limit Cycle from Unit Step Input

Limit Cycle Error (Radians)  $\left( \frac{0.3}{\Delta} \right)$  for  $\frac{\rho^2 J_L}{J_m}$  Variable

$$\frac{\rho^2 f_L}{F_T} = \frac{1}{\frac{f_m}{\rho^2 f_L} + 1} = 0$$

$$e = 0.6$$



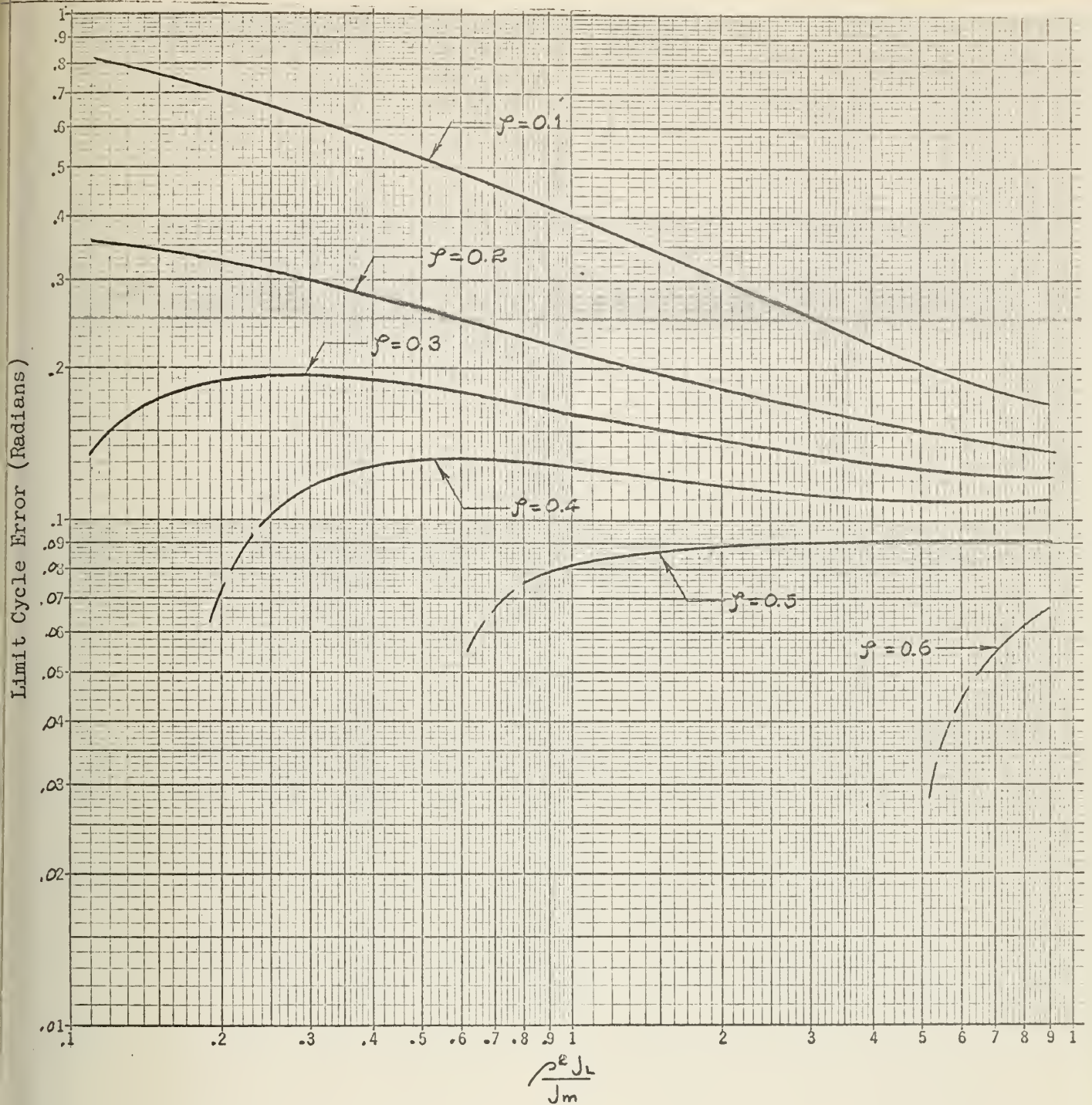


Fig. 5-12

Maximum Error of Limit Cycle from Unit Step Input

Limit Cycle Error (Radians)  $\left( \frac{0.3}{\Delta} \right)$  for  $\frac{\rho^2 J_L}{J_m}$  Variable

$$\frac{\rho^2 f_L}{F_T} = \frac{1}{\frac{f_m}{\rho^2 f_L} + 1} = 0.2$$

$$e = 0.6$$

No limit cycle exists for  $\zeta \geq 0.8$







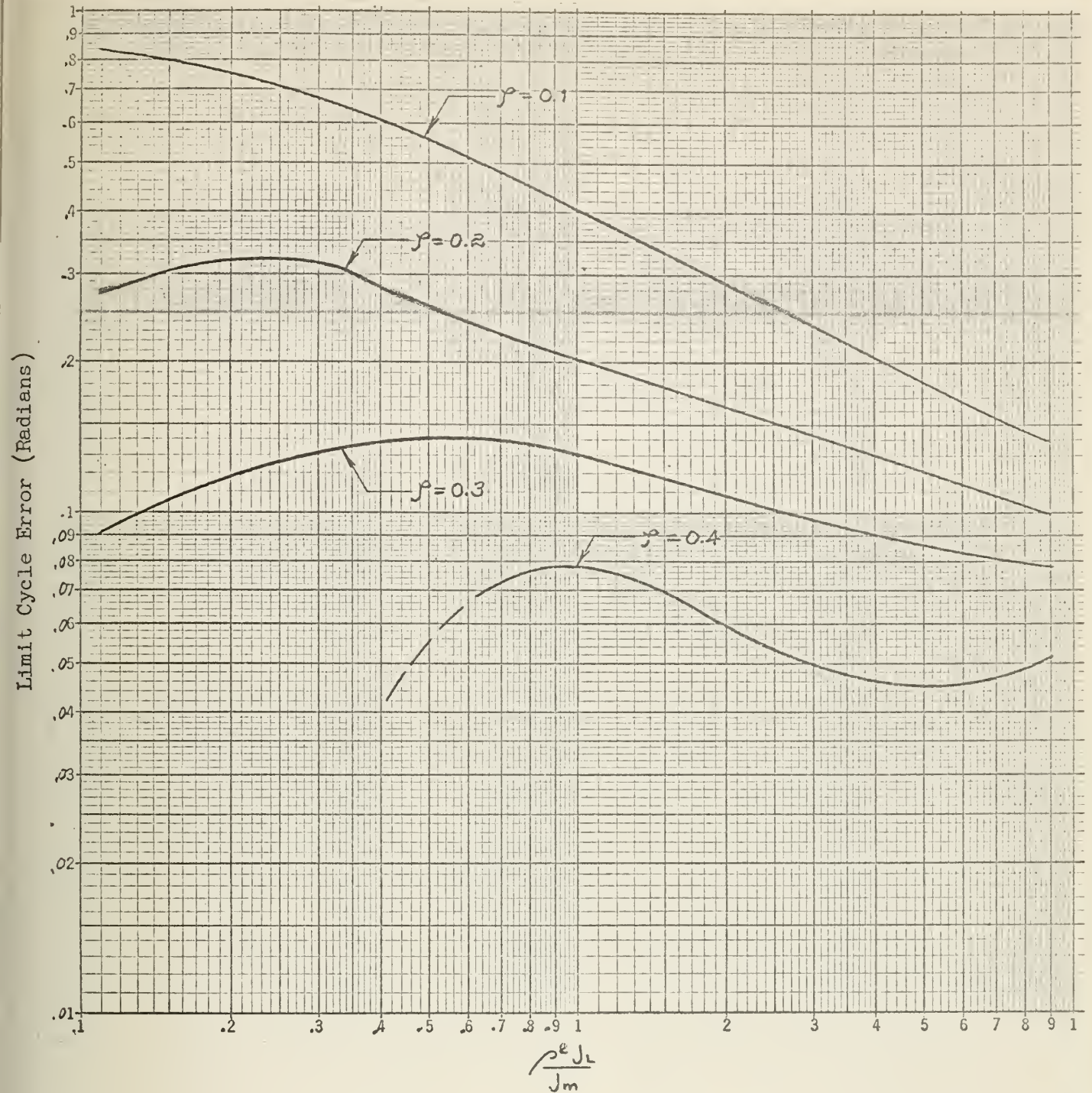


Fig. 5-13

Maximum Error of Limit Cycle from Unit Step Input

Limit Cycle Error (Radians)  $\left( \frac{0.3}{\Delta} \right)$  for  $\frac{\rho^2 J_L}{J_m}$  Variable

$$\frac{\rho^2 f_L}{F\tau} = \frac{1}{\frac{f_m}{\rho^2 f_L} + 1} = 0.4$$

$$e = 0.6$$

No limit cycle exists for  $\rho \geq 0.5$



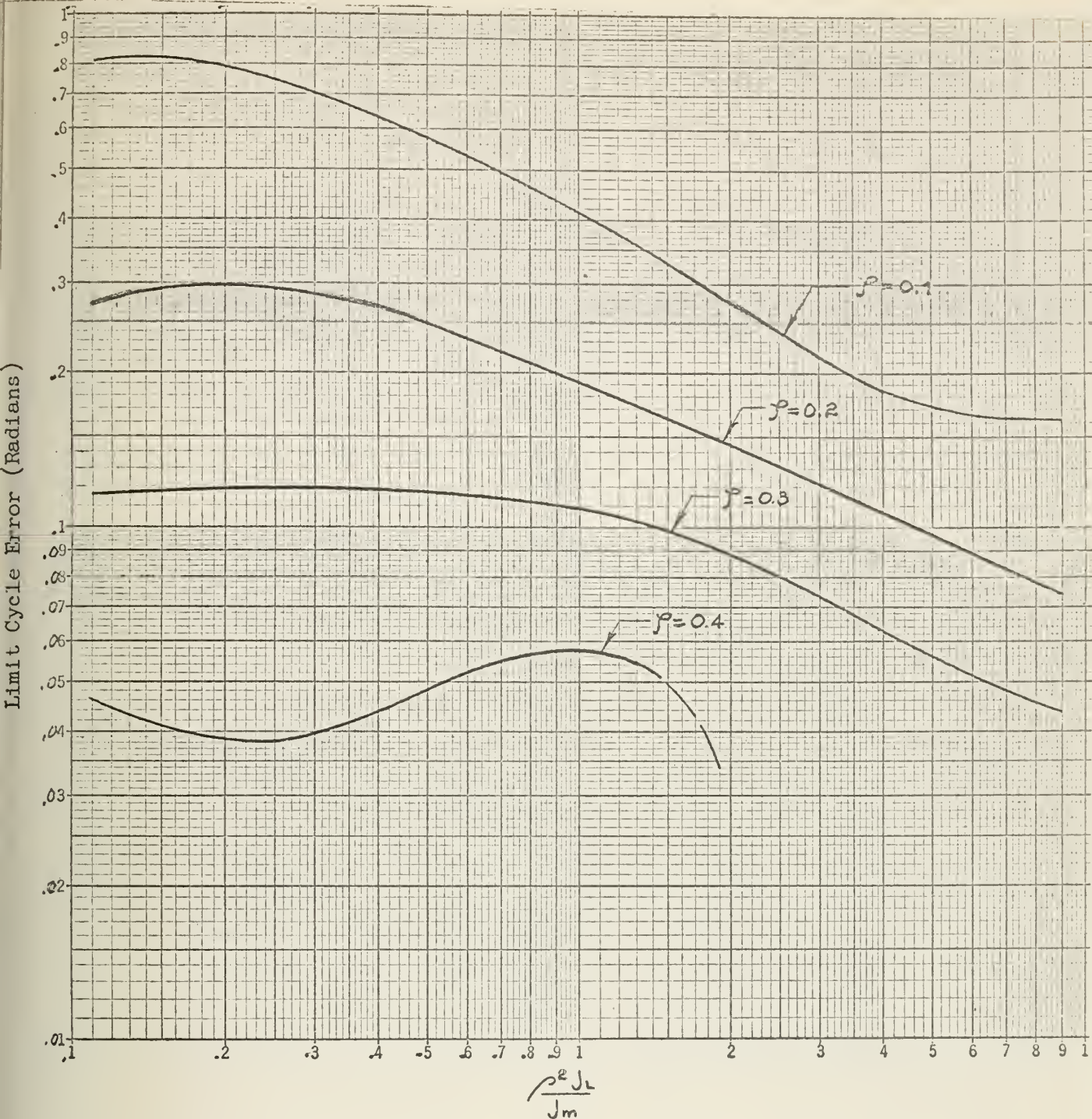


Fig. 5-14

Maximum Error of Limit Cycle from Unit Step Input

Limit Cycle Error (Radians)  $\left( \frac{0.3}{\Delta} \right)$  for  $\frac{\rho^2 J_L}{J_m}$  Variable

$$\frac{\rho^2 f_L}{F_T} = \frac{1}{\frac{f_m}{\rho^2 f_L} + 1} = 0.6$$

$$e = 0.6$$

No limit cycle exists for  $\rho \geq 0.5$





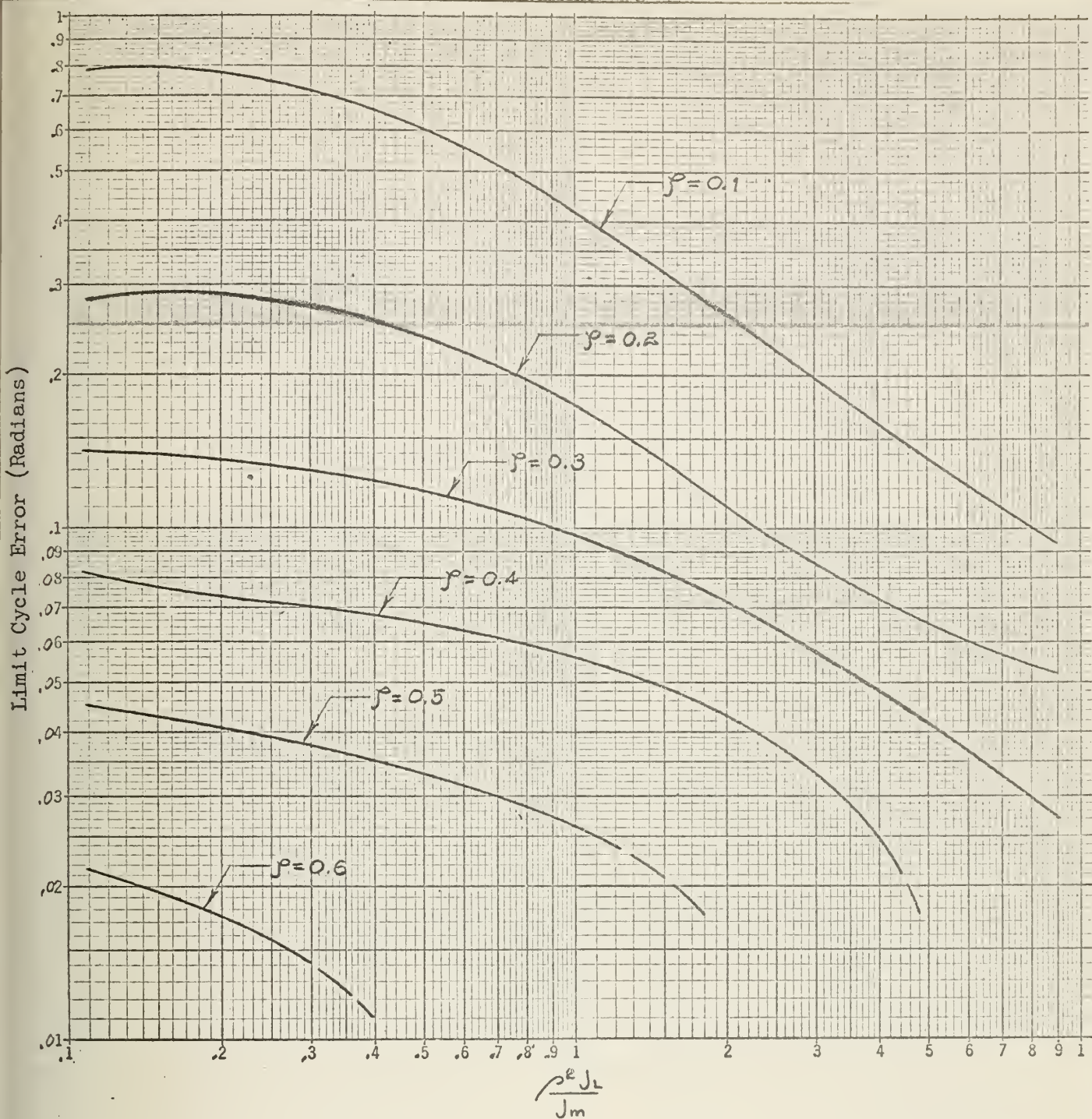


Fig. 5-15

Maximum Error of Limit Cycle from Unit Step Input

Limit Cycle Error (Radians)  $\left( \frac{0.3}{\Delta} \right)$  for  $\frac{\rho^2 J_L}{J_m}$  Variable

$$\frac{\rho^2 f_L}{F\tau} = \frac{1}{\frac{f_m}{\rho^2 f_L} + 1} = 0.8$$

$$e = 0.6$$

No limit cycle exists for  $\rho \geq 0.8$





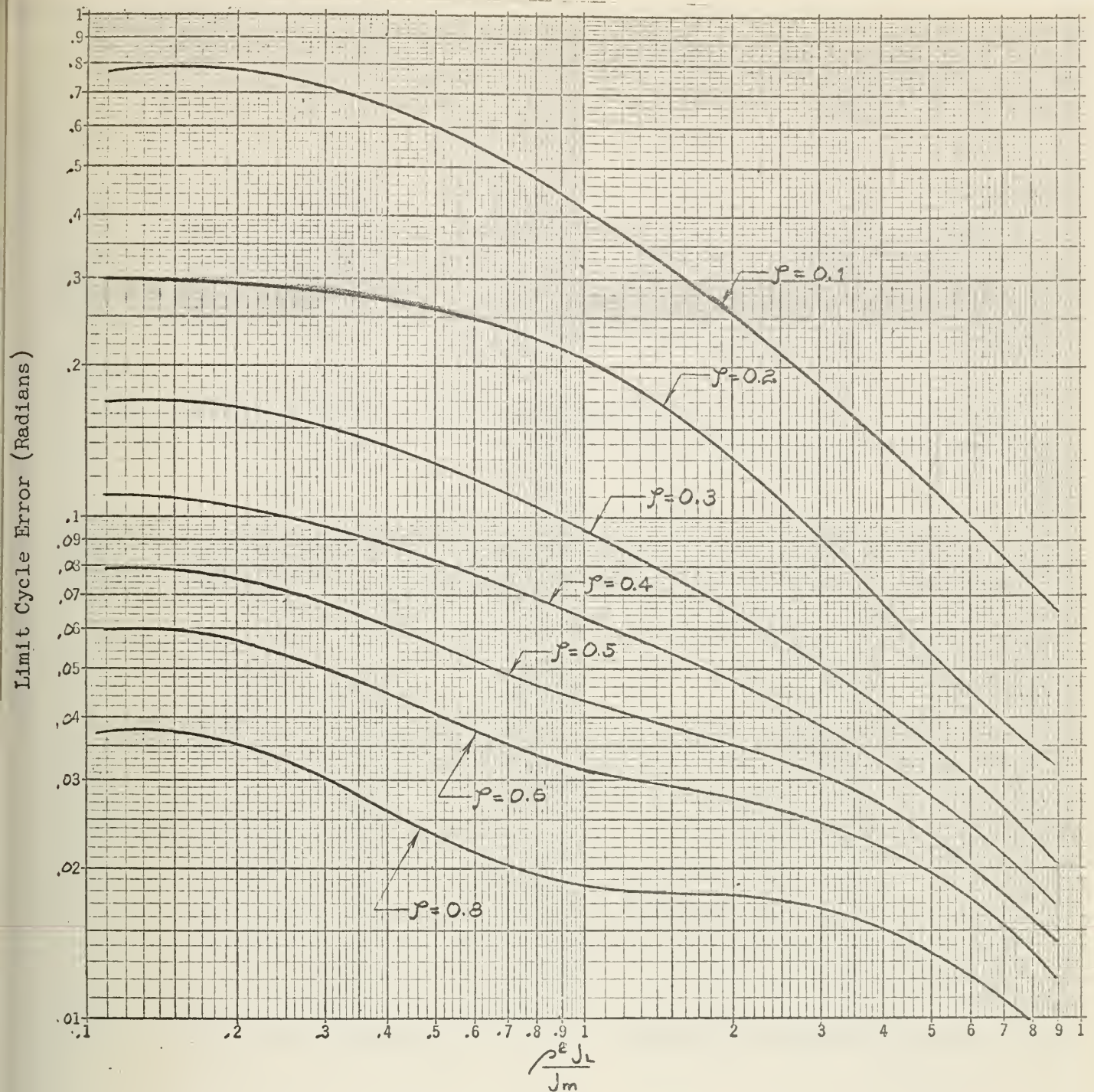


Fig. 5-16

Maximum Error of Limit Cycle from Unit Step Input

Limit Cycle Error (Radians)  $\left( \frac{0.3}{\Delta} \right)$  for  $\frac{\rho^2 J_L}{J_m}$  Variable

$$\frac{\rho^2 f_L}{F\tau} = \frac{1}{\frac{f_m}{\rho^2 f_L} + 1} = 1.0$$

$$e = 0.6$$

No limit cycle exists for  $\rho \geq 1.0$





Limit Cycle Error (Radians)

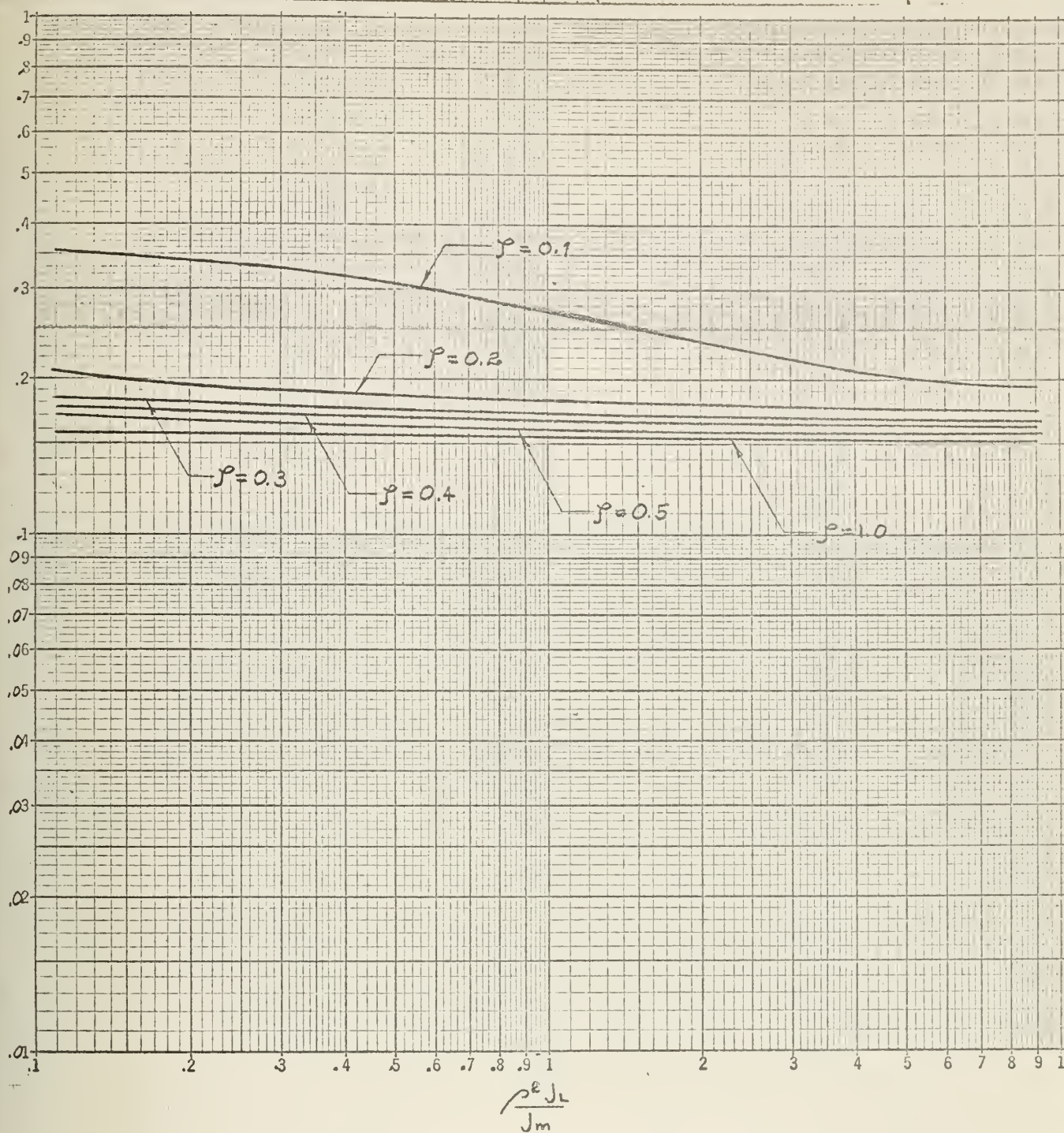


Fig. 5-17

Maximum Error of Limit Cycle from Unit Step Input

Limit Cycle Error (Radians)  $\left( \frac{0.3}{\Delta} \right)$  for  $\frac{\rho^2 J_L}{J_m}$  Variable

$$\frac{\rho^2 f_L}{F_T} = \frac{1}{\frac{f_m}{\rho^2 f_L} + 1} = 0$$

$$e = 0.8$$



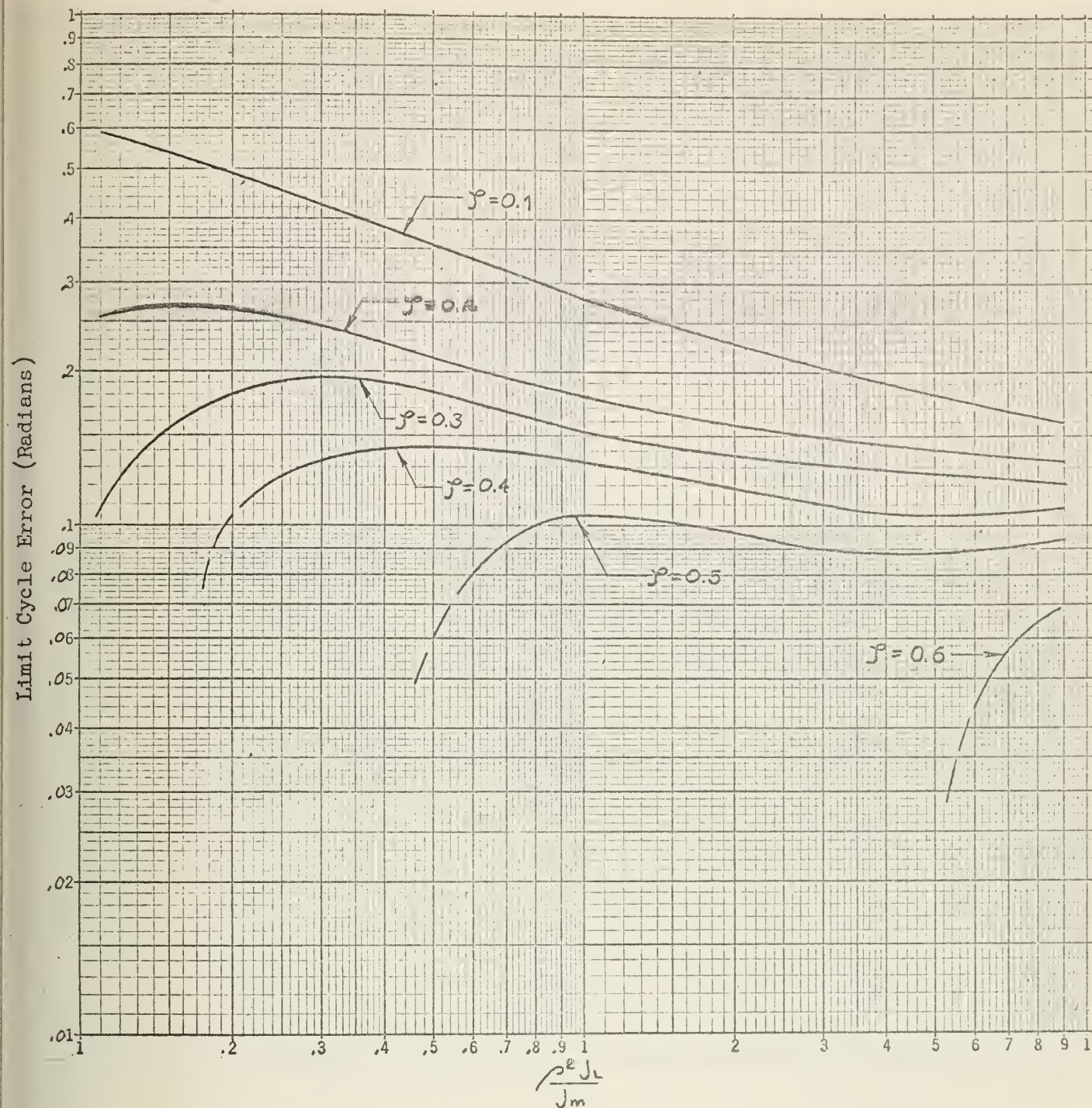


Fig. 5-18

Maximum Error of Limit Cycle from Unit Step Input

Limit Cycle Error (Radians)  $\left( \frac{0.3}{\Delta} \right)$  for  $\frac{\rho^2 J_L}{J_m}$  Variable

$$\frac{\rho^2 f_L}{F_T} = \frac{1}{\frac{f_m}{\rho^2 f_L} + 1} = 0.2$$

$$e = 0.8$$

No limit cycle exists for  $\gamma \geq 0.8$





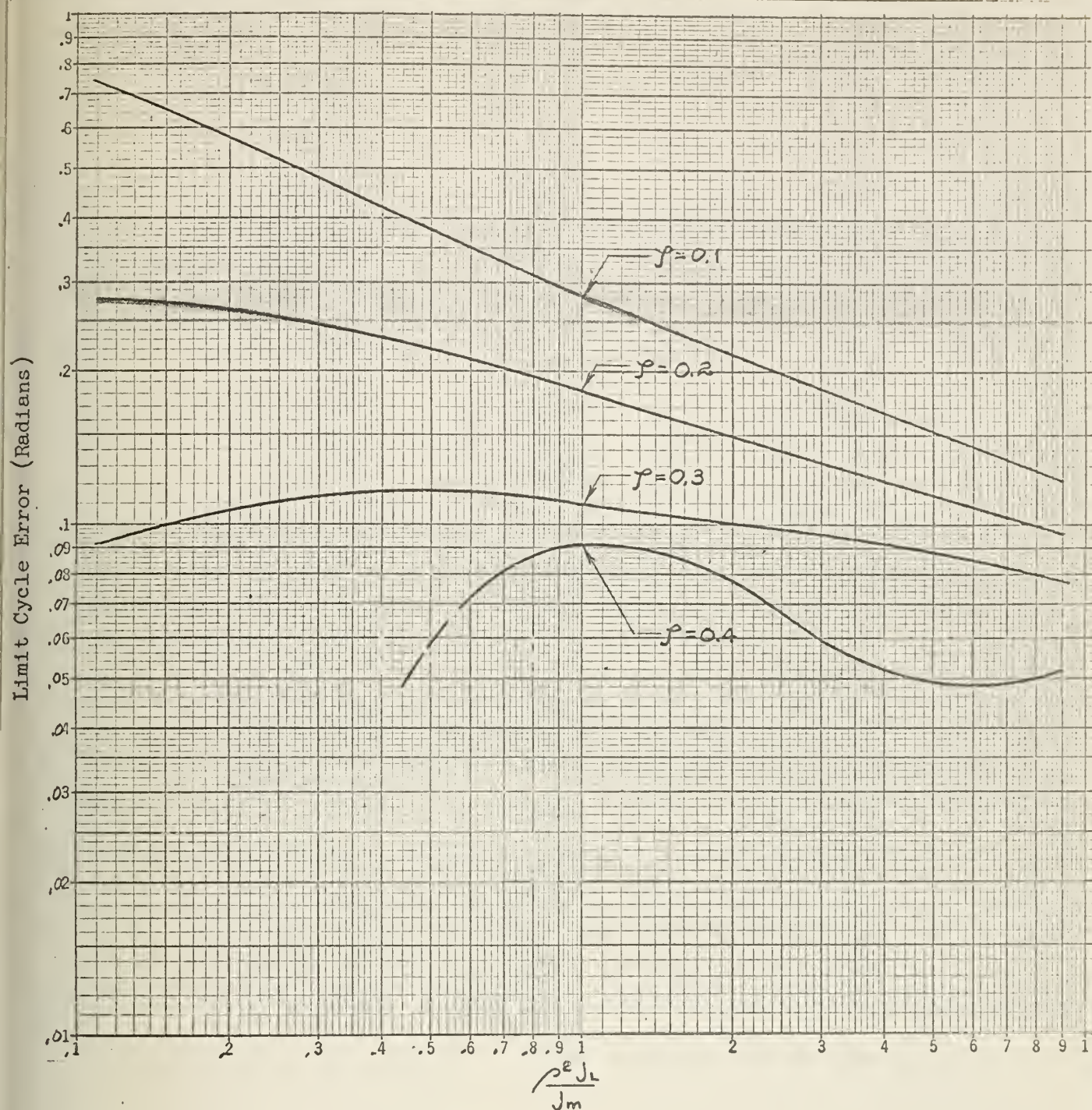


Fig. 5-19

Maximum Error of Limit Cycle from Unit Step Input

Limit Cycle Error (Radians)  $\left( \frac{0.3}{\Delta} \right)$  for  $\frac{\rho^2 J_L}{J_m}$  Variable

$$\frac{\rho^2 f_L}{F\tau} = \frac{1}{\frac{f_m}{\rho^2 f_L} + 1} = 0.4$$

$$e = 0.8$$

No limit cycle exists for  $\rho \geq 0.5$





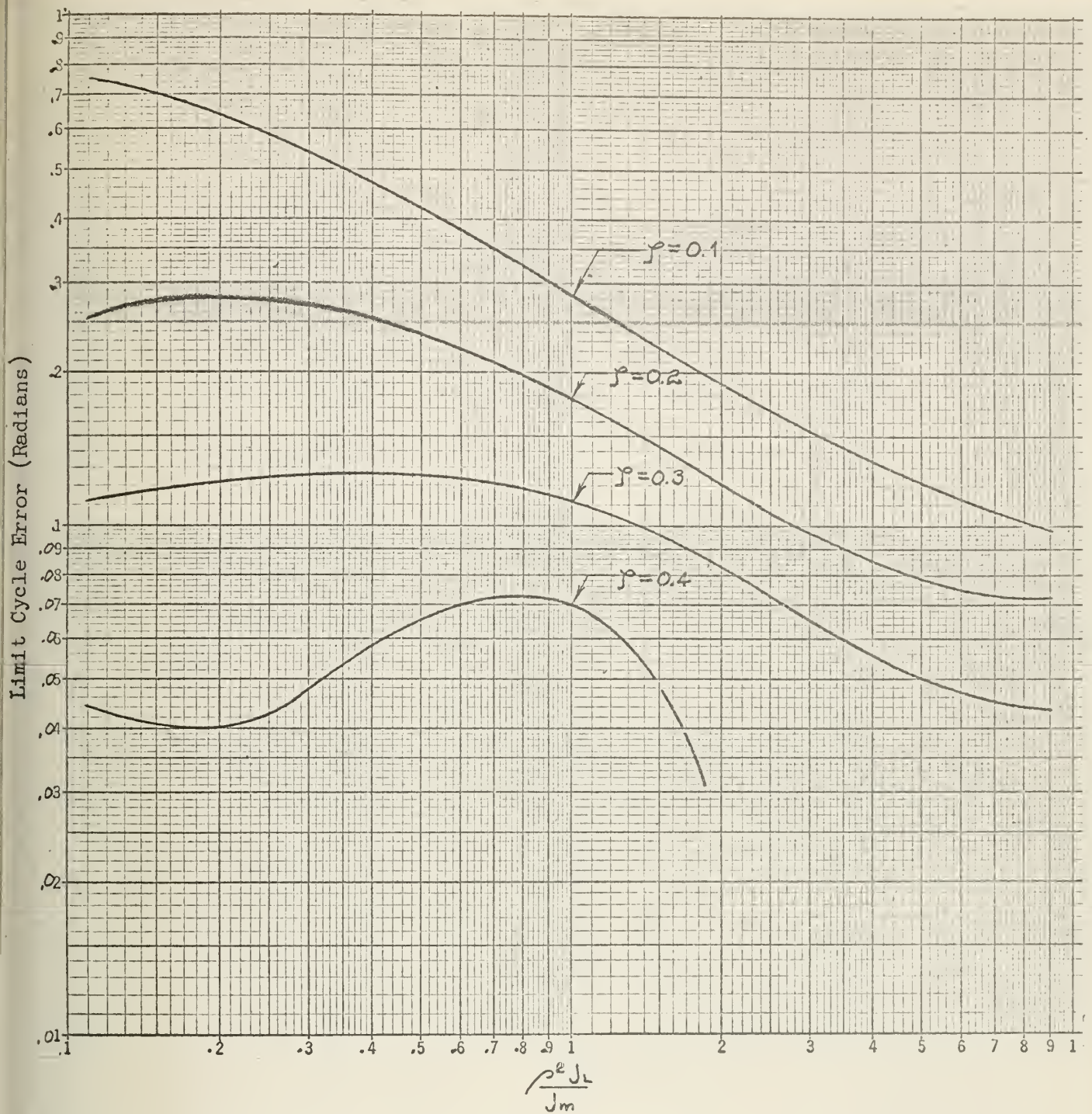


Fig. 5-20

Maximum Error of Limit Cycle from Unit Step Input

Limit Cycle Error (Radians)  $\left( \frac{0.3}{\Delta} \right)$  for  $\frac{\rho^2 J_L}{J_m}$  Variable

$$\frac{\rho^2 f_L}{F_T} = \frac{1}{\frac{f_m}{\rho^2 f_L} + 1} = 0.6$$

$$e = 0.8$$

No limit cycle exists for  $\gamma \geq 0.5$





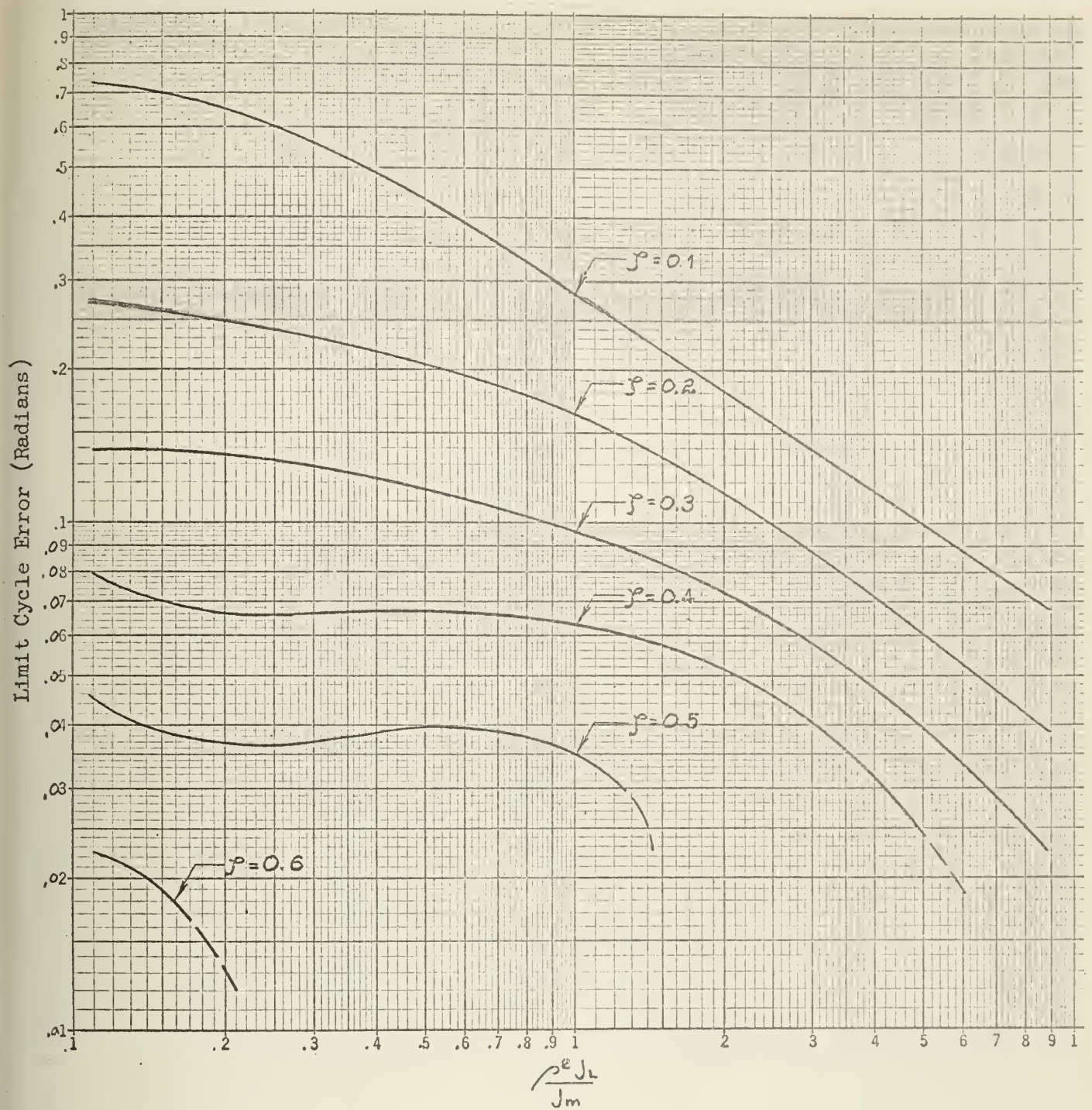


Fig. 5-21

Maximum Error of Limit Cycle from Unit Step Input

Limit Cycle Error (Radians)  $\left( \frac{0.3}{\Delta} \right)$  for  $\frac{\rho^2 J_L}{J_m}$  Variable

$$\frac{\rho^2 f_L}{F_T} = \frac{1}{\frac{f_m}{\rho^2 f_L} + 1} = 0.8$$

$$e = 0.8$$

No limit cycle exists for  $\gamma \geq 0.8$



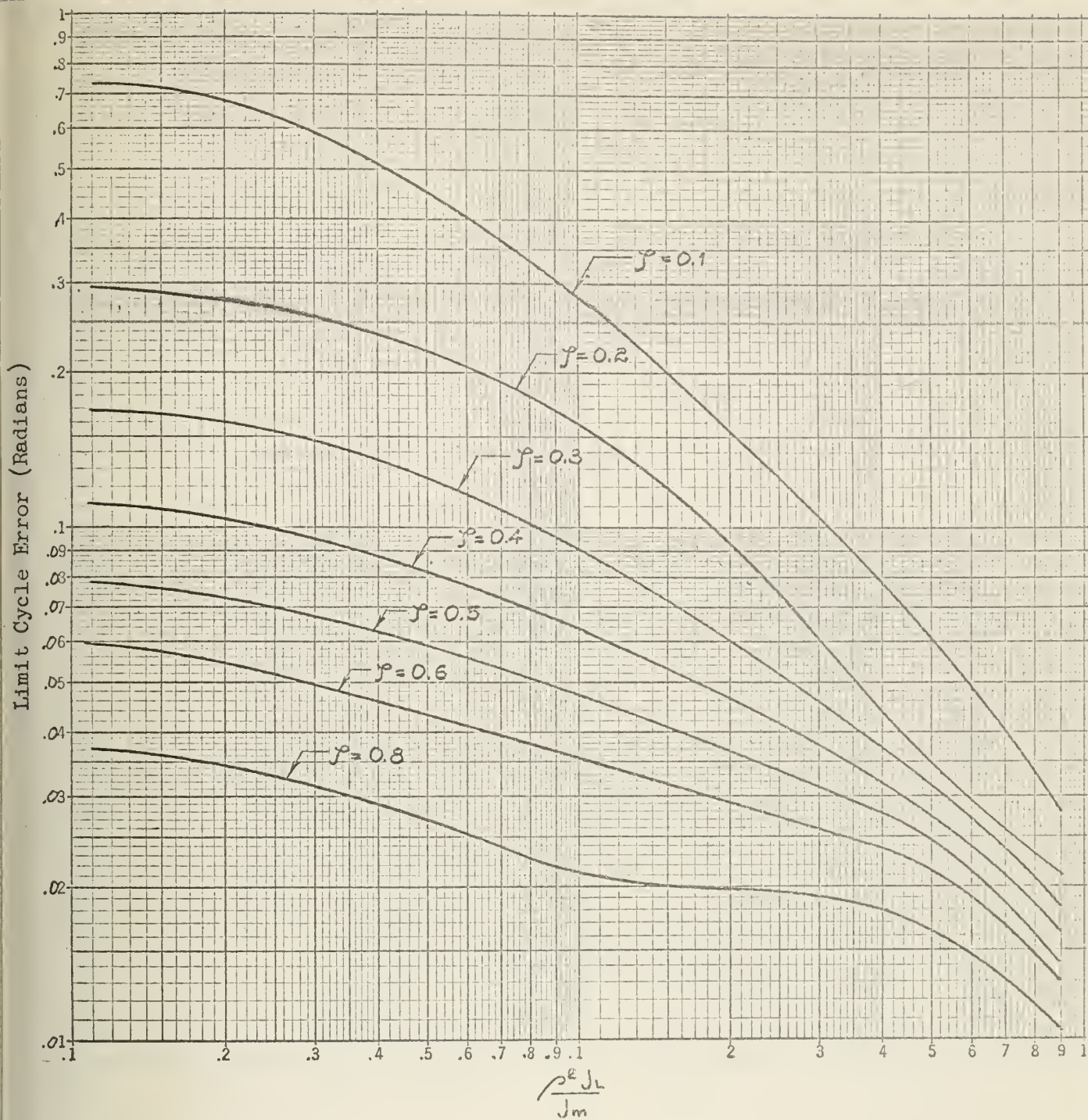


Fig. 5-22

Maximum Error of Limit Cycle from Unit Step Input

Limit Cycle Error (Radians)  $\left( \frac{0.3}{\Delta} \right)$  for  $\frac{\rho^2 J_L}{J_m}$  Variable

$$\frac{\rho^2 f_L}{F_T} = \frac{1}{\frac{f_m}{\rho^2 f_L} + 1} = 1.0$$

$$e = 0.8$$

No limit cycle exists for  $\gamma \geq 1.0$





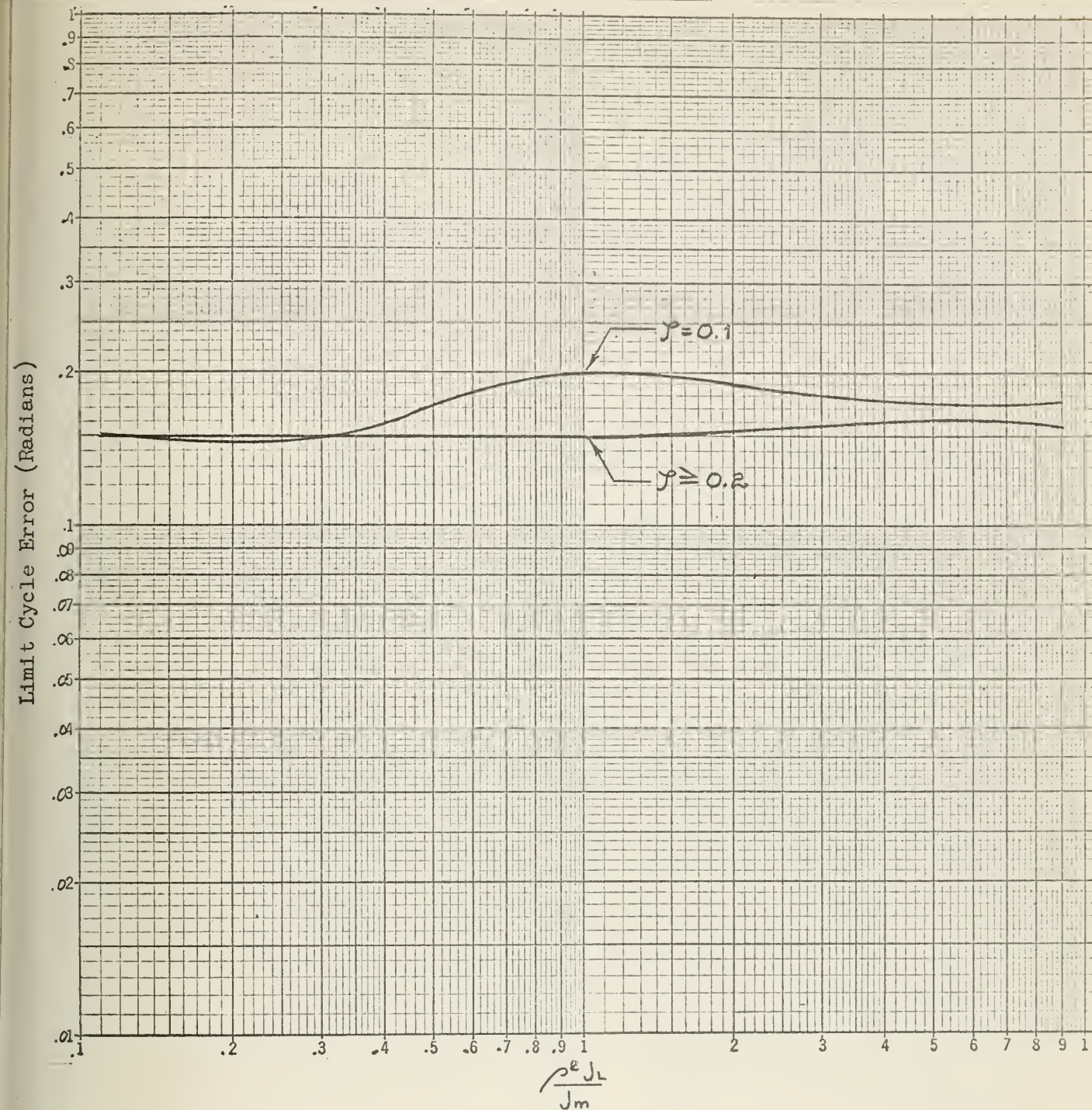


Fig. 5-23

Maximum Error of Limit Cycle from Unit Step Input

Limit Cycle Error (Radians)  $\left( \frac{0.3}{\Delta} \right)$  for  $\frac{\rho^2 J_L}{J_m}$  Variable

$$\frac{\rho^2 f_L}{F_T} = \frac{1}{\frac{f_m}{\rho^2 f_L} + 1} = 0$$

$$e = 1.0$$





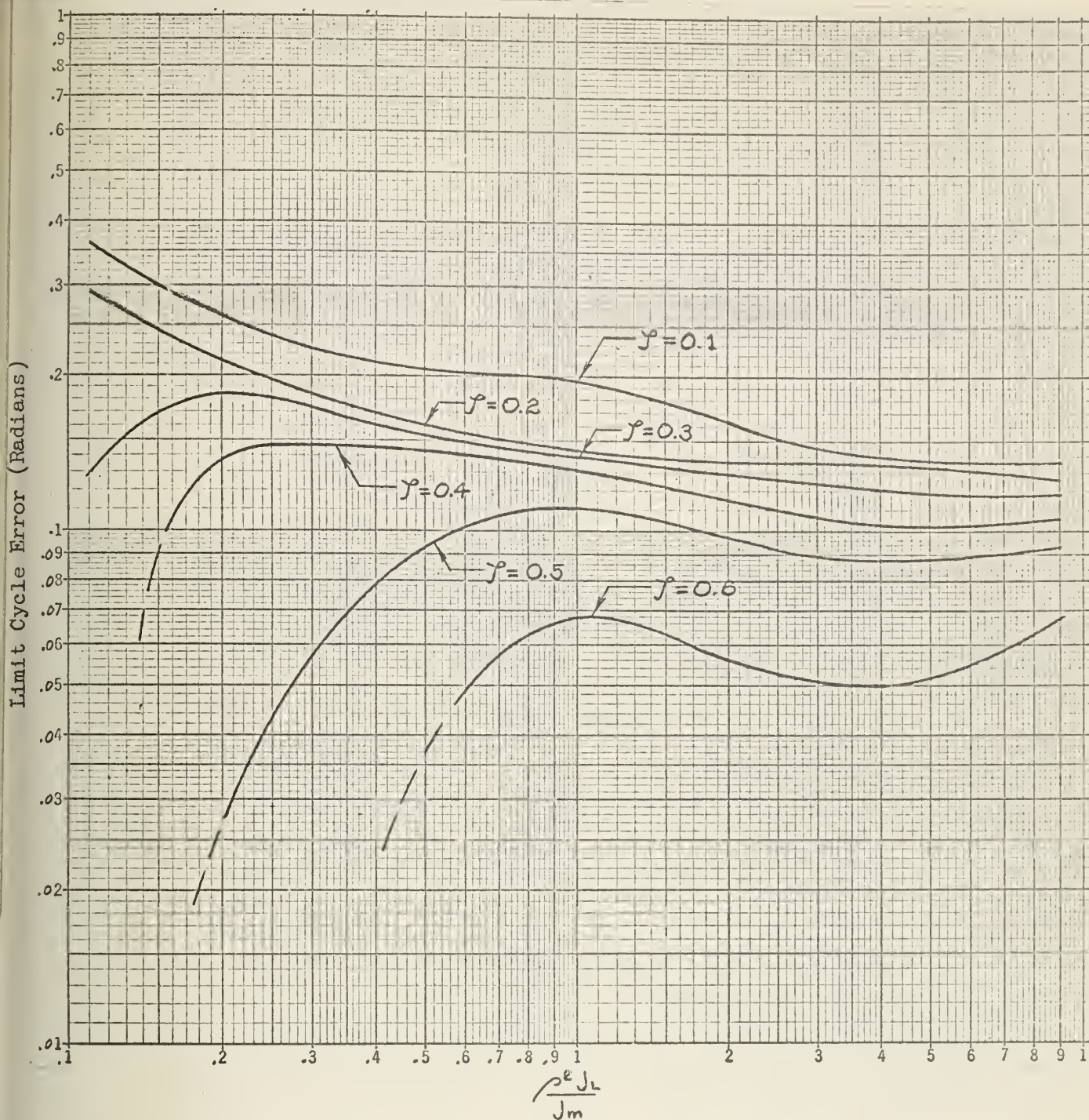


Fig. 5-24

Maximum Error of Limit Cycle from Unit Step Input

Limit Cycle Error (Radians)  $\left( \frac{0.3}{\Delta} \right)$  for  $\frac{\rho^2 J_L}{J_m}$  Variable

$$\frac{\rho^2 f_L}{F\tau} = \frac{1}{\frac{f_m}{\rho^2 f_L} + 1} = 0.2$$

$$e = 1.0$$

No limit cycle exists for  $\gamma \geq 0.8$





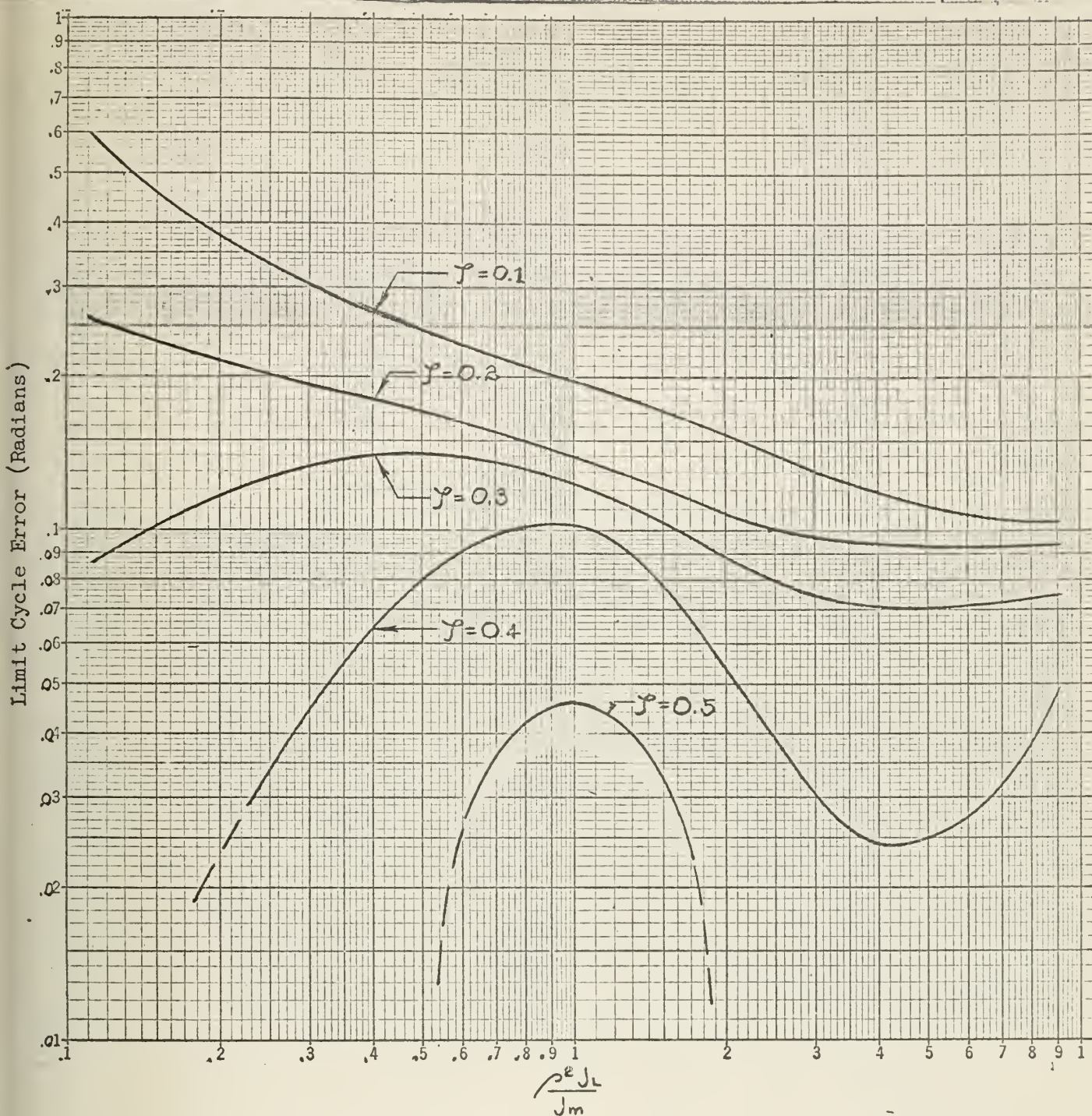


Fig. 5-25

Maximum Error of Limit Cycle from Unit Step Input

Limit Cycle Error (Radians)  $\left( \frac{0.3}{\Delta} \right)$  for  $\frac{\rho^2 J_L}{J_m}$  Variable

$$\frac{\rho^2 f_L}{F_T} = \frac{1}{\frac{f_m}{\rho^2 f_L} + 1} = 0.4$$

$$e = 1.0$$

No limit cycle exists for  $\gamma \geq 0.6$





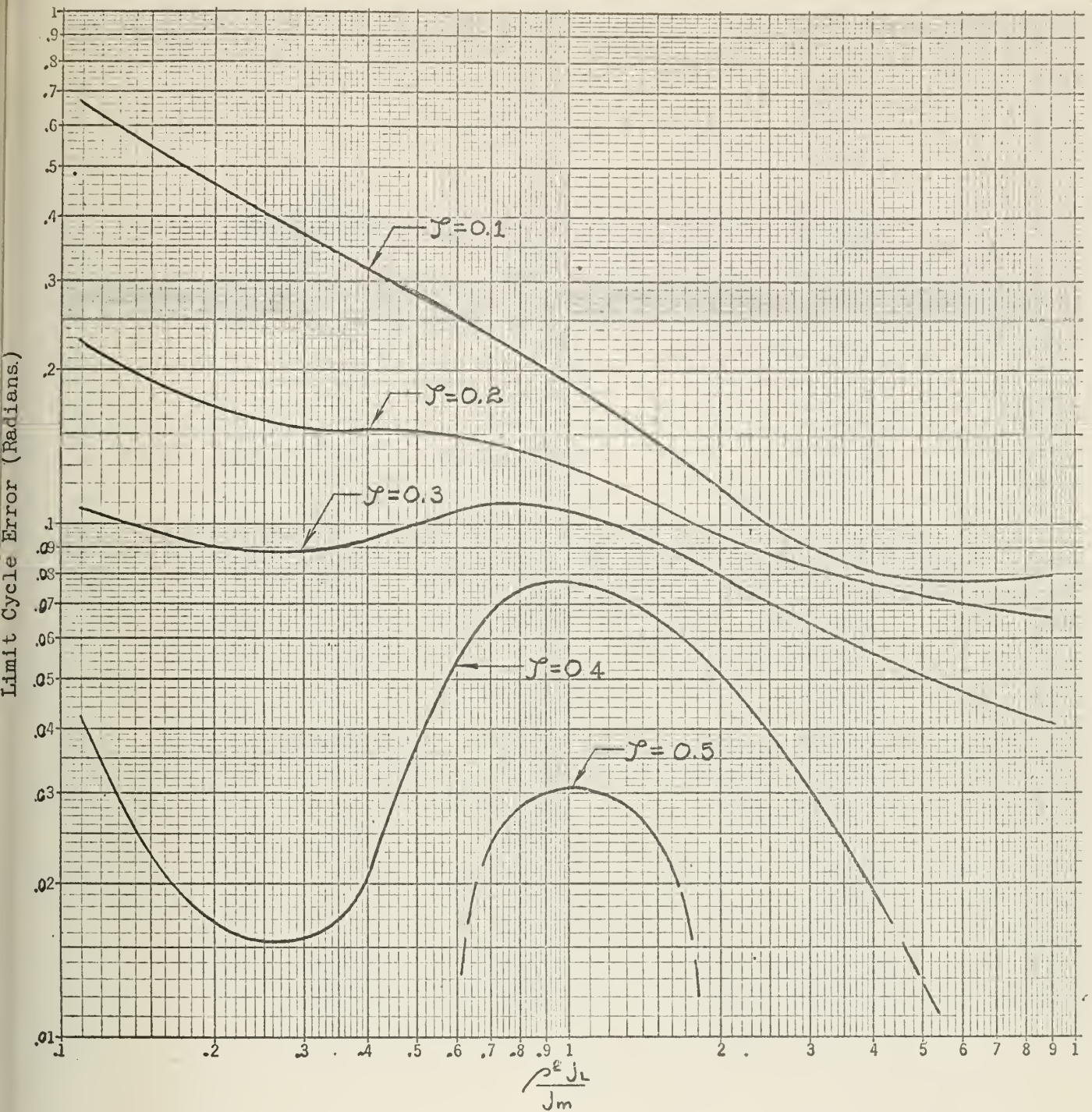


Fig. 5-26

Maximum Error of Limit Cycle from Unit Step Input

Limit Cycle Error (Radians)  $\left( \frac{0.3}{\Delta} \right)$  for  $\frac{\rho^2 J_L}{J_m}$  Variable

$$\frac{\rho^2 f_L}{F\tau} = \frac{1}{\frac{f_m}{\rho^2 f_L} + 1} = 0.6$$

$$e = 1.0$$

No limit cycle exists for  $\gamma \geq 0.6$





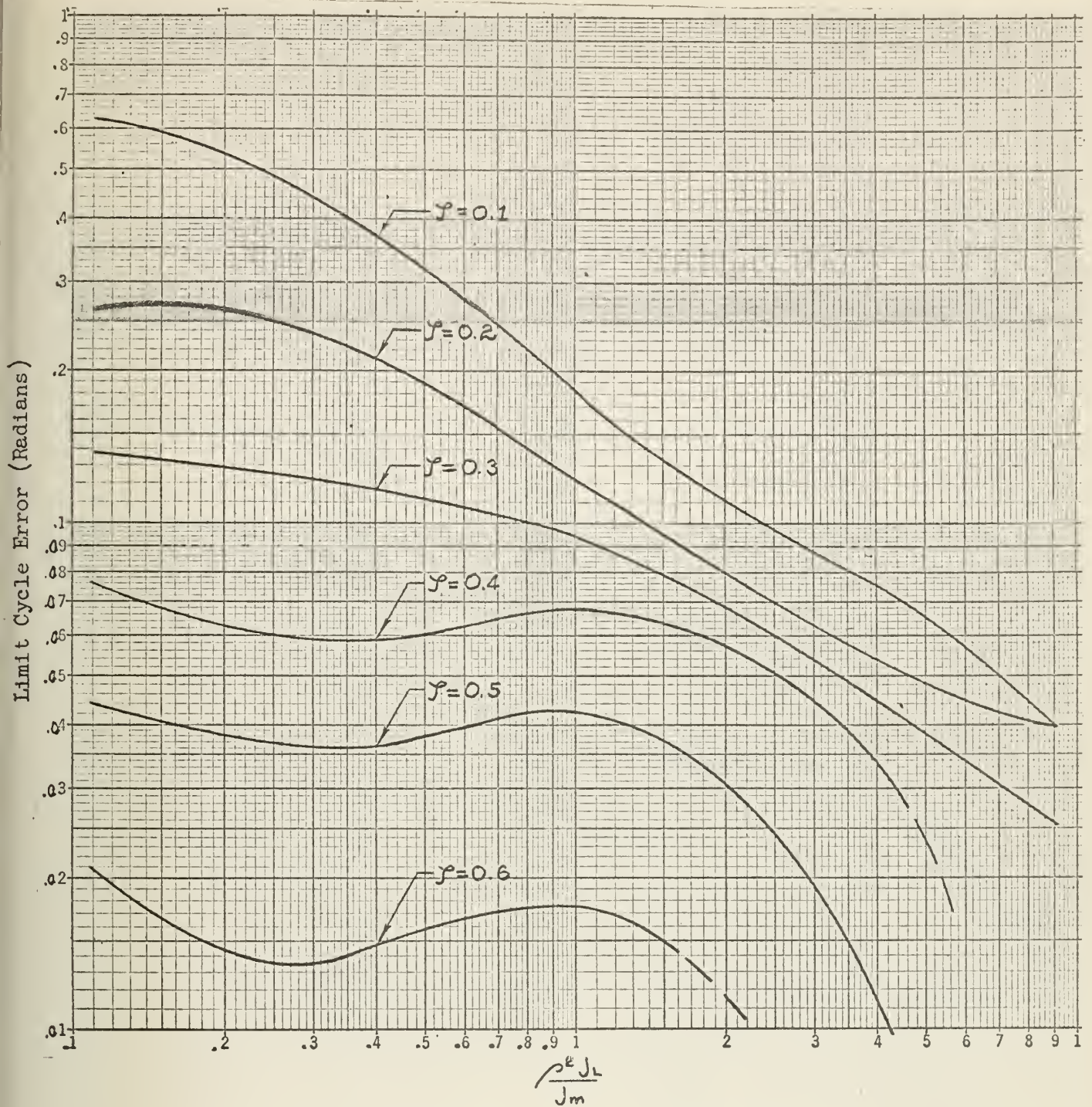


Fig. 5-27

Maximum Error of Limit Cycle from Unit Step Input

Limit Cycle Error (Radians)  $\left( \frac{0.3}{\Delta} \right)$  for  $\frac{\rho^2 J_L}{J_m}$  Variable

$$\frac{\rho^2 f_L}{F\tau} = \frac{1}{\frac{f_m}{\rho^2 f_L} + 1} = 0.8$$

$$e = 1.0$$

No limit cycle exists for  $\gamma \geq 0.8$





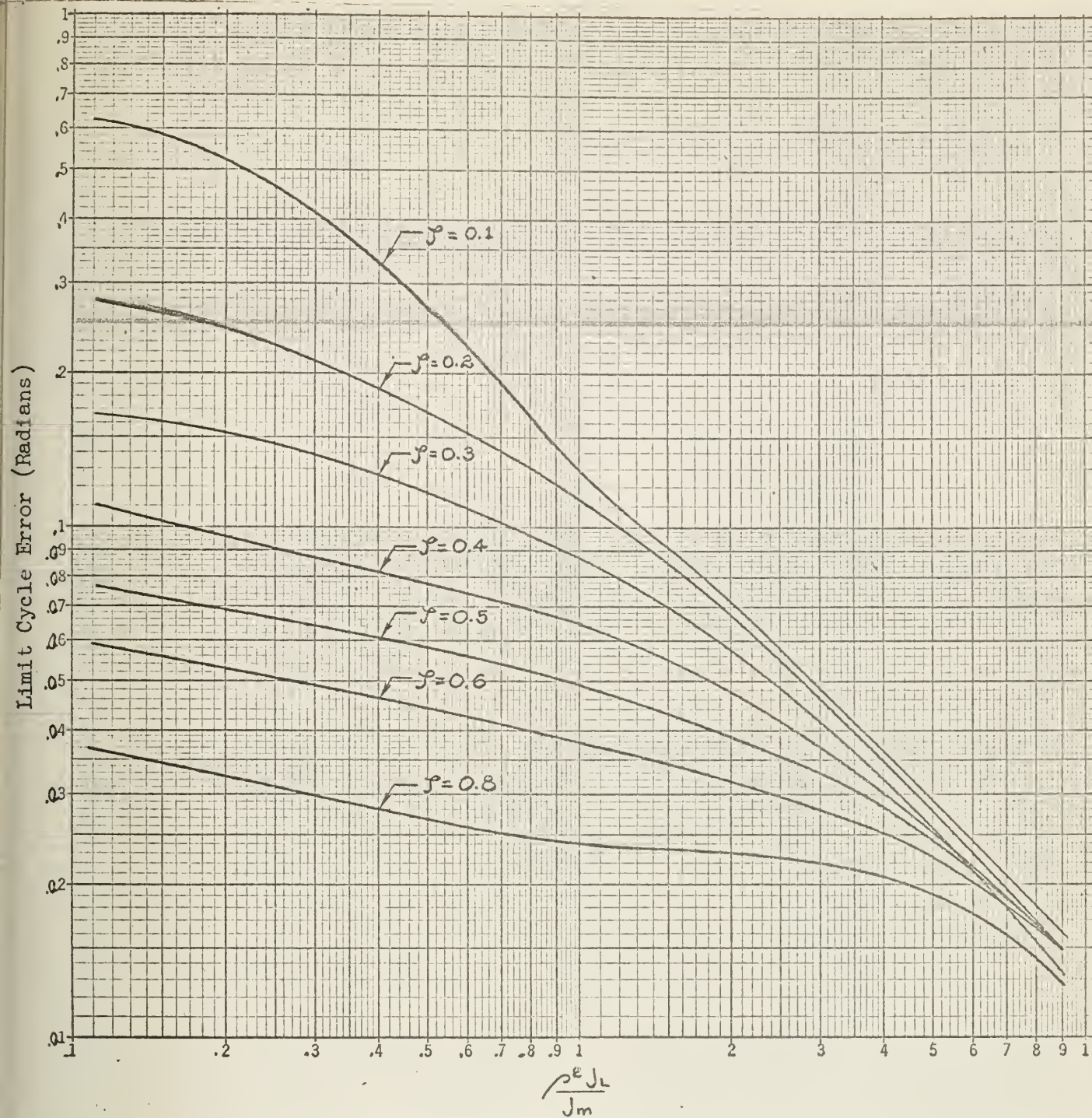


Fig. 5-28

Maximum Error of Limit Cycle from Unit Step Input

Limit Cycle Error (Radians)  $\left( \frac{0.3}{\Delta} \right)$  for  $\frac{\rho^2 J_L}{J_m}$  Variable

$$\frac{\rho^2 f_L}{F\tau} = \frac{1}{\frac{f_m}{\rho^2 f_L} + 1} = 1.0$$

$$e = 1.0$$

No limit cycle exists for  $\gamma \geq 1.0$

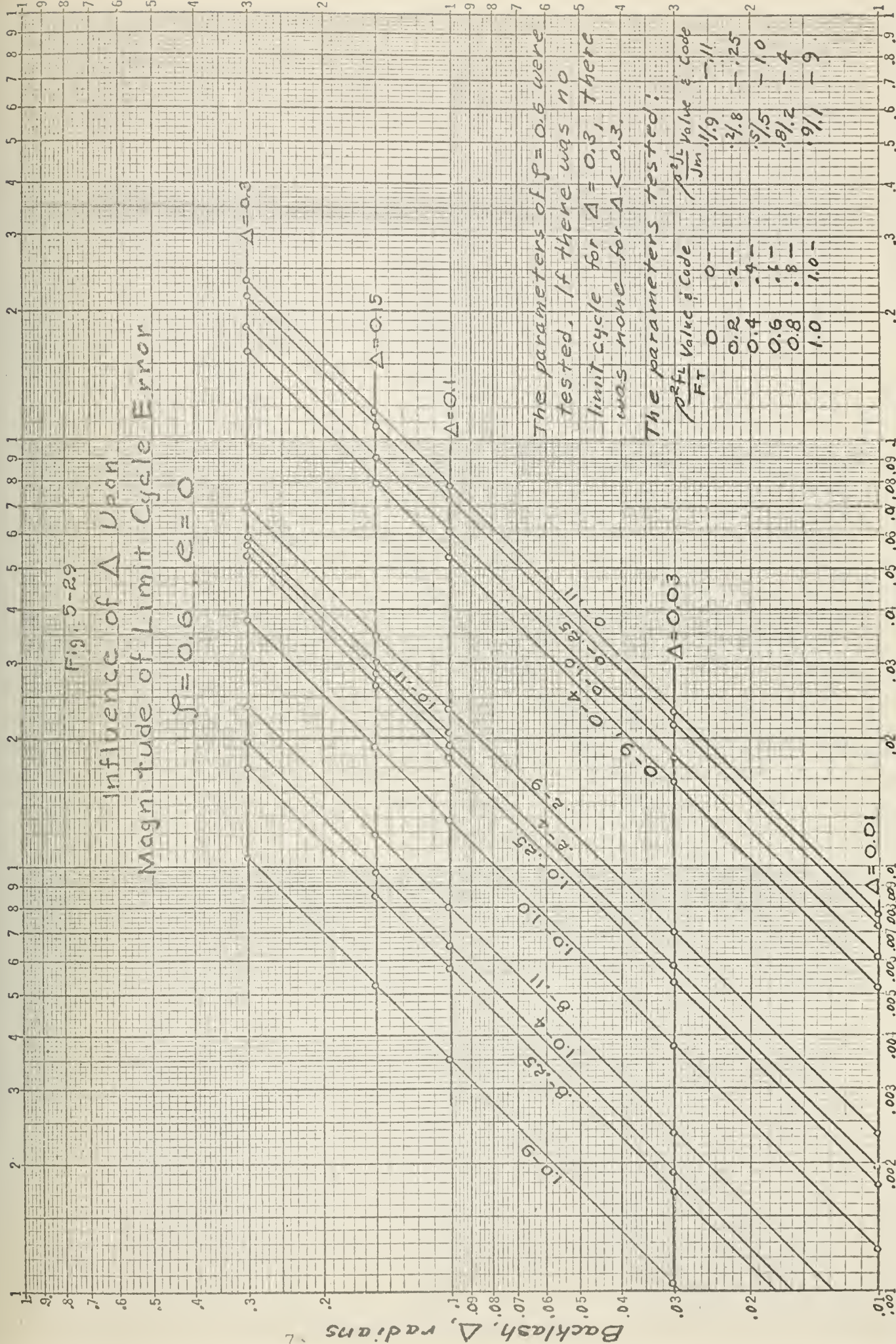




Fig. 5-29

# Influence of $\Delta$ Upon Magnitude of Limit Cycle Error

$p = 0.6, e = 0$



The parameters of  $p = 0.6$  were tested. If there was no limit cycle for  $\Delta = 0.3$ , there was none for  $\Delta < 0.3$ .

The parameters tested:

$\frac{\sigma^2 F_L}{F_T}$	Value & Code	$\frac{\sigma^2 F_L}{J_m}$	Value & Code
0	0	1/9	1/1
0.2	2	2/8	2/25
0.4	4	5/5	5/10
0.6	6	8/2	8/4
0.8	8	9/1	9/9
1.0	10		

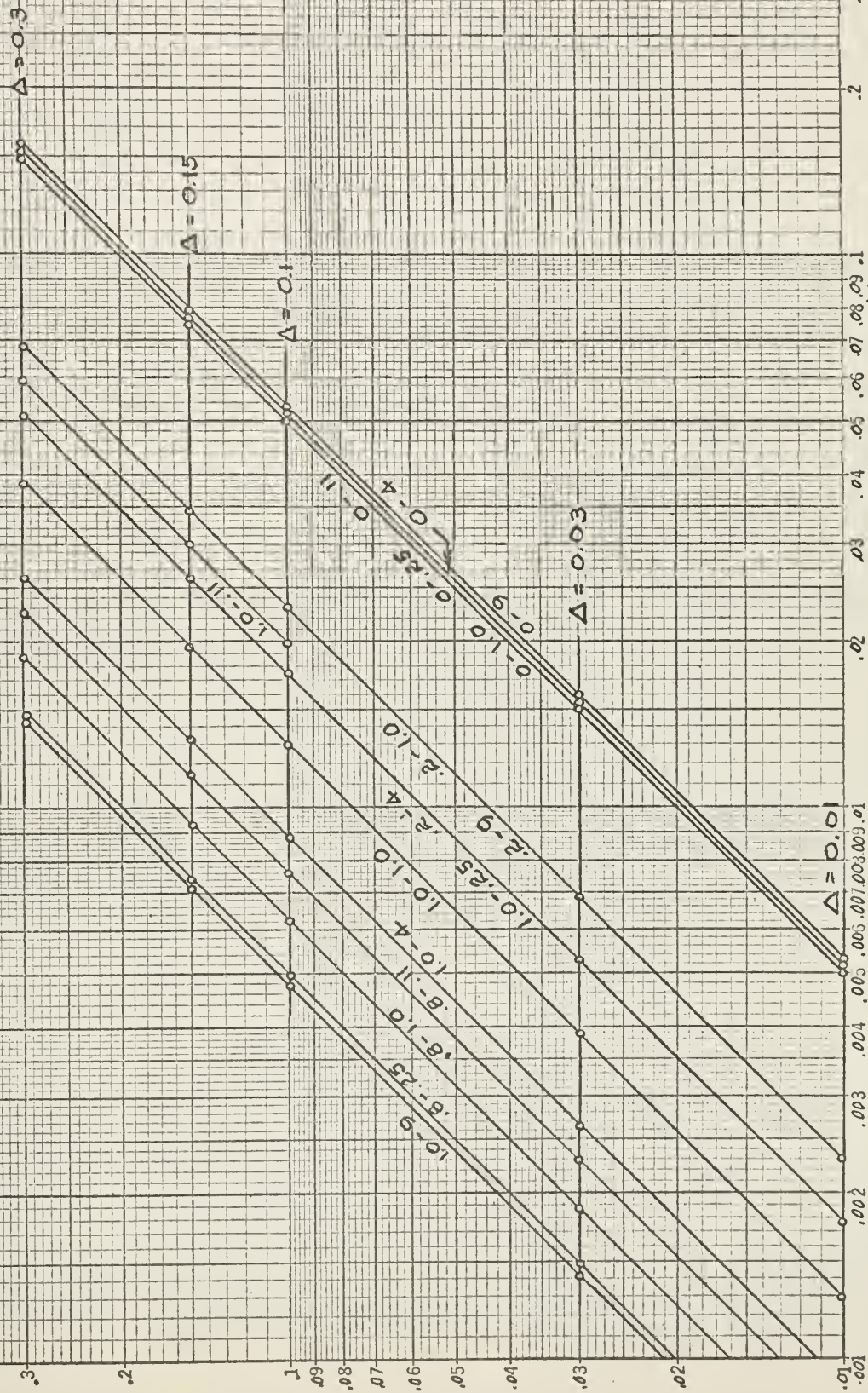
Limit Cycle Error, radians





Fig. 5-30

Influence of  $\Delta$  Upon  
Magnitude of Limit Cycle Error  
 $\rho=0.6, e=1.0$



Limit Cycle Error, radians





Fig. 5-31

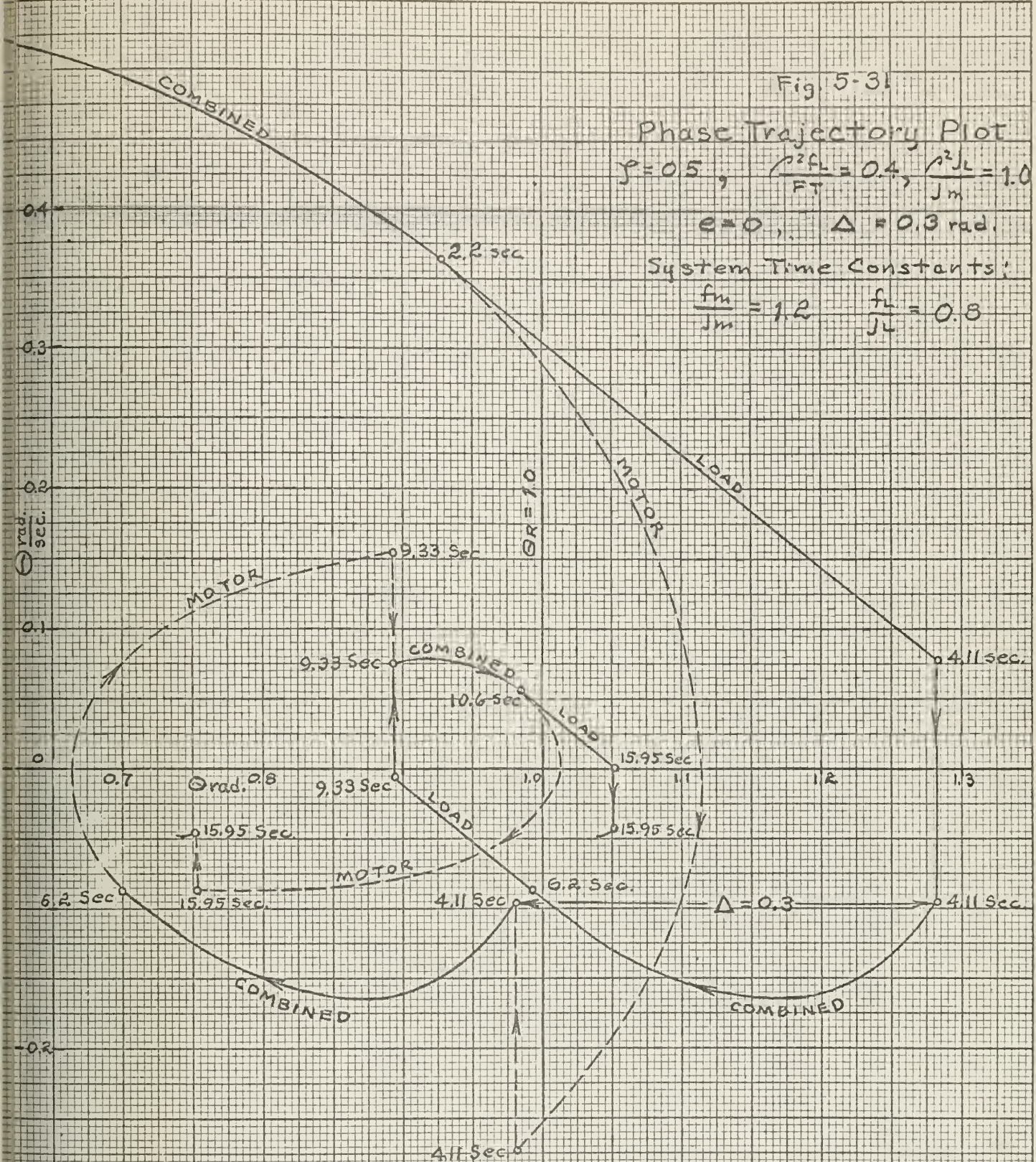
# Phase Trajectory Plot

$$\gamma = 0.5, \quad \frac{f_L^2}{F_T} = 0.4, \quad \frac{f_L^2}{J_m} = 1.0$$

$$e = 0, \quad \Delta = 0.3 \text{ rad.}$$

System Time Constants:

$$\frac{f_m}{J_m} = 1.2 \quad \frac{f_L}{J_L} = 0.8$$



Initial Conditions:

$$\Theta_R = 1.0$$

$$\Theta_c = \Theta_m = 0$$

$$\dot{\Theta}_c = \dot{\Theta}_m = 0$$

Steady State Error = 0  
(No limit cycle resulted)

See Figs. 5-1 and 5-7





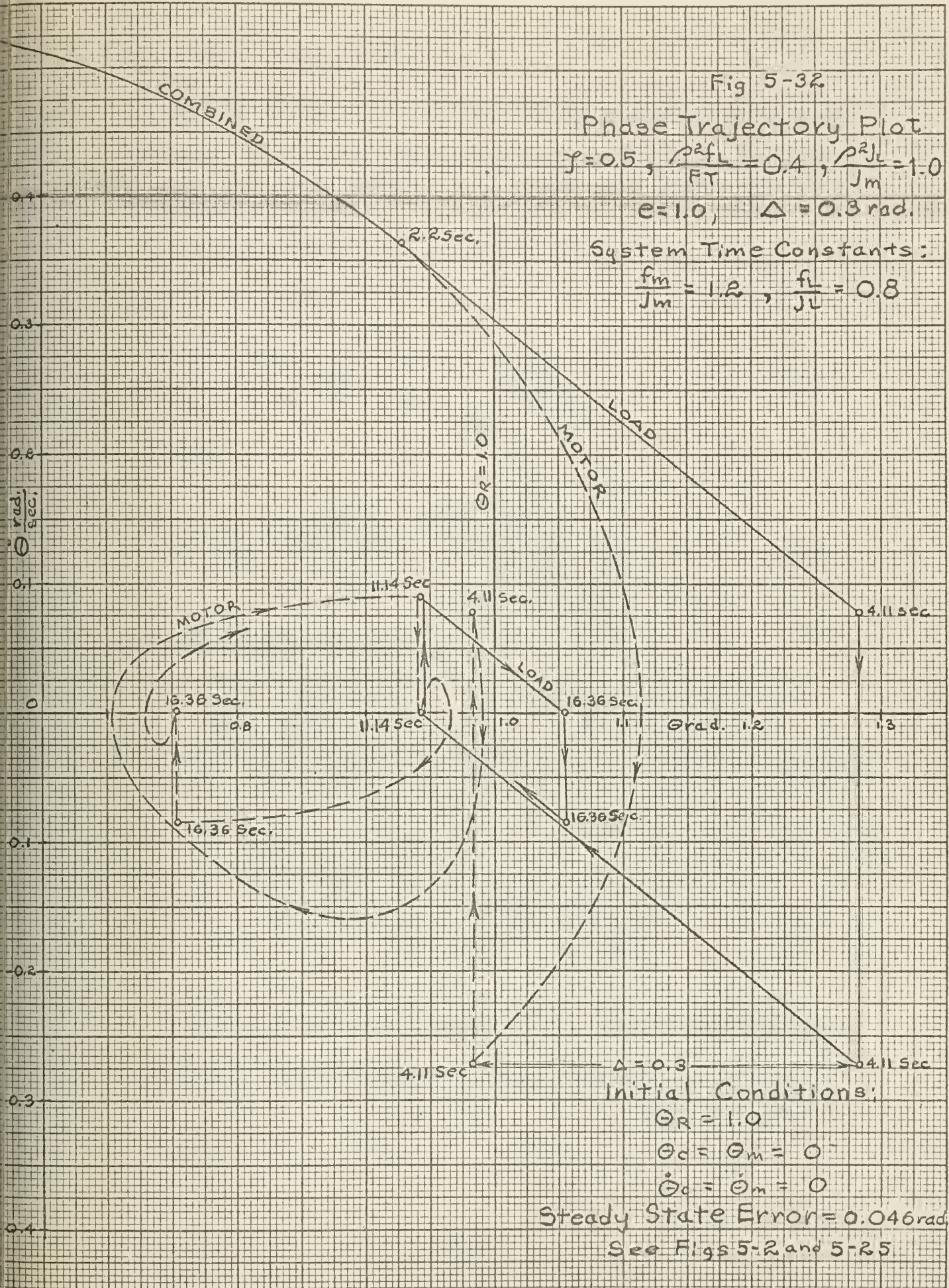
Fig 5-32

Phase Trajectory Plot  
 $\gamma = 0.5$ ,  $\frac{p^2 f_L}{F_T} = 0.4$ ,  $\frac{p^2 J_L}{J_m} = 1.0$

$e = 1.0$ ,  $\Delta = 0.3 \text{ rad.}$

System Time Constants:

$\frac{f_m}{J_m} = 1.2$ ,  $\frac{f_L}{J_L} = 0.8$



Initial Conditions:

$\Theta_R = 1.0$

$\Theta_c = \Theta_m = 0$

$\dot{\Theta}_c = \dot{\Theta}_m = 0$

Steady State Error = 0.046 rad.

See Figs 5-2 and 5-25





## 6. APPLICATION OF RESULTS

In this section, the results are applied to hypothetical physical systems. Methods are indicated by which physical systems may be analyzed or designed.

It is desirable to find an equation relating certain system variables, therefore the equations:

$$\omega_n^2 = \frac{p K}{J_m + p^2 J_L} = \frac{p K}{J_m} \left[ \frac{1}{1 + p^2 \frac{J_L}{J_m}} \right] \quad (6-1)$$

and

$$2 \zeta \omega_n = \frac{f_m + p^2 f_L}{J_m + p^2 J_L} = \frac{p^2 f_L \left[ \frac{f_m}{p^2 f_L} + 1 \right]}{J_m \left[ 1 + p^2 \frac{J_L}{J_m} \right]} \quad (6-2)$$

will be manipulated to the form

$$\zeta = \frac{1}{2} p \frac{p^2 f_L}{J_m} \frac{\left[ \frac{f_m}{p^2 f_L} + 1 \right]}{\left[ 1 + p^2 \frac{J_L}{J_m} \right]} \frac{\sqrt{\frac{1}{J_m}} \sqrt{1 + p^2 \frac{J_L}{J_m}}}{\sqrt{p} \sqrt{K}} \quad (6-3)$$

or

$$= \frac{1}{2} f_L \left[ \frac{f_m}{p^2 f_L} + 1 \right] \left[ \frac{p^3}{J_m K \left( 1 + p^2 \frac{J_L}{J_m} \right)} \right]^{1/2} \quad (6-4)$$

In view of the form of Equation 6-4 for  $\zeta$  and recalling that the variable parameters used on the figures were  $p^2 \frac{J_L}{J_m}$  and  $p^2 \frac{f_L}{f_T} =$





$$\frac{\rho^2 f_L}{f_m + \rho^2 f_L} = \frac{1}{\frac{f_m}{\rho^2 f_L} + 1} \quad \text{it is seen that the expression for } \zeta$$

in fact includes the other two variable parameters.

The value of overshoot and hence limit cycle are not affected by  $\omega_n$ ; however, the time and velocity are scaled for  $\omega_n \neq 1.0$ . Thus the transient response characteristics may be related to the same parameters used in these applications.

If a motor and load are selected for a system and the limitation is imposed that system operation shall not result in a limit cycle, Equation 6-4 and the limit cycle existence charts may be used to determine the unspecified system parameters  $\zeta$ ,  $K$  and  $\rho$ . The coefficient of restitution for the proposed gear train material must also be determined.

To proceed, select a value of  $K$  and  $\rho$ , then determine the value of  $\zeta$  from Equation 6-4. Enter the limit cycle existence chart for the value of  $e$ , system  $\zeta$  and the parameters  $\rho^2 \frac{J_L}{J_m}$  and

$$\frac{1}{\frac{f_m}{\rho^2 f_L} + 1}$$

Determine if the selected parameters describe a point of no limit cycle. Since limit cycle existence is independent of backlash ( $\Delta = 0$  excluded), backlash is not a variable parameter. Successive trial



values of the unspecified parameters may be required to meet the limitation of no limit cycle. If it is also required that certain transient response characteristics be met, these conditions could be examined by a similar method.

In the event that no acceptable parameters are found to satisfy the system requirements for no limit cycle, the figures for limit cycle size may be examined to obtain a minimum size limit cycle. The method of solution is similar to that previously described.

Example: The material intended for use in the gears has an  $e = 0.6$ . The motor and load have the parameters  $f_m = 0.64$ ,  $J_m = 0.25$ ,  $f_L = 0.64$ ,  $J_L = 1.0$  and it desired that the system operate with no limit cycle. If the values are selected  $K = 4.0$ ,  $p = 0.5$ , the values

$$p^2 \frac{J_L}{J_m} = 1.0 \quad \text{and} \quad \frac{f_m}{p^2 f_L} = 4.0, \quad \frac{1}{\frac{f_m}{p^2 f_L} + 1} = 0.2 \text{ result.}$$

Solve Equation 6-4 for  $\zeta = .5 \left( \frac{.5}{.25 (4) (1+1)} \right)^{3/2}$ , thus  $\zeta = 0.4$ . Enter the chart for limit cycle existence, Fig. 5-1,

$$e = 0.6, \zeta = 0.4, \quad \frac{1}{\frac{f_m}{p^2 f_L} + 1} = 0.2, \quad p^2 \frac{J_L}{J_m} = 1.0$$

It can be seen that limit cycle will exist for these parameters.

Since  $K$  is most easily varied in equation 6-4, a new  $K$  is selected at 1.0 in an effort to find parameters for no limit cycle. It is seen

$$\text{that } \zeta_{K=1.0} = \zeta_{K=4.0} \sqrt{\frac{4}{1}} = 0.4 \quad (2)$$



with all other parameters constant, thus  $\zeta = 0.8$  Enter Fig. 5-1

with  $e = 0.6$

$$\zeta = 0.8 \quad \rho^2 \frac{J_L}{J_m} = 1.0 \quad \frac{1}{\frac{f_m}{\rho^2 f_L} + 1} = 0.2$$

These parameters describe system operation with no limit cycle and are well within the area limits. The transient response of this system may be undesirable and various combinations of  $\rho$  and  $K$  would have to be tested to satisfy the additional requirements of the problem. It will be restated that the existence areas of Figs. 5-1 and 5-2 are not exact.

The figures of limit cycle size may be used in the same manner as the existence charts. The same parameters of the first case are

$$\text{assumed: } k = 4.0, \quad \rho = 0.5, \quad \rho^2 \frac{J_L}{J_m} = 1.0, \quad \frac{1}{\frac{f_m}{\rho^2 f_L} + 1} = 0.2$$

$$\zeta = 0.4$$

$e = 0.6, \Delta = 0.1$  radians. Enter Fig. 5-12 with the parameters given.

The ordinate, Limit Cycle Error  $\frac{(0.3)}{\Delta} = 0.13$  radians, is obtained.

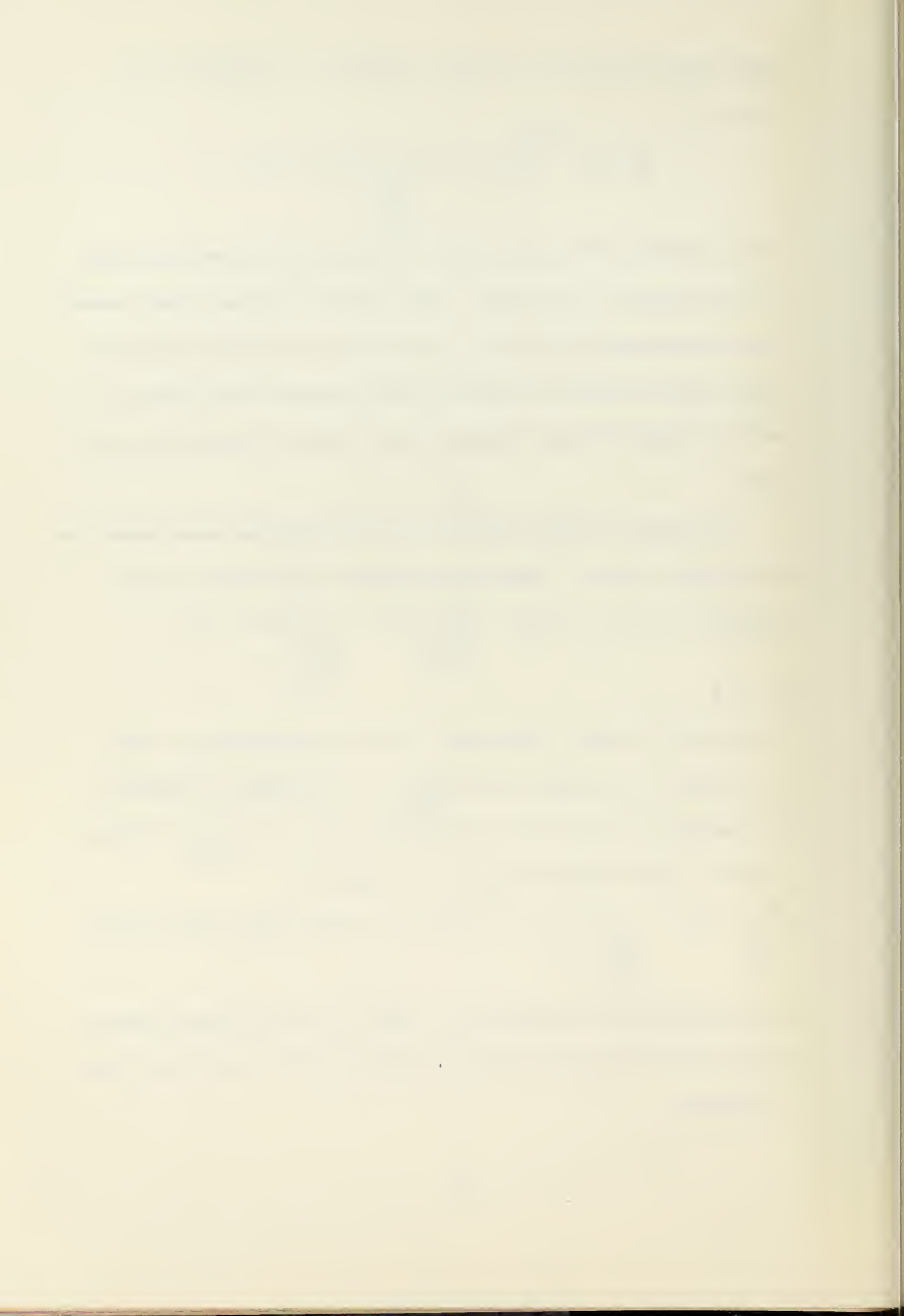
The maximum positive error in the limit cycle  $= 0.13 \frac{(0.1)}{0.3} = 0.0434$

radians. Enter the same figure for  $e = 0.6, \zeta = 0.8$

$$\rho^2 \frac{J_L}{J_m} = 1.0, \quad \frac{1}{\frac{f_m}{\rho^2 f_L} + 1} = 0.2, \quad \Delta = 0.5 \text{ radians; this is the second}$$

case of examination for existence. No  $\zeta = 0.8$  curve exists; hence no limit cycle exists for this choice of parameters for any nominal value of backlash.





## 7. TRANSIENT RESPONSE CHARACTERISTICS, PLASTIC IMPACT

The effects of backlash on the transient response to a step displacement input is also of interest, so a relatively exhaustive study was made of the plastic impact case. The characteristics of interest are the peak overshoot,  $M_{pt}$ , the settling time and the peak time. Of these, the peak overshoot,  $M_{pt}$ , produced the most satisfactory pattern with the result that data charts and equations have been prepared to assist in analysis and design. Settling time and peak time were much less satisfactory to work with. The results obtained to date are presented here, but more work remains to be done.

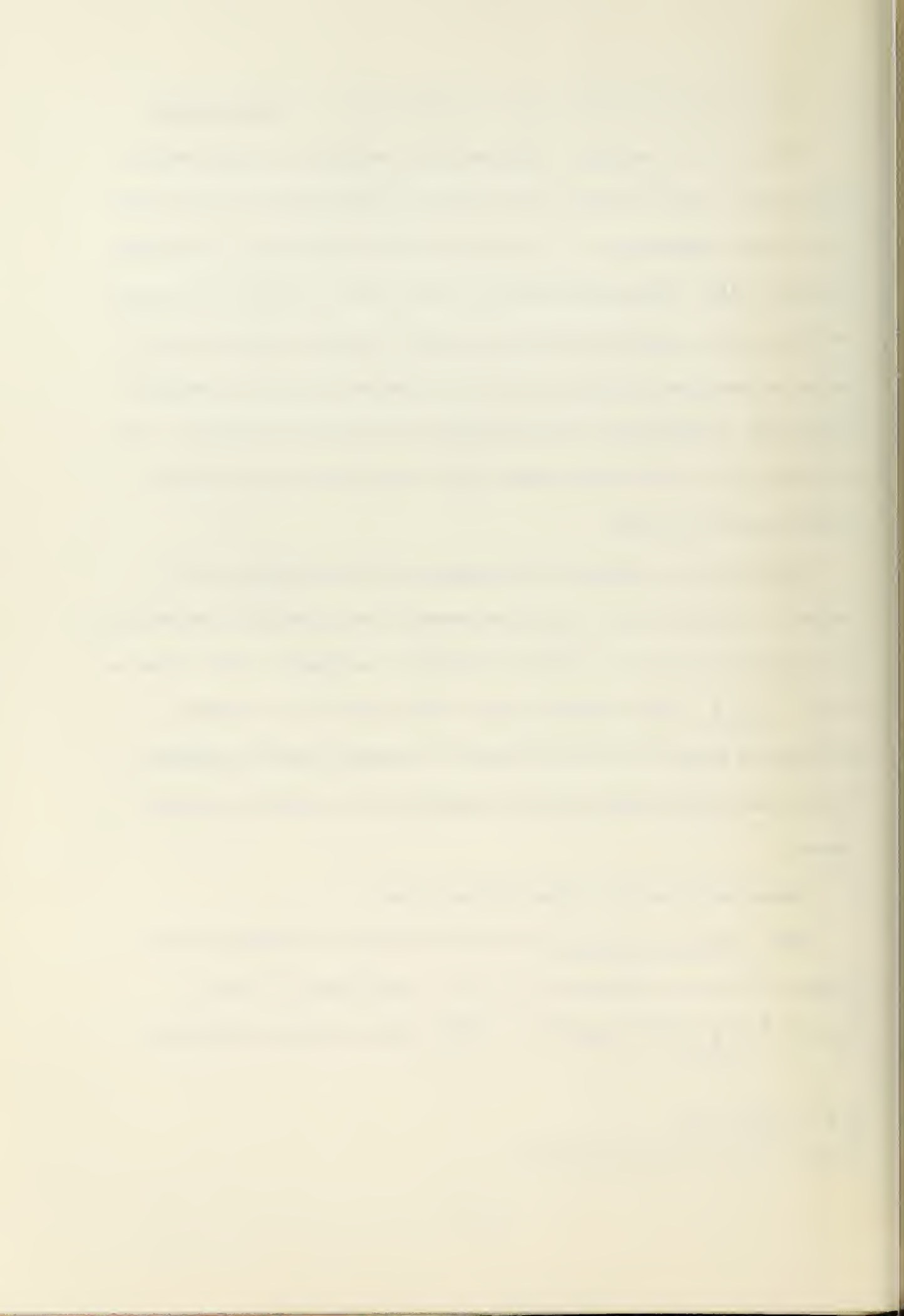
The bulk of the computed data assumes that the backlash is 0.3 radians. To use this data with other values of backlash it is first necessary to establish the effect of varying the amount of backlash. This is done on Figs. 7-1, 2, 3. These figures merely verify the intuitively obvious fact that the amount of overshoot must vary linearly with the backlash, but that the proportionality constant depends on the various parameter values.

### 7.1 Maximum Overshoot; Plastic Impact Case

Figs. 7-4, 5, 6, 7, 8, and 9 present the results of computer calculations in the form of families of curves. Each family is a plot of  $M_{pt}$  vs  $\rho^2 J_L / J_m$  for a specific  $\rho^2 f / FT$  ratio with  $\zeta$  as the family

K & A Figs. 5, 6, 7

Figs. 10, 11, 12, 13, 14, 15 in K & A





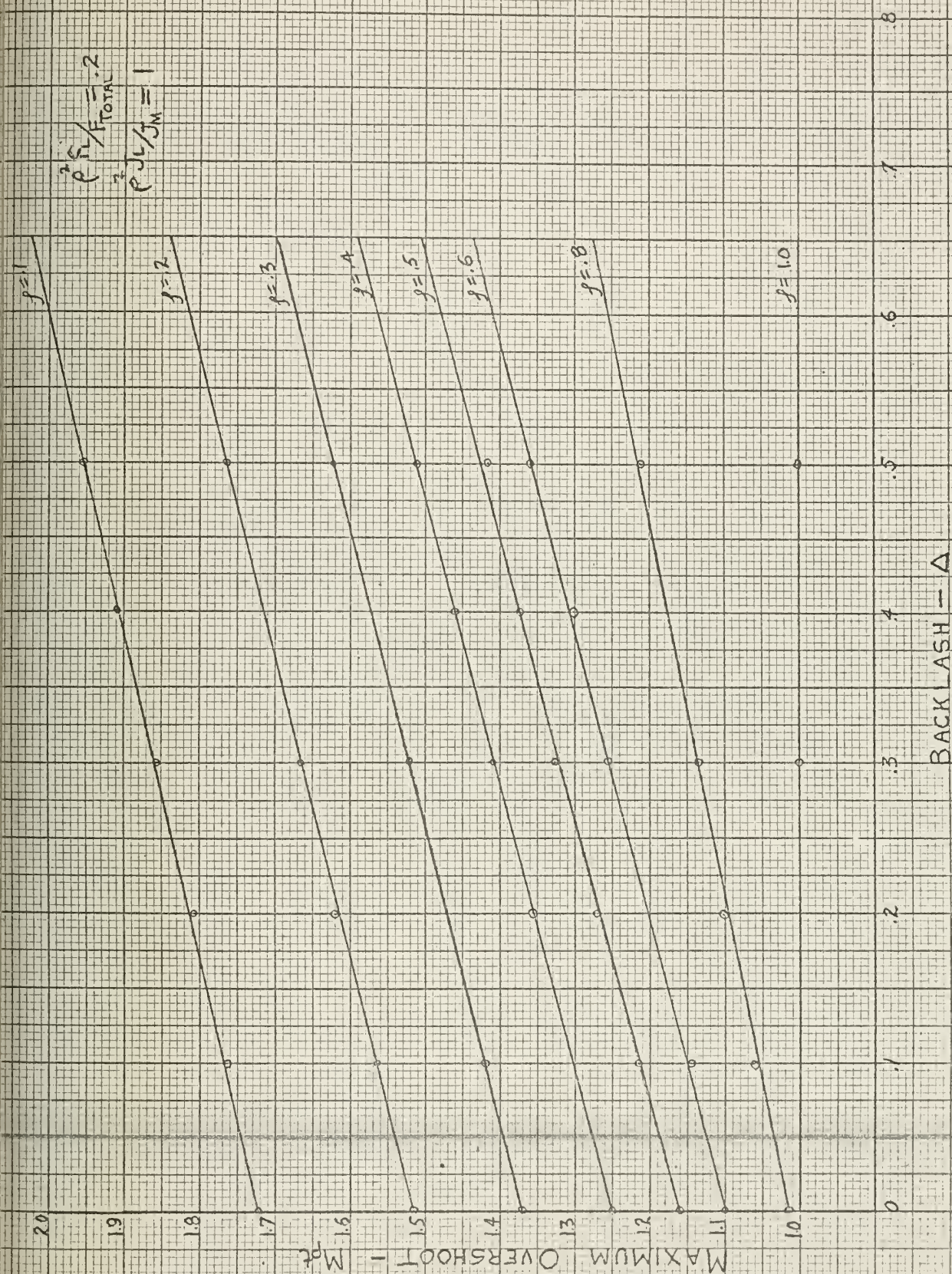


FIG. 7-1 MAXIMUM OVERSHOOT VS. BACKLASH FOR FRICTION RATIO OF 0.2 AND  $\frac{P_{FL}}{P_{JM}}$  OF 1.0





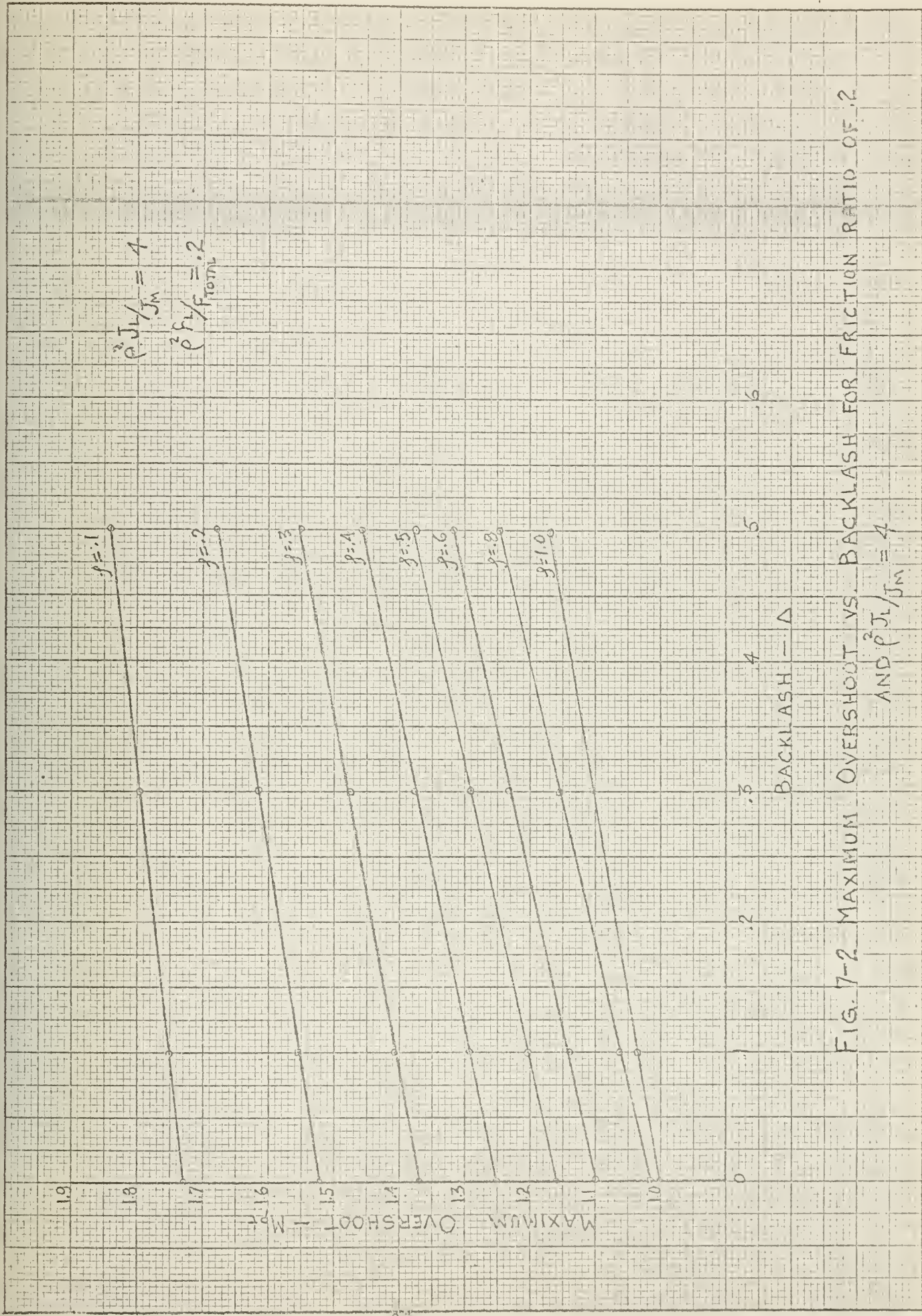


FIG. 7-2 MAXIMUM OVERSHOOT VS. BACKLASH FOR FRICTION RATIO OF .2  
 AND  $\rho J_L / J_M = 4$





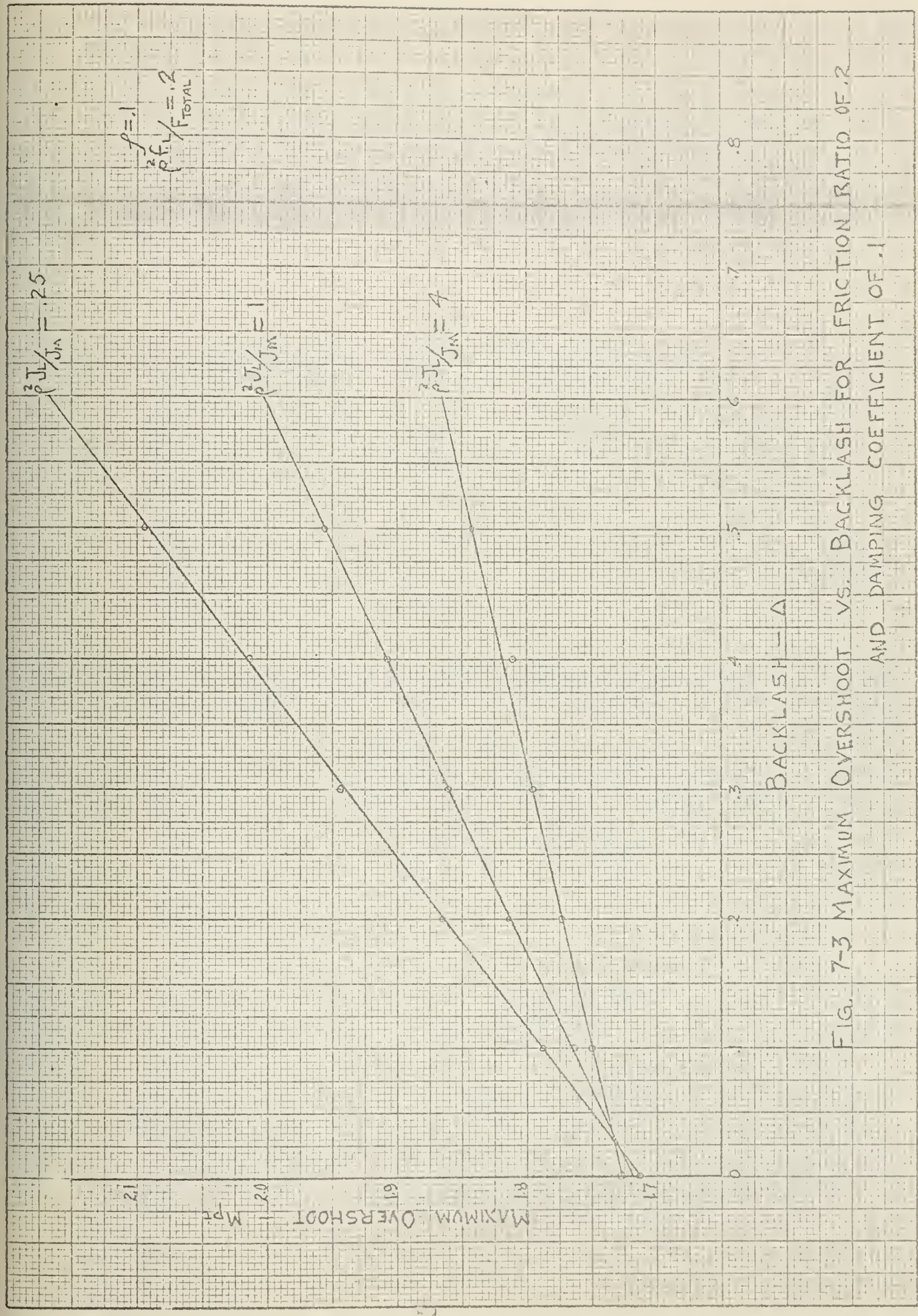


FIG. 7-3 MAXIMUM OVERSHOOT VS. BACKLASH FOR FRICTION RATIO OF 0.2 AND DAMPING COEFFICIENT OF .1





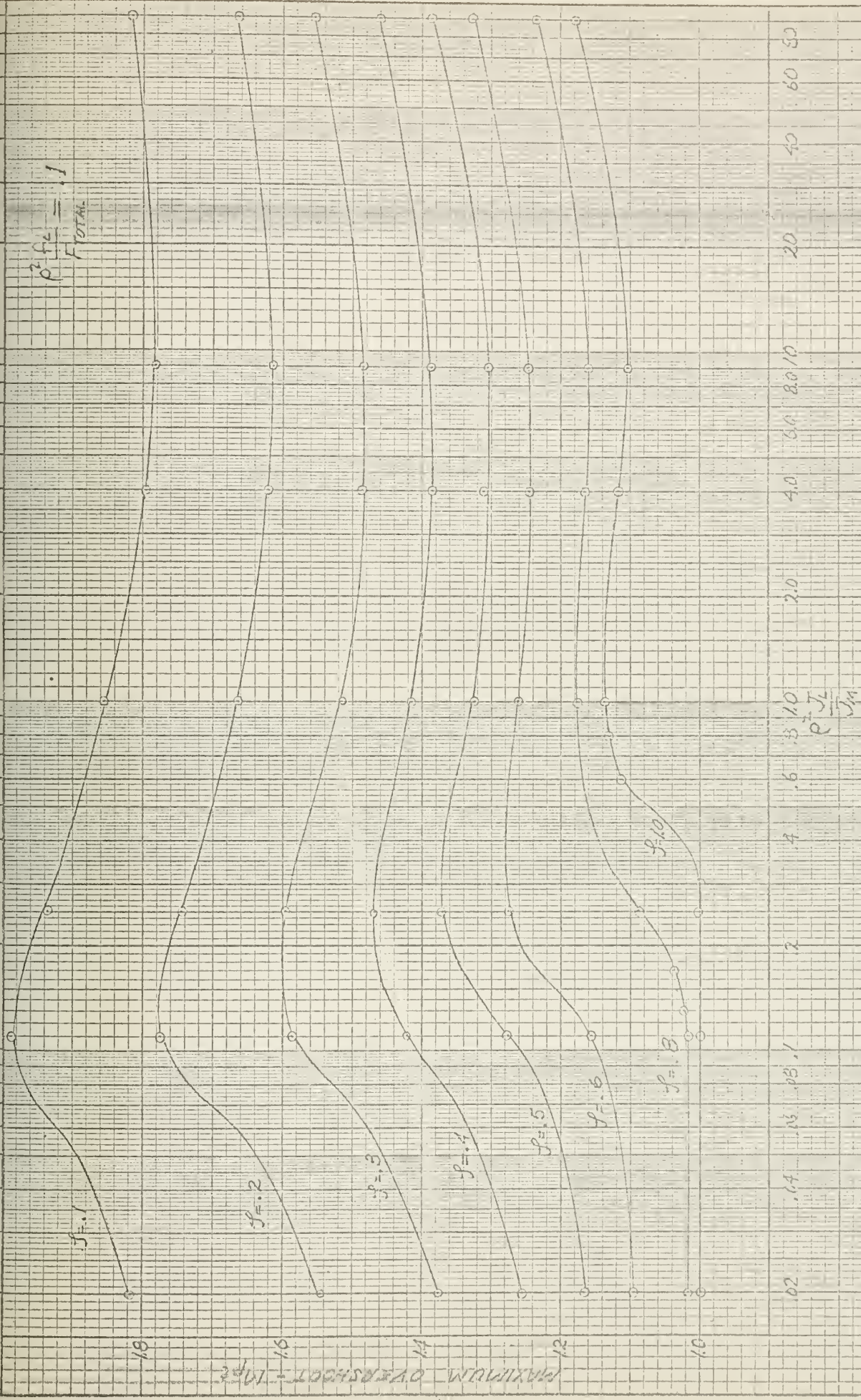


FIG. 7-4 MAXIMUM OVERSHOOT VS.  $P^2 \frac{J_c}{J_m}$  FOR FRICTION RATIO OF 0.1 AND BACKLASH OF 0.3





$$\left(\frac{J}{J_{TOTAL}}\right)^2 = .2$$

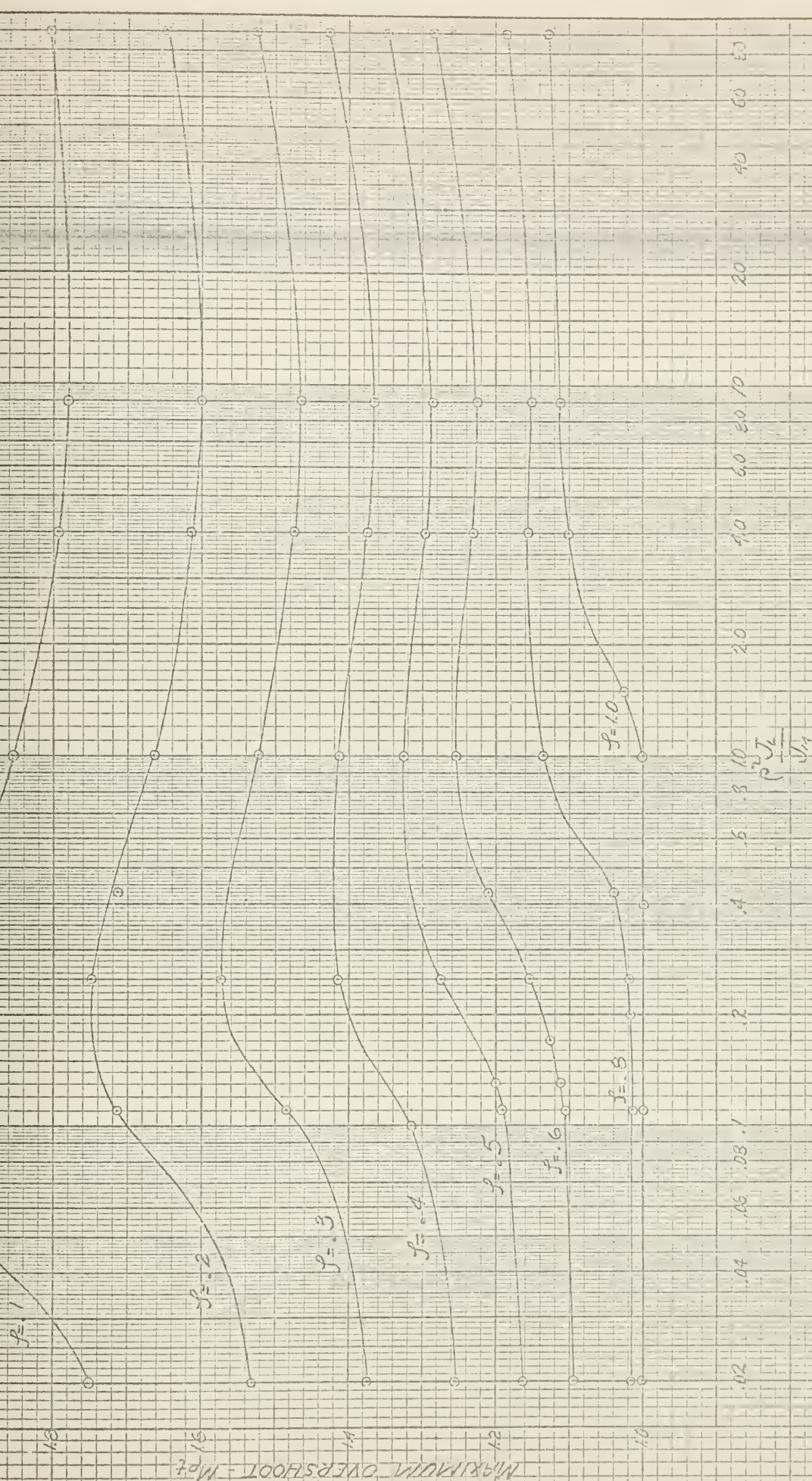


FIG. 7-5 MAXIMUM OVERSHOOT VS.  $\frac{P}{J_1}$  FOR FRICTION RATIO OF 0.2 AND DACKLASH OF 0.3





$$\rho \frac{J_L}{J_M} = 0.4$$

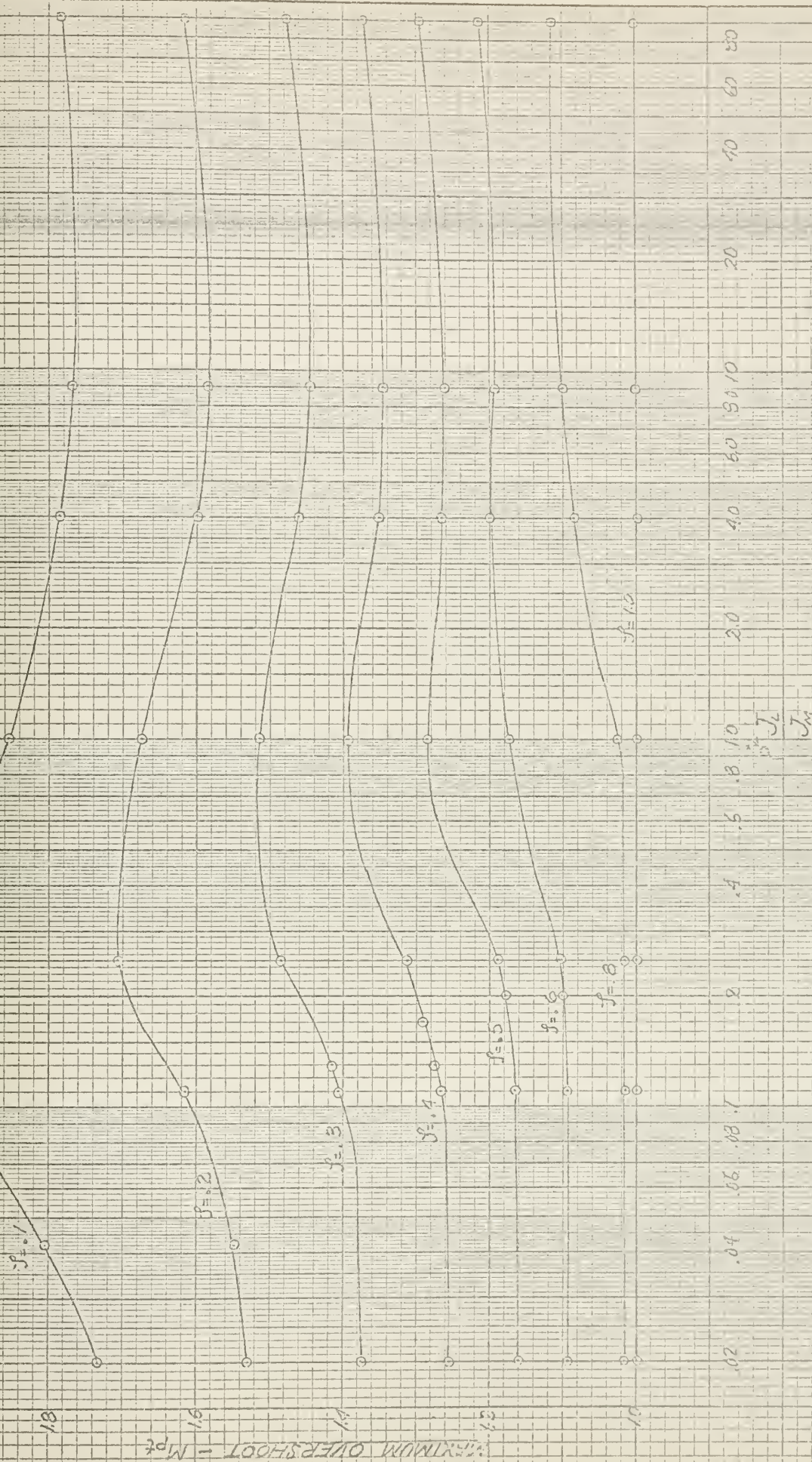


FIG. 7-6 MAXIMUM OVERSHOOT VS.  $\rho \frac{J_L}{J_M}$  FOR FRICTION RATIO OF 0.4 AND BACKLASH OF 0.3





$$\frac{J_e}{J_m} = 0.6$$

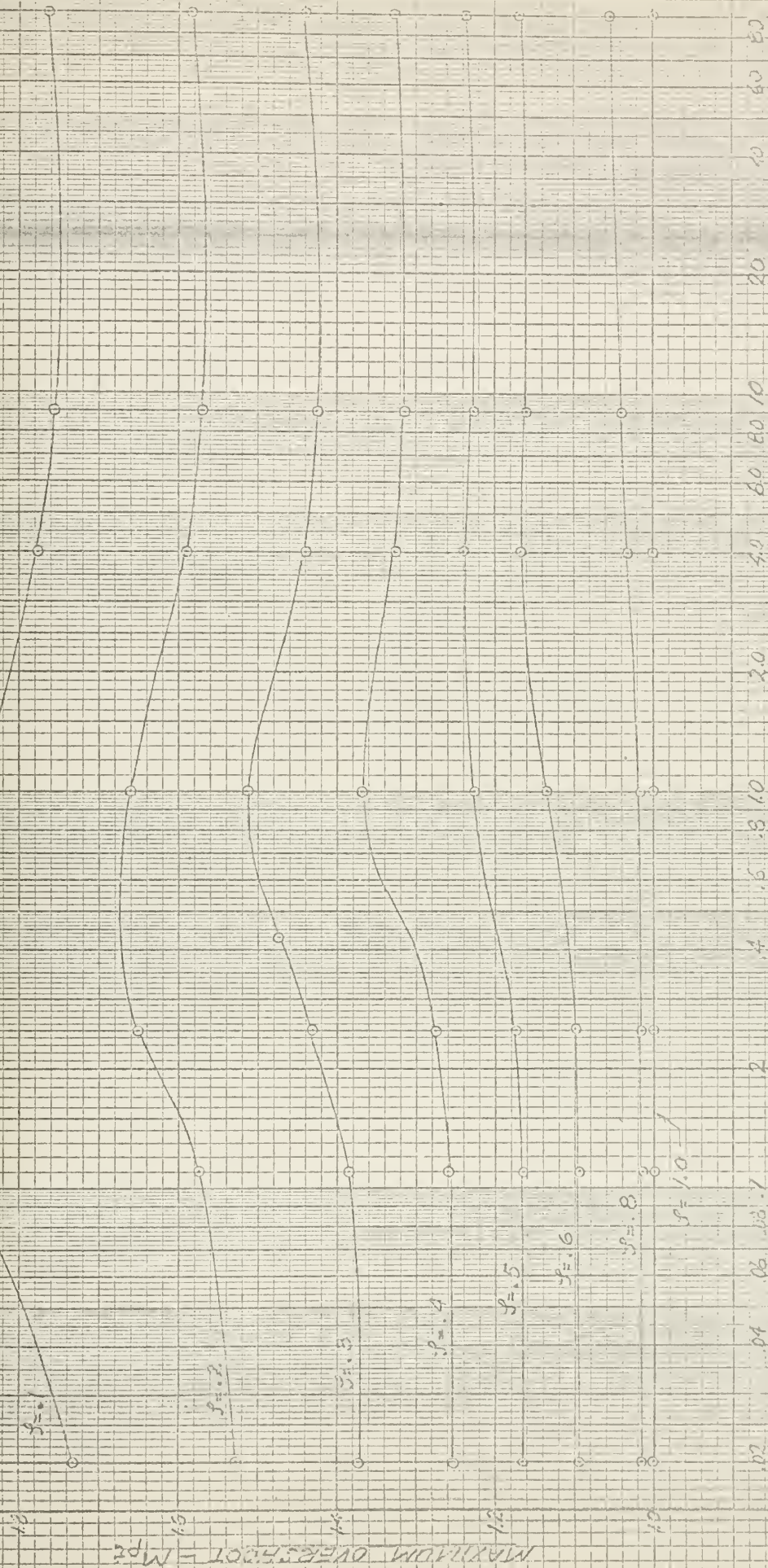


FIG. 7-7 MAXIMUM OVERSHOOT VS.  $\frac{J_e}{J_m}$  FOR FRICTION RATIO OF 0.6 AND BACKLASH OF 0.3





$$\frac{p \cdot J_2}{J_1} = .8$$

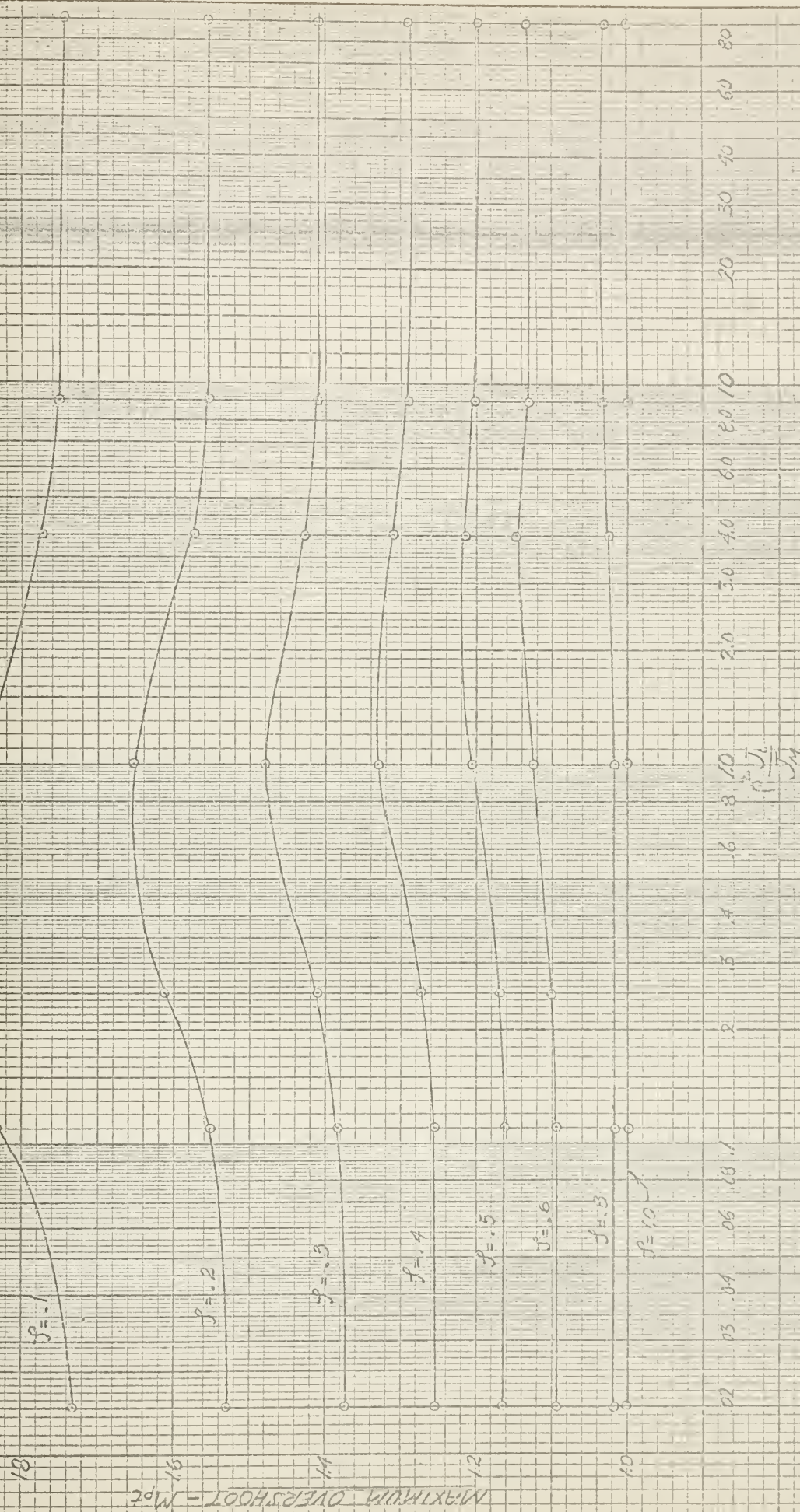


FIG 7-8 MAXIMUM OVERSHOOT VS.  $\frac{J_2}{J_1}$  FOR FRICTION RATIO OF 0.8 AND BACKLASH OF 0.3





$$\frac{P_{f_c}}{F_{TOTAL}} = 1.0$$

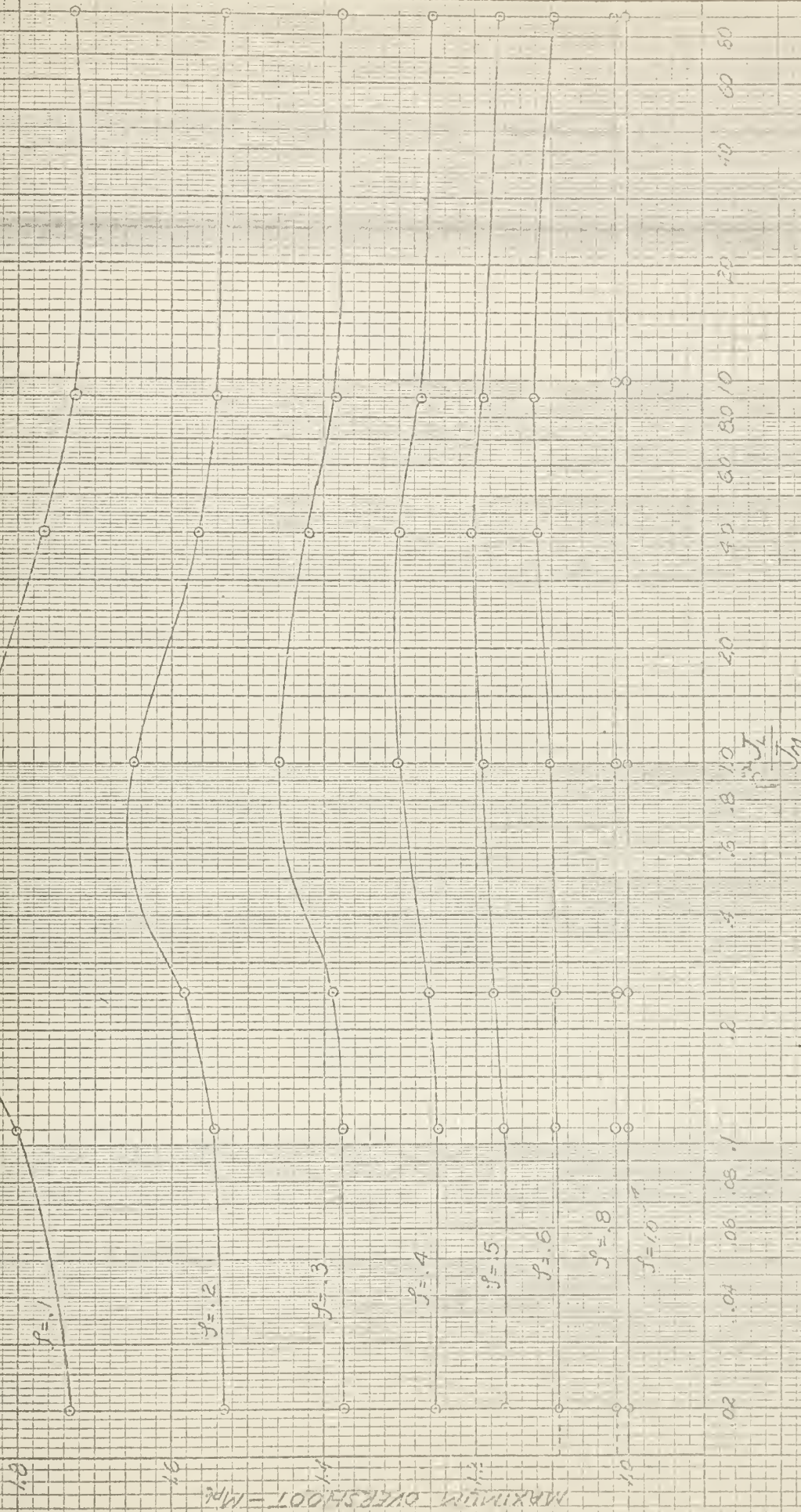


FIG. 7-9. MINIMUM OVERSHOOT IS  $\frac{P_{f_c}}{J_1}$  FOR FRICTION RATIO OF 1.0 AND BACKLASH OF 0.3





parameter. All are for the case of plastic impact. These curves can be used to predict the peak overshoot of any arbitrary second order system with backlash and plastic impact by reading off the pertinent values and inserting in the equation

$$M_{pt} \left| \begin{matrix} \Delta = \Delta_1 \\ \zeta = \zeta_1 \end{matrix} \right. = M_{pt} \left| \begin{matrix} \Delta = 0 \\ \zeta = \zeta_1 \end{matrix} \right. + \frac{\Delta_1}{0.3} \left[ M_{pt} \left| \begin{matrix} \Delta = .3 \\ \zeta = \zeta_1 \end{matrix} \right. - M_{pt} \left| \begin{matrix} \Delta = 0 \\ \zeta = \zeta_1 \end{matrix} \right. \right] \quad (7-1)$$

As was pointed out earlier, the solutions were made and the results were plotted using a backlash angle of 0.3 radian. Thus the values of amplitude of maximum overshoot on the curves are significant only in that they represent the slope of the overshoot versus backlash straight lines. This slope must be calculated in order to scale the value of overshoot read from the curve for the magnitude of backlash actually expected. Therefore, in order to refine the prediction scheme, other design curves, figures 7-10 through 7-15, were calculated using the curves of figures 7-4 through 7-9 just discussed. Along the curves the slope  $\frac{dM_{pt}}{d\Delta}$  was calculated by,

$$\frac{dM_{pt}}{d\Delta} \left| \begin{matrix} \zeta = \zeta_1 \end{matrix} \right. = \left[ M_{pt} \left| \begin{matrix} \Delta = .3 \\ \zeta = \zeta_1 \end{matrix} \right. - M_{pt} \left| \begin{matrix} \Delta = 0 \\ \zeta = \zeta_1 \end{matrix} \right. \right] \div .3 \quad (7-2)$$

These values of  $dM_{pt}/d\Delta$  were then plotted versus inertia ratios at constant friction ratios as before. These curves give a more straightforward prediction method with the following equation:





$$\frac{\rho_{IL}^2}{F_{TOTAL}} = .1$$

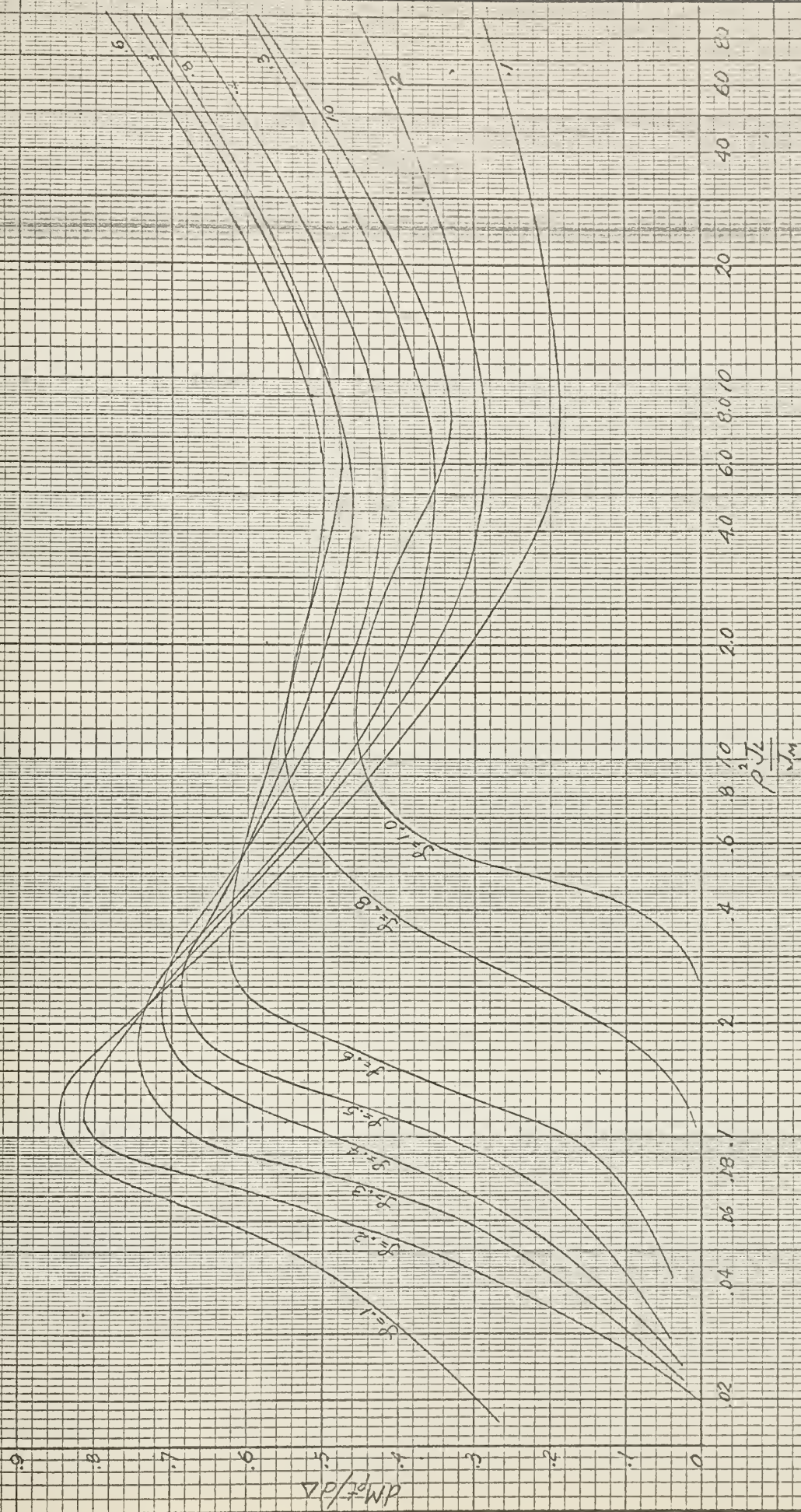


FIG. 7-10 DESIGN CHART FOR PREDICTING MAXIMUM OVERSHOOT  $\left(\frac{\rho_{IL}^2}{F_{TOTAL}} = .1\right)$





$$\frac{P_{TL}}{F_{TOTAL}} = .2$$

9

8

7

6

5

4

3

2

1

0

$$\frac{\Delta P}{\rho V^2} \frac{W}{D}$$

26

0.2

0.4

0.6

0.8

1.0

1.2

1.4

1.6

1.8

2.0

2.2

2.4

2.6

2.8

3.0

3.2

3.4

3.6

3.8

4.0

4.2

4.4

4.6

4.8

5.0

5.2

5.4

5.6

5.8

6.0

6.2

6.4

6.6

6.8

7.0

7.2

7.4

7.6

7.8

8.0

8.2

8.4

8.6

8.8

9.0

9.2

9.4

9.6

9.8

10.0

10.2

10.4

10.6

10.8

11.0

11.2

11.4

11.6

11.8

12.0

12.2

12.4

12.6

12.8

13.0

13.2

13.4

13.6

13.8

14.0

14.2

14.4

14.6

14.8

15.0

15.2

15.4

15.6

15.8

16.0

16.2

16.4

16.6

16.8

17.0

17.2

17.4

17.6

17.8

18.0

18.2

18.4

18.6

18.8

19.0

19.2

19.4

19.6

19.8

20.0

20.2

20.4

20.6

20.8

21.0

21.2

21.4

21.6

21.8

22.0

22.2

22.4

22.6

22.8

23.0

23.2

23.4

23.6

23.8

24.0

24.2

24.4

24.6

24.8

25.0

25.2

25.4

25.6

25.8

26.0

26.2

26.4

26.6

26.8

27.0

27.2

27.4

27.6

27.8

28.0

28.2

28.4

28.6

28.8

29.0

29.2

29.4

29.6

29.8

30.0

30.2

30.4

30.6

30.8

31.0

31.2

31.4

31.6

31.8

32.0

32.2

32.4

32.6

32.8

33.0

33.2

33.4

33.6

33.8

34.0

34.2

34.4

34.6

34.8

35.0

35.2

35.4

35.6

35.8

36.0

36.2

36.4

36.6

36.8

37.0

37.2

37.4

37.6

37.8

38.0

38.2

38.4

38.6

38.8

39.0

39.2

39.4

39.6

39.8

40.0

40.2

40.4

40.6

40.8

41.0

41.2

41.4

41.6

41.8

42.0

42.2

42.4

42.6

42.8

43.0

43.2

43.4

43.6

43.8

44.0

44.2

44.4

44.6

44.8

45.0

45.2

45.4

45.6

45.8

46.0

46.2

46.4

46.6

46.8

47.0

47.2

47.4

47.6

47.8

48.0

48.2

48.4

48.6

48.8

49.0

49.2

49.4

49.6

49.8

50.0

50.2

50.4

50.6

50.8

51.0

51.2

51.4

51.6

51.8

52.0

52.2

52.4

52.6

52.8

53.0

53.2

53.4

53.6

53.8

54.0

54.2

54.4

54.6

54.8

55.0

55.2

55.4

55.6

55.8

56.0

56.2

56.4

56.6

56.8

57.0

57.2

57.4

57.6

57.8

58.0

58.2

58.4

58.6

58.8

59.0

59.2

59.4

59.6

59.8

60.0

60.2

60.4

60.6

60.8

61.0

61.2

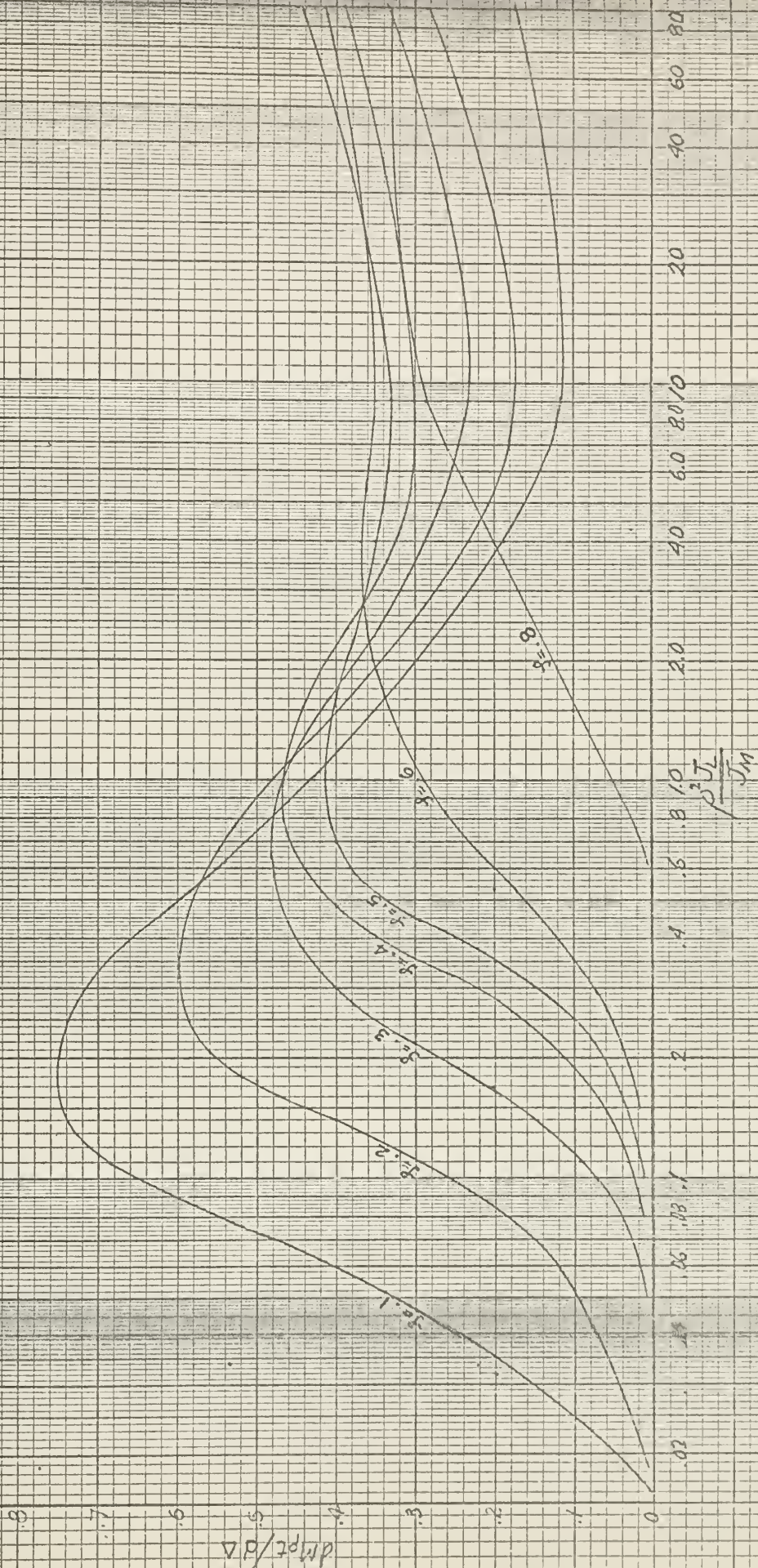
61.4

</

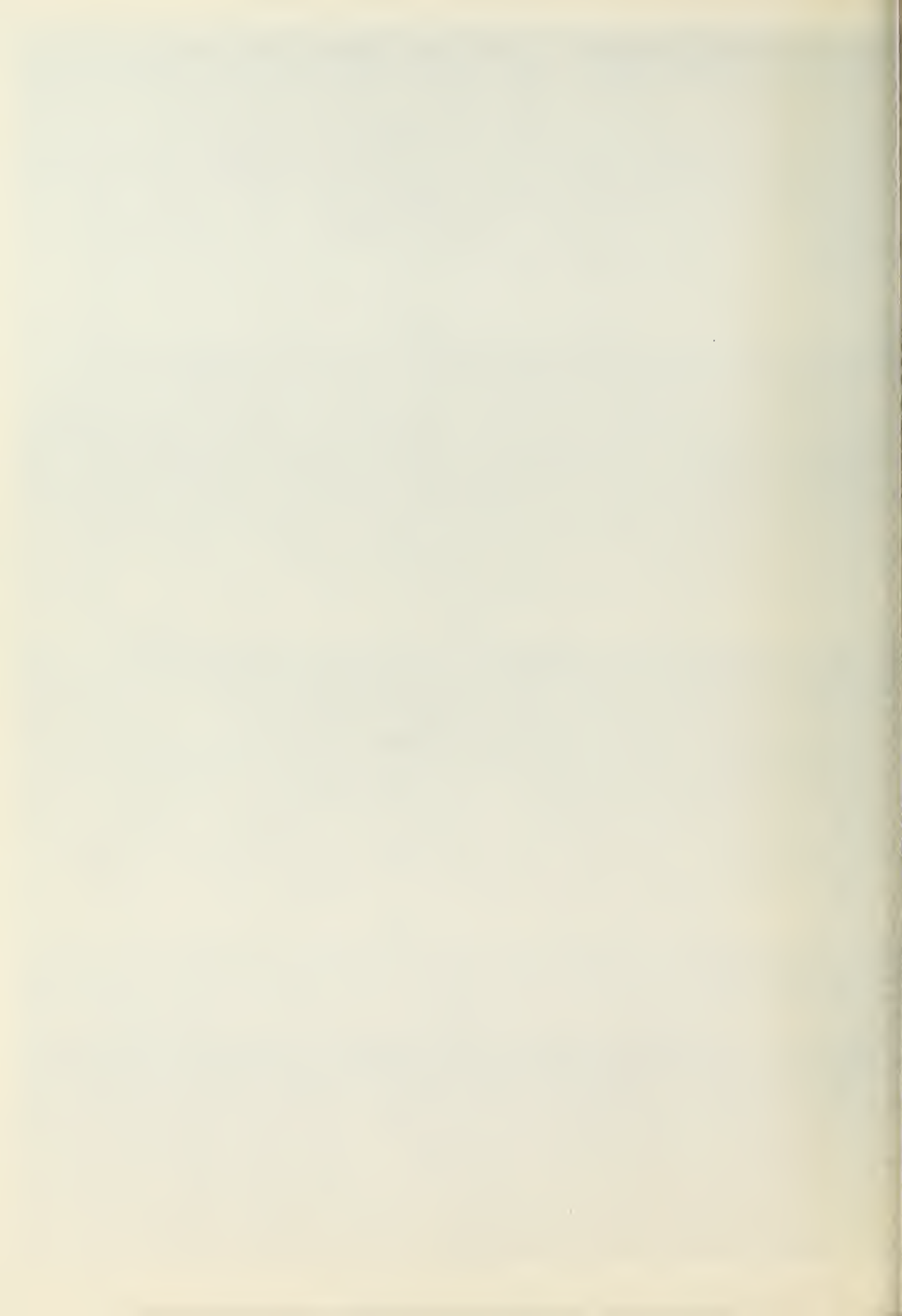




$$\frac{\rho^2 I}{F_{TOTAL}} = 4$$



F G, 7-12 DESIGN CHART FOR PREDICTING MAXIMUM OVERSHOOT  $\left( \frac{\rho^2 I}{F_{TOTAL}} = 4 \right)$





$$\frac{\rho_{TL}^2}{F_{TOTAL}} = .6$$

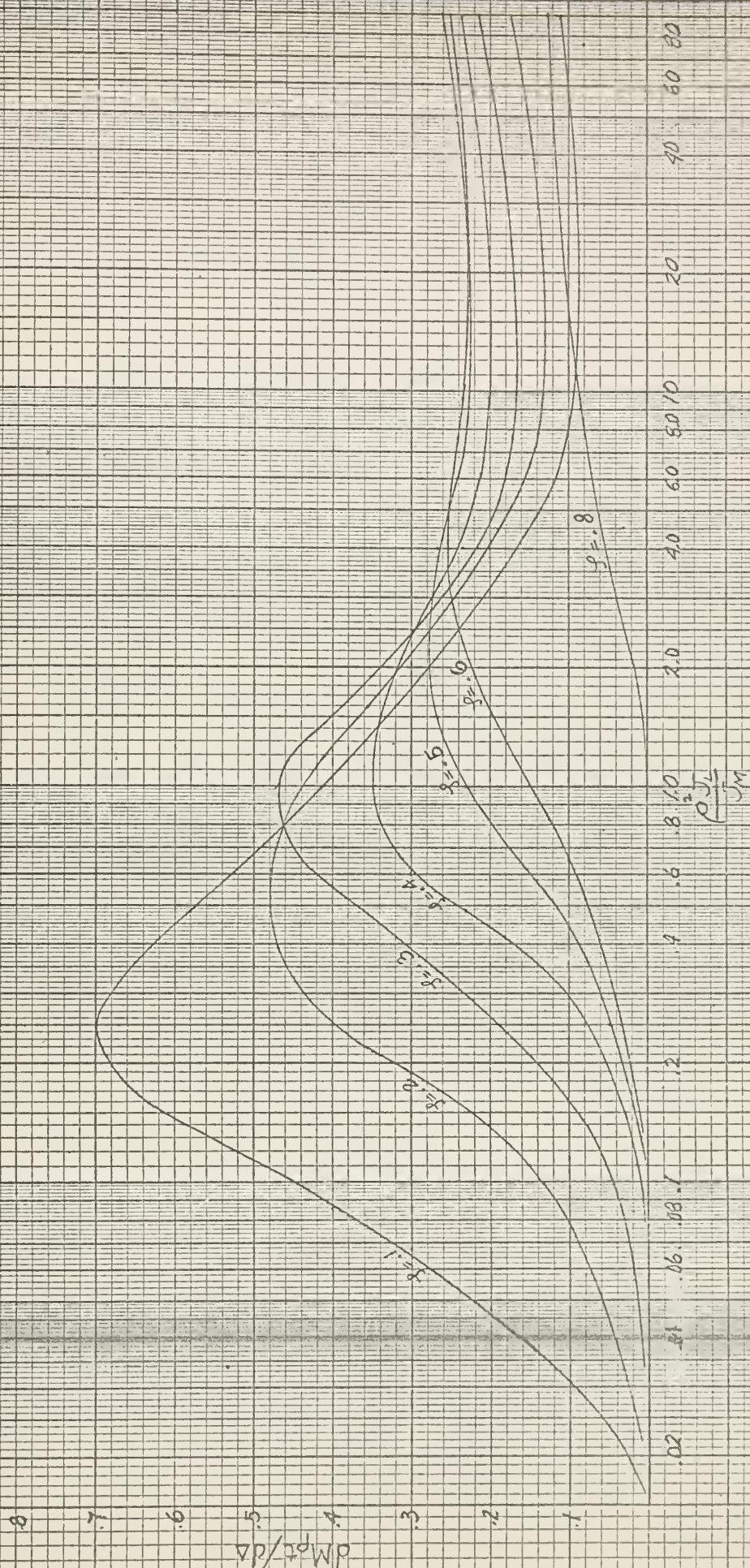


FIG. 7-13 DESIGN CHART FOR PREDICTING MAXIMUM OVERSHOOT  $\left(\frac{\rho_{TL}^2}{F_{TOTAL}} = .6\right)$





$$\frac{\rho^2 f}{F_{TOTAL}} = .8$$

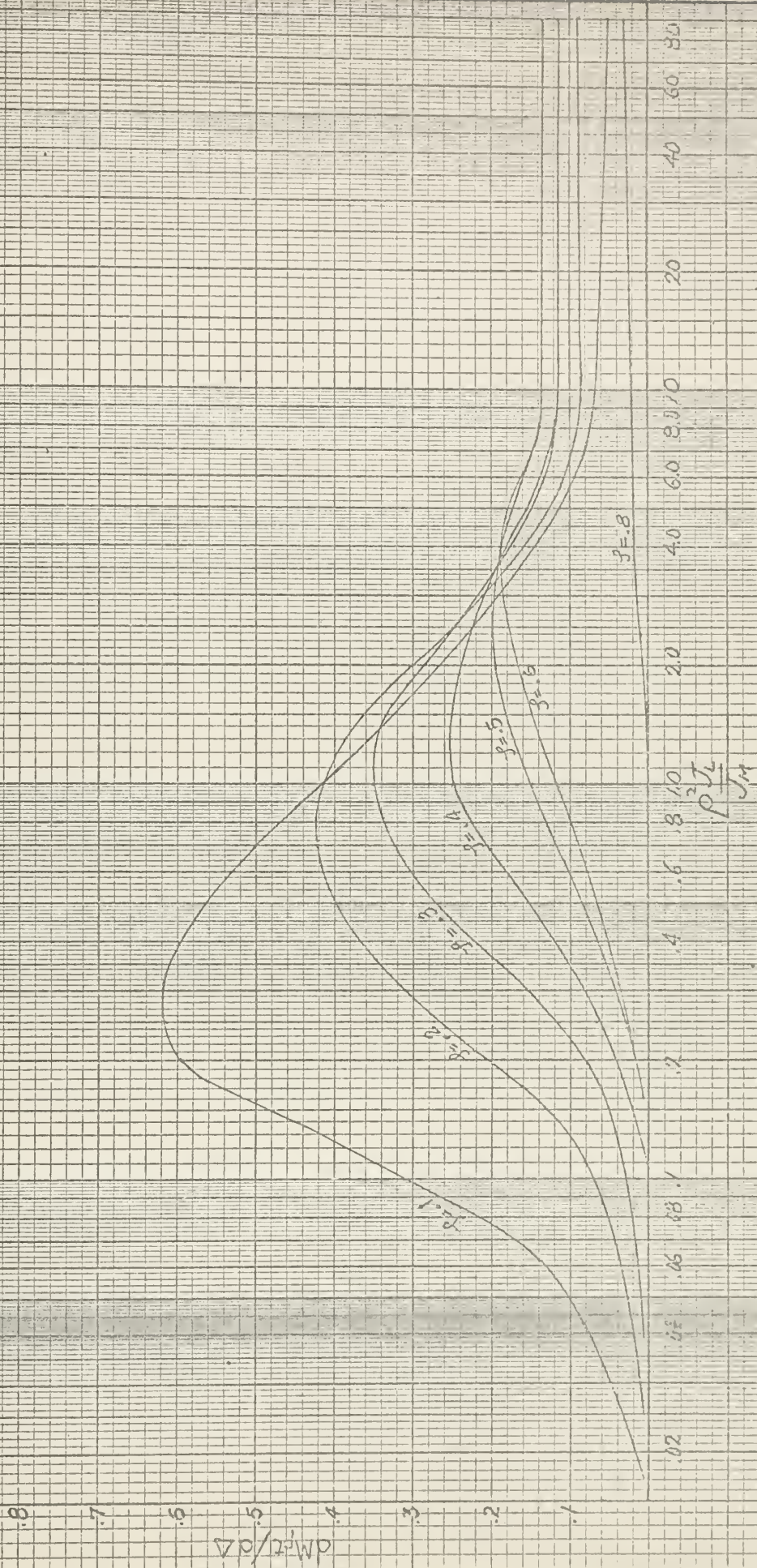
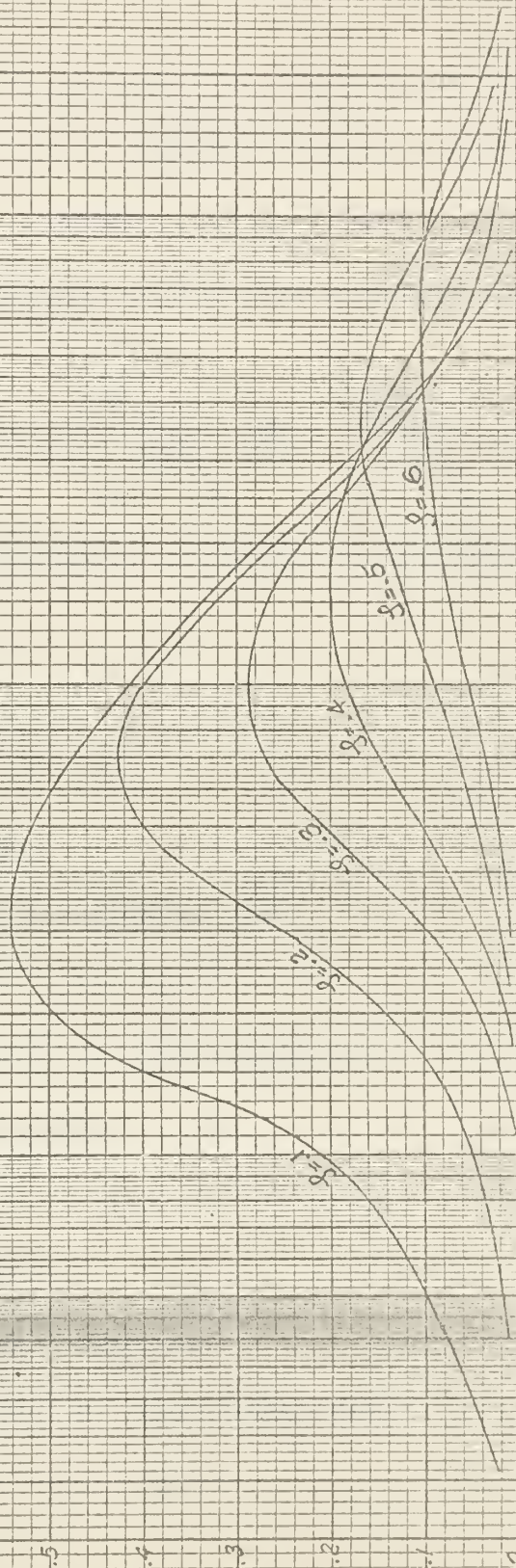


FIG. 7-14 DESIGN CHART FOR PREDICTING MAXIMUM OVERSHOOT  $(\frac{\rho^2 f}{F_{TOTAL}} = .8)$





$$\frac{\rho_{TL}^2}{F_{TOTAL}} = 1.0$$

 $\Delta p / \Delta v$ 


0 1 2 3 4 5 6

$$\left( \frac{\rho_{TL}^2}{F_{TOTAL}} = 1.0 \right)$$

FIG. 7-15 DESIGN CHART FOR PREDICTING MAXIMUM OVERSHOOT





$$M_{pt} \bigg|_{\substack{\Delta=\Delta_1 \\ \mathcal{S}=\mathcal{S}_1}} = M_{pt} \bigg|_{\substack{\Delta=0 \\ \mathcal{S}=\mathcal{S}_1}} + \frac{dM_{pt}}{d\Delta} \bigg|_{\mathcal{S}=\mathcal{S}_1} \times \Delta_1 \quad (7-3)$$

In order to demonstrate the procedure for using the design charts shown in figures 7-4 through 7-15, an example problem is solved obtaining the maximum overshoot,  $M_{pt}$ , for a second order servo with backlash. The differential equation for the combined motion of an armature controlled motor is:

$$\ddot{\Theta}_c + \frac{f_t + f_l}{J_m + \rho^2 J_L} \dot{\Theta}_c + \frac{\rho K_a}{J_m + \rho^2 J_L} \Theta_c = \frac{\rho K_a}{J_m + \rho^2 J_L} \Theta_r \quad (7-4)$$

Given the following specifications of a D. C. shunt motor coupled through a gear box to a load:

Horsepower	= .008
Rated RPM	= 4000
R	= 282 ohms
$K_g$	= .233 volts/radian/second
$J_m$	= $8.2 \times 10^{-6}$ slug feet <sup>2</sup>
$f_m$	= $3.34 \times 10^{-6}$ lb.-feet/radian/sec.
$K_e$	= 10 volts/radian
$\rho$	= 1
$\Delta$	= .05 radians
$J_L$	= $16.4 \times 10^{-6}$ slug-feet <sup>2</sup>
$f_L$	= $10.4 \times 10^{-6}$ lb.-feet/radian/sec.
$K_t$	= .1464 lb.-feet/ampere



The required values shown in Equation 7-4 are obtained as follows:

$$K_a = \frac{K_t K_e}{R} = \frac{.1464 \times 10}{282} = .0052 \text{ LB-FT}$$

$$\omega_n = \sqrt{\frac{\rho K_a}{J_m + \rho^2 J_L}} = \sqrt{\frac{(1) .0052}{8.2 \times 10^{-6} + (1)^2 16.4 \times 10^{-6}}} = \frac{14.5}{\text{SEC}} \frac{\text{RAD}}{\text{SEC}}$$

$$f_t = \rho^2 f_L + f_m = (1)^2 10.4 \times 10^{-6} + 3.34 \times 10^{-6}$$

$$= \frac{13.74 \times 10^{-6}}{\text{RAD/SEC}} \frac{\text{LB-FT}}{\text{RAD/SEC}}$$

$$F_T = f_T + f_1 = (13.74 + 121) \times 10^{-6} = \frac{135 \times 10^{-6}}{\text{RAD/SEC}} \frac{\text{LB-FT}}{\text{RAD/SEC}}$$

$$f_1 = \frac{K_t K_g}{R} = \frac{.1464 \times .233}{282} = \frac{121 \times 10^{-6}}{\text{RAD/SEC}} \frac{\text{LB-FT}}{\text{RAD/SEC}}$$

$$\zeta = \frac{f_T + f_1}{J_m + \rho^2 J_L} \left( \frac{1}{2 \omega_n} \right) = .19$$

$$\rho^2 J_L / J_m = \frac{(1)^2 16.4 \times 10^{-6}}{8.2 \times 10^{-6}} = 2.0$$

$$\rho^2 \frac{f_L}{F_T} = \frac{10.4 \times 10^{-6}}{135 \times 10^{-6}} = .077$$

Two methods are shown for obtaining the maximum overshoot with a backlash angle of .05 radians in the gear trains.

The first method is accomplished using the curves of figures 7-4 through 7-9. The procedure is simple, but requires more steps than does the second. Also one must remember that these curves are drawn for a backlash of 0.3 radian and must be scaled for the expected amount of backlash. The second method makes use of the design charts of figures 7-10 through 7-15.



### Method 1

Entering figure 7-4 ( $\rho^2 f_L / F_T = 0.1$ ), at  $\rho^2 J_L / J_m = 2.0$ , and a damping ratio,  $\zeta = 0.19$ , the amount of overshoot for a backlash angle,  $\Delta = 0.3$  rad. is  $M_{pt} = 1.658$ . Then:

$$M_{pt} \left| \begin{array}{l} \Delta = .05 \\ \zeta = .19 \end{array} \right. = M_{pt} \left| \begin{array}{l} \Delta = 0 \\ \zeta = .19 \end{array} \right. + .05 / .3 \left[ M_{pt} \left| \begin{array}{l} \Delta = .3 \\ \zeta = .19 \end{array} \right. - M_{pt} \left| \begin{array}{l} \Delta = 0 \\ \zeta = .19 \end{array} \right. \right]$$

From second order linear characteristics

$$M_{pt} = 1.545$$

hence,

$$\begin{aligned} M_{pt} &= 1.545 + .05 / .3 \quad 1.658 - 1.545 \\ &= 1.545 + .0189 \\ &= \underline{1.564} \end{aligned}$$

### Method 2

$$M_{pt} \left| \begin{array}{l} \Delta = .05 \\ \zeta = .19 \end{array} \right. = M_{pt} \left| \begin{array}{l} \Delta = 0 \\ \zeta = .19 \end{array} \right. + \left. \frac{dM_{pt}}{d\Delta} \right|_{\zeta = .19} \times \Delta$$

from figure 7-10, ( $\rho^2 f_L / F_T = 0.1$ ), at  $\rho^2 J_L / J_m = 2.0$ , and a damping ratio  $\zeta = 0.19$ ,  $dM_{pt} / d\Delta = 0.357$

Also:

$$M_{pt} \left| \begin{array}{l} \Delta = 0 \\ \zeta = .19 \end{array} \right. = 1.545$$

hence,

$$\begin{aligned} M_{pt} &= 1.545 + .357 \times .05 \\ &= 1.545 + .018 \\ &= \underline{1.563} \end{aligned}$$





The procedure for using the charts remains unchanged for servo systems which utilize other types of motors. The only difference which arises is in the calculation of the chart parameters from the known system constants. For a field control motor if the field time constant is negligible, the equation is similar to the armature control motor equation.

$$\ddot{\Theta}_c + \frac{F_t}{J_m + \rho^2 J_L} \dot{\Theta}_c + \frac{\rho K_a}{J_m + \rho^2 J_L} \Theta_c = \frac{\rho K_a}{J_m + \rho^2 J_L} \Theta_R \quad (7-5)$$

In like manner the equation for the system with a two phase motor is

$$\ddot{\Theta}_c + \frac{F_t K_n}{J_m + \rho^2 J_L} \dot{\Theta}_c + \frac{\rho K_m}{J_m + \rho^2 J_L} \Theta_c = \frac{\rho K_m}{J_m + \rho^2 J_L} \Theta_R \quad (7-6)$$

where

$$K_n = - \frac{\partial T}{\partial n} \quad (\text{from characteristic curves of two phase motor})$$

$$K_m = \frac{\partial T}{\partial e_1} \quad (\text{from characteristic curves of two phase motor})$$

The calculation of the chart parameters is a simple matter once the defining equations are known.



## 7.2 Maximum Overshoot, Elastic Impact Case.

Investigation of a limited number of cases reveal that the amount of overshoot with plastic impact is always greater than that with elastic impact. The difference between this maximum overshoot decreases as

$\frac{2_f L}{F_T}$  increases. However, under no circumstances was the effect on maximum overshoot greater than .01 radians. The effect on the time of maximum overshoot appears negligible. In a few cases the time was different for the plastic and the elastic cases but the difference was very small and no pattern of difference could be ascertained.

These results point out the validity of the original assumption made for this study. In a practical system there will exist, of course, some amount of gear bounce when the gears contact each other. The effect on maximum overshoot, however, is so small that the curves obtained in this study remain reasonably accurate.





### 7.3 Settling Time

In determining the effect of backlash on the settling time of a second order servo system, it was necessary to first find a definition for settling time which would be suitable for all of the cases which were investigated. Normally, settling time is defined as the time for the output to reach 98% of its final value. This definition has real meaning, however, only for linear stable systems in which there are no sustained oscillations. For systems which do exhibit small sustained oscillations, the settling time is sometimes defined as the time required for the amplitude of oscillations to decrease to within 2% of the final value. For very small amplitudes of oscillations this definition gives an unrealistic value for settling time. For the purpose of this study settling time is considered as the time required for the system output to settle to 98% of the difference between the magnitude of the input and the amplitude of the sustained oscillations.

For all cases for which the damping coefficient was less than 0.6 there were no conclusions as to effects of backlash on the system settling time since the magnitudes of the sustained oscillations were always quite large for the amount of backlash used in the solutions and the settling time was difficult to obtain accurately. For those cases for which the damping coefficient was greater than 0.6, the sustained oscillations were small if they existed and an analysis revealed the following general conclusions:



1. As the size of the backlash angle increases, the settling time will increase provided the other parameters are kept constant. For the cases investigated, this increase in settling time was nearly proportional to the backlash angle.

2. As the ratio  $\rho^2 J_L / J_m$  increases, with other parameters constant, the settling time increases.

3. At the ratio  $\rho^2 f_L / F_T$  is increased, with other parameters constant, the settling time decreases.

The data included in Tables I-III show these general conclusions and also some quantitative effects of backlash on settling time.



TABLE I  
SETTLING TIME DATA  
 $\omega_n = 1.0$

$\mathcal{J}$	$\rho^{2.J_L/J_M}$	$\rho_{f.L}^2 \cdot \frac{L}{FT}$	Radians $\Delta$	Seconds $t_s$
.6	1/9	.2	.3	28
.6	1/9	.4	.3	21
.6	1/9	.6	.3	16
.6	1/9	.8	.3	13
.6	1/9	1.0	.3	7
.6	1/4	.2	.3	28
.6	1/4	.4	.3	24
.6	1/4	.6	.3	16
.6	1/4	.8	.3	14
.6	1/4	1.0	.3	9
.6	1	.2	.3	29
.6	1	.4	.3	28
.6	1	.6	.3	23
.6	1	.8	.3	17
.6	1	1.0	.3	10
.6	4	.2	.3	29
.6	4	.4	.3	28
.6	4	.6	.3	26
.6	4	.8	.3	23
.6	4	1.0	.3	10
.6	9	.2	.3	29
.6	9	.4	.3	29
.6	9	.6	.3	26
.6	9	.8	.3	23
.6	9	1.0	.3	10





TABLE II  
SETTLING TIME DATA  
 $\omega_n = 1.0$

$\mathcal{J}$	$\rho^{2J_L}/J_M$	$\rho^{2f_L} \frac{L}{FT}$	Radians $\Delta$	Seconds $t_s$
.6	1/9	.8	.03	5
.6	1/9	.8	.10	7
.6	1/9	.8	.15	8
.6	1/9	.8	.30	13
.6	1	.8	.03	11
.6	1	.8	.10	14
.6	1	.8	.15	16
.6	1	.8	.30	17
.6	4	.8	.03	12
.6	4	.8	.10	14
.6	4	.8	.15	17
.6	4	.8	.30	23
.6	9	.8	.03	13
.6	9	.8	.10	16
.6	9	.8	.15	18
.6	9	.8	.30	23



TABLE III  
SETTLING TIME DATA  
 $\omega n = 1.0$

$\gamma$	$\rho^2_{J_L/J_M}$	$\rho^2_{\frac{f_L}{FT}}$	Radians $\Delta$	Seconds $t_s$
.8	1/9	.2	.3	8
.8	1/9	.4	.3	7
.8	1/9	.6	.3	6
.8	1/9	.8	.3	5
.8	1/9	1.0	.3	5
.8	1/4	.2	.3	20
.8	1/4	.4	.3	9
.8	1/4	.6	.3	7
.8	1/4	.8	.3	6
.8	1/4	1.0	.3	5
.8	1	.2	.3	43
.8	1	.4	.3	31
.8	1	.6	.3	10
.8	1	.8	.3	8
.8	1	1.0	.3	6
.8	4	.2	.3	48
.8	4	.4	.3	36
.8	4	.6	.3	12
.8	4	.8	.3	9
.8	4	1.0	.3	6
.8	9	.2	.3	52
.8	9	.4	.3	43
.8	9	.6	.3	13
.8	9	.8	.3	9
.8	9	1.0	.3	6





#### 7.4 Time of Maximum Overshoot

For each of the cases investigated the time of maximum overshoot (peak time) was recorded from the printout of the solution. It was found that the presence of backlash causes a slight increase in the peak time over the linear system for those cases where  $\zeta > .5$ , and has negligible effect in those where  $\zeta < .5$ . When  $\rho_{\frac{f_L}{F_T}}^2$  is increased from zero to 0.5, other parameters constant and  $\zeta > .5$ , peak time increases slightly and remains essentially constant for  $\rho_{\frac{f_L}{F_T}}^2 > .5$ . As  $\rho_{J_L/J_m}^2$  is increased, other parameters constant and  $\zeta > .5$ , peak time is decreased.



### 7.5 Other System Characteristics.

A careful study of the results as plotted in figures 7-4 through 7-9 reveals some interesting phenomena. At all friction ratios it is observed that as the ratio of load inertia to motor inertia is made smaller the amplitude of the overshoot is less. There is a point where the overshoot is identical to that of a linear second order system, in other words, where backlash has no effect on the overshoot. Note that this point occurs at different inertia ratios for each value of damping ratio. Also this point varies depending on the value of friction ratio. If the inertia ratio is decreased beyond this point then the amplitude of overshoot remains constant at the value of the linear case. Figure 7-16 is a plot of the boundaries of the combinations of variables which will cause an effect on the amplitude of overshoot if the system has any appreciable amount of backlash. The coordinates are friction ratio and inertia ratio with the boundaries labeled with values of damping ratio. Areas to the right of a boundary are combinations of the variables which affect overshoot. These curves were plotted using information deducted from figures 7-4 through 7-9. Three points were selected as test points to prove the validity of the boundaries as plotted. These points are shown on the figures as points "A", "B", and "C". The system parameters used at the test points were:

$$\begin{array}{l} \text{Point A} \\ \hline \zeta = 0.8 \\ \rho_{fL}^2 / F_T = 0.8 \end{array}$$

$$\rho_{JL/J_m}^2 = 1.0$$

$$\begin{array}{l} \text{Point B} \\ \hline \zeta = 0.6 \\ \rho_{fL/F_T}^2 = 0.6 \end{array}$$

$$\rho_{JL/J_m}^2 = 0.25$$

$$\begin{array}{l} \text{Point C} \\ \hline \zeta = 0.3 \\ \rho_{fL/F_T}^2 = 0.4 \end{array}$$

$$\rho_{JL/J_m}^2 = 0.111$$





$B=0$

$f=0$

$\frac{P^2 J_L}{5M}$

$f=1.6$

$f=1.5$

$f=1.4$

$f=1.3$

$f=1.2$

$f=1.1$

(A)

(B)

(C)

0.2 0.3 0.4 0.5 0.6 0.7 0.8 1 2 3 4 5 6 8 10 20 30 40 50 60 80

FIG. 7-16 REGIONS OF PARAMETER COMBINATIONS FOR WHICH BACKLASH AFFECTS MAXIMUM OVERSHOOT





The system was solved on the digital computer to obtain the maximum overshoot for these three sets of parameters. According to the curves point A falls to the left of the boundary of the  $\zeta = .8$  area. Therefore, the overshoot should be the same as that of the linear case. The computer solution gave an overshoot of 1.019, which is, in fact, identical to that of the linear case. Similarly, point B falls to the right of the  $\zeta = 0.6$  boundary and in the area where the amplitude of overshoot should not be the same as for the linear case. The computer solution gave a maximum overshoot of 1.110 which is slightly greater than the linear case. Point C falls to the right of the  $\zeta = 0.3$  boundary and in the area where the amplitude of overshoot should be different from that of the linear system. The computer solution gave a maximum overshoot of 1.41 while that of the linear system is 1.372. From these boundary curves one cannot determine the exact effect of backlash on the maximum overshoot of a system, but can determine in which systems backlash will cause an appreciable effect.

Another phenomena which is revealed in the results as plotted in figures 7-4 through 7-9 is that for all cases the greatest maximum overshoot occurs in the range  $0.1 < \rho^2 J_L / J_m < 10.0$  for the range of  $\rho^2 J_L / J_m$  tested. However, it appears that since the curves are trending upwards at the high end of the  $\rho^2 J_L / J_m$  axis that at very large inertia ratios the overshoot would be greater. It is felt that these large inertia



ratios are outside the practical range. An attempt was made to explain these phenomena but without success. It is often very difficult, if not impossible, to find a physical explanation for certain behavior caused by non-linearities. They can merely be pointed out from analyses of experimental information and accounted for accordingly

It is interesting to note that when the ratio of load friction to motor friction is below 0.4, as in figures 7-4 and 7-5 and 11, there is a possibility of an overshoot for the critically damped case, i.e.  $\zeta = 1.0$ , depending on the inertia ratio. At first glance one would reason that if the system is critically damped there should be no overshoot. However, it can be seen that if the friction ratio is small and the inertia ratio is large then the ratio of  $F_L/J_L$ , which is the slope of the drifting load trajectory, is made small. Therefore, when the load separates from the motor, its velocity remains fairly constant at a relatively high value and its momentum carries it past the correspondence point.





## 8. CONCLUSIONS

Since this report is to be the first of a series, it is apparent that the results are incomplete and the conclusions must therefore be brief:

1. It has been established by calculation that a second order feedback control system with backlash may or may not exhibit a limit cycle.
2. The existence of a limit cycle as a function of various parameters has been established, and a series of charts suitable for analysis and design have been prepared.
3. The amplitude of the limit cycle depends on the amount of backlash, and charts illustrating this dependence have been prepared.
4. Peak overshoot depends on the system parameters and the amount of backlash. Charts and equations suitable for analysis and design have been prepared.
5. The effect of elastic impact at the gear teeth is significant, but much less so than was anticipated. Most of the design charts include this effect.



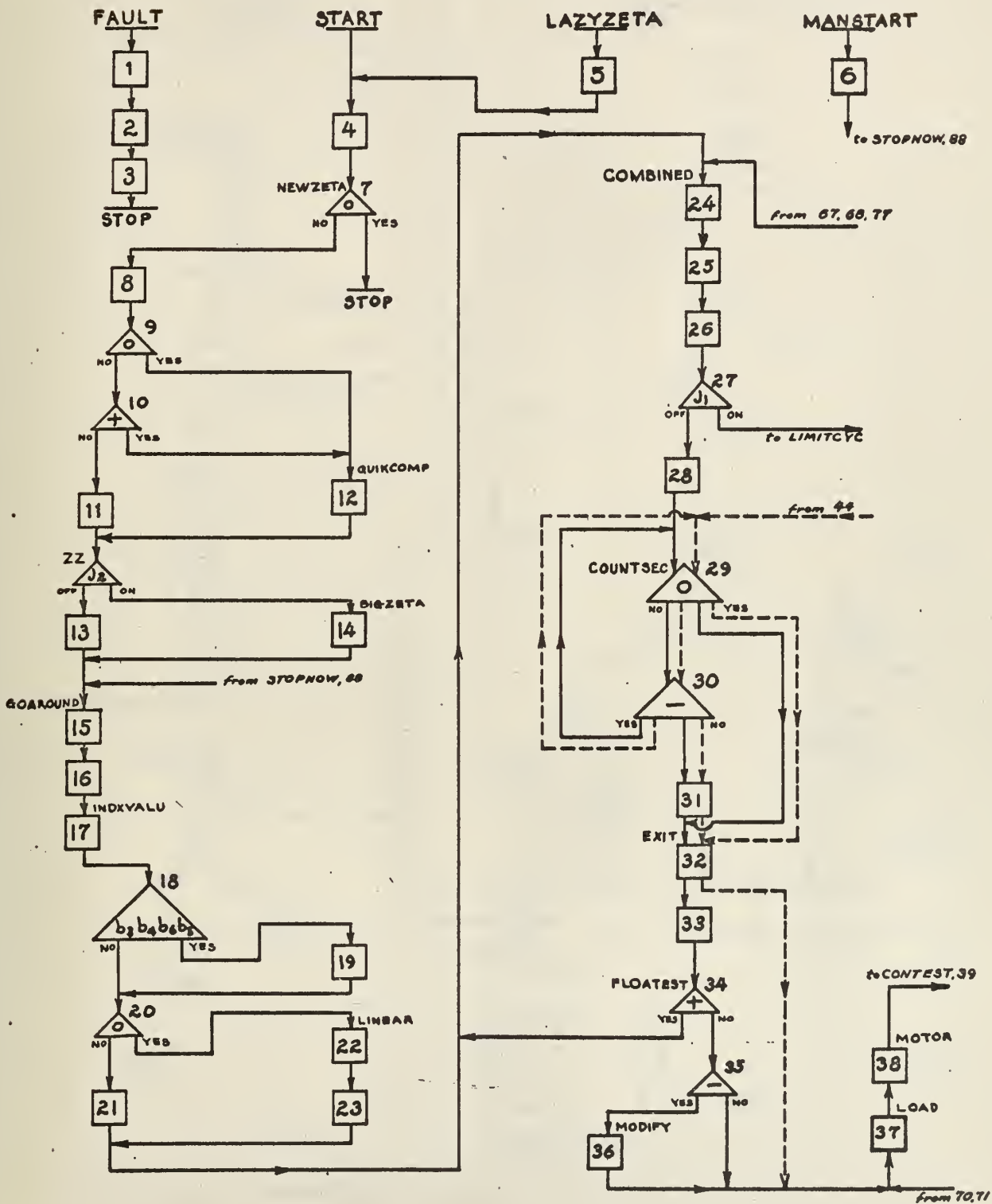
## REFERENCES

- a. Chestnut, H. and Mayer, R. W., Servomechanisms and Regulating System Design, John Wiley & Sons, Inc., New York, N. Y., 1955.
- b. Lutkenhouse, W. J., "Dividing Lines for Backlash in the Phaseplane," Unpublished Master's Thesis, United States Naval Postgraduate School, 1959.
- c. Pastel, M. P. and Thaler, G. J., "Instrument Servomechanisms with Backlash, Coulomb Friction, and Stiction," Trans. A.I.E.E. (Applications and Industry) July 1960.
- d. Knoll, A. L. and Narud, J. A., "Phase Plane Investigation of a Servomechanism with Backlash between Motor and Load," Technical Report 309 for Office of Naval Research, NR-375-017, Cruft Laboratory, Harvard University, Cambridge, Massachusetts, July 30, 1959.
- e. New, N. C., "Effects of Backlash in the Second Order Servo," Unpublished Master's Thesis, United States Naval Postgraduate School, 1960.
- f. Anderson, Jr., N. O., and Luckett, T. W., "Steady State Response of a Second Order Servomechanisms with Backlash and Resilience in the Gears between Motor and Load," Unpublished Master's Thesis, United States Naval Postgraduate School, 1961.
- g. Andrews, C. E., and Kelley, R. A., "Effects of Maximum Over-shoot and Settling Time when Backlash is present in a Second Order Servomechanism." Unpublished Master's Thesis, United States Naval Postgraduate School, 1961.



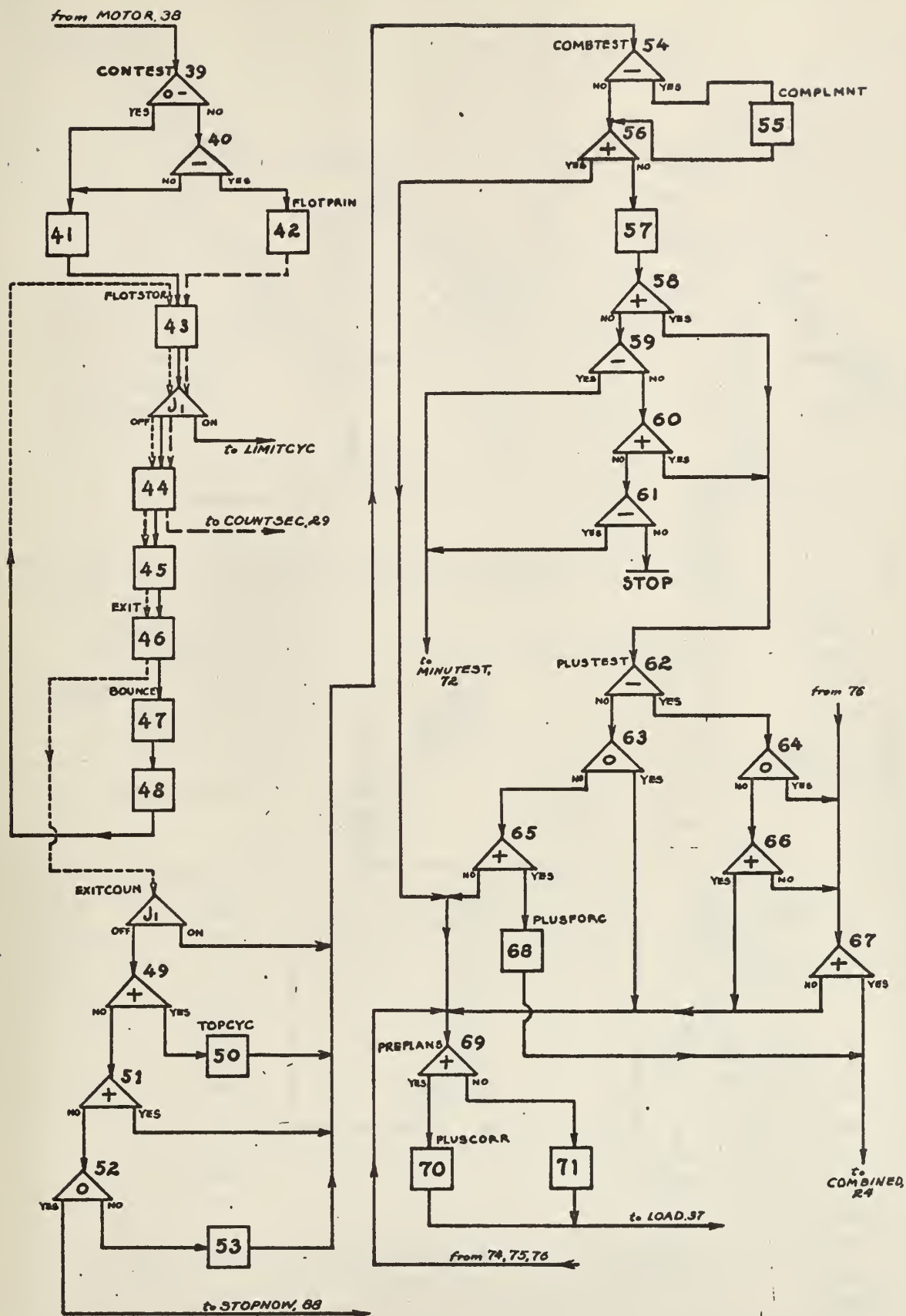
# APPENDIX A

## COMPUTATION FLOW DIAGRAM for CDC 1604 DIGITAL COMPUTER

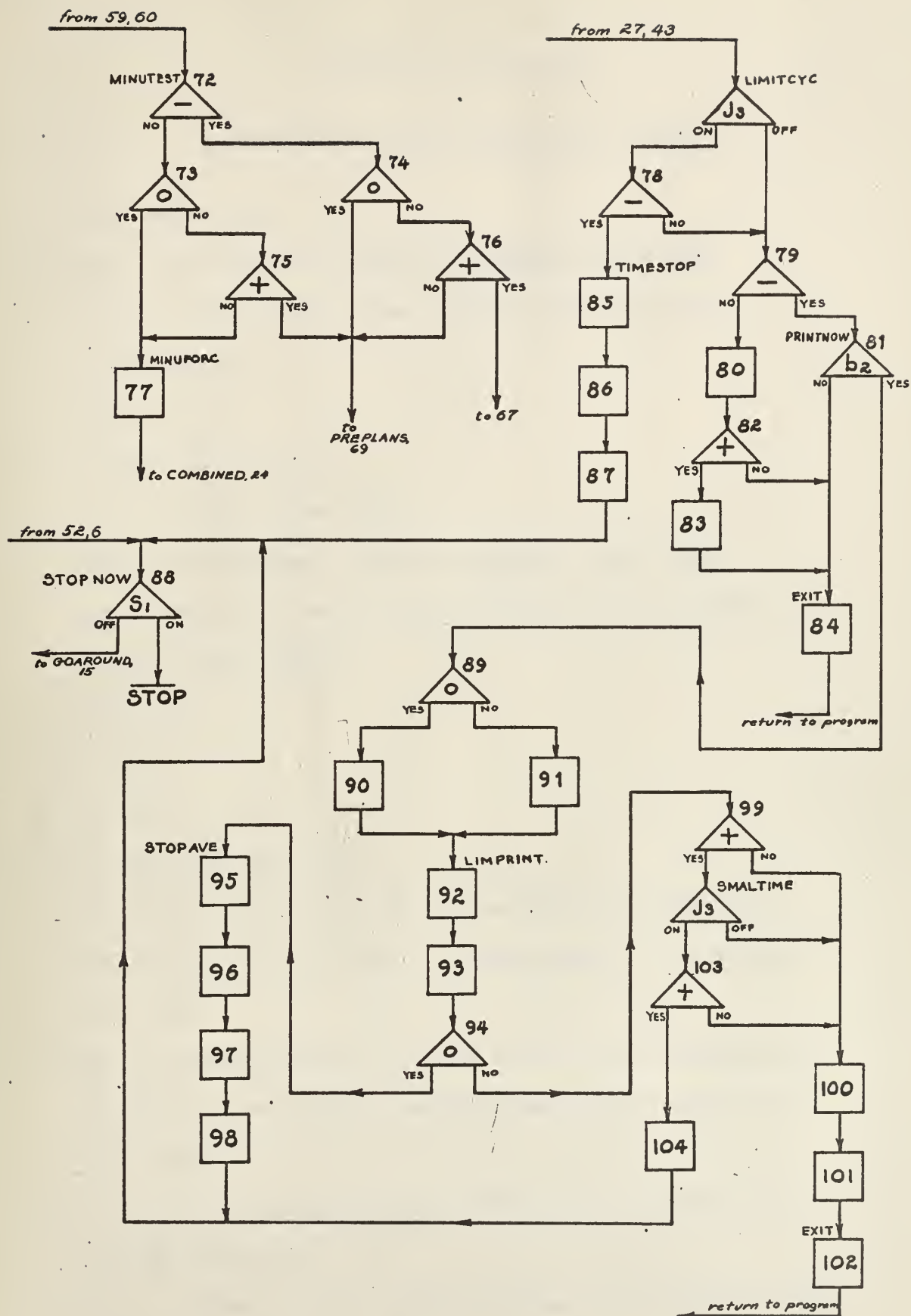
















## APPENDIX A (continued)

### EXPLANATION OF FLOW DIAGRAM BLOCK SYMBOLS

1. Clear fault stop.
2. Print last overshoot stored in LIMITBUF (symbol 888).  
Print out position in phase trajectory of fault stop  
(symbol 666).
3. End of file.
4. Actuate fault stop.
5. Load zeta from Index 1 ( $b_1$ ).
6. Print last overshoot stored on LIMITBUF (symbol 888).  
Print position in phase trajectory where it was manually  
stopped (symbol 1961).
7. Stop if Zeta = 0.
8.  $2\zeta\omega_n = A$
9. Is zeta = 0.1?
10. Is zeta less than 0.1?
11. Set up computation time of 0.01 seconds for problem and  
set up for print at every 0.1 seconds when zeta is greater  
than 0.1.
12. Set up computation time of 0.004 seconds for problem and set  
up for print at every 0.1 seconds when zeta is equal to or  
less than 0.1.
13. Set up limit cycle print-out routine for 20 overshoots and  
average the last 8.
14. Set up number of limit cycle print-outs and averaging routine  
depending upon the size of zeta:



<u><math>\rho</math></u>	<u>Overshoots</u>	<u>Start Averaging</u>	<u>Divide by *</u>	<u>Comp. Time</u>
$\geq 0.8$	6	4	2.0	0.01
0.6	7	5	2.0	0.01
0.5	8	5	3.0	0.01
0.4	10	7	3.0	0.01
0.3	14	10	4.0	0.01
0.2	20	12	8.0	0.01
$\leq 0.1$	17	12	5.0	0.004

\*The last row printed has this number printed on the far left if the problem has a normal solution. This number indicates how many overshoots were averaged. The average value has 1.0 subtracted from it and is printed in the far right of the same last row.

15. Page reject.

16. Clear buffers and set up for new problem.

17. Restitution,  $e$ , from Index 3 ( $b_3$ ).

Backlash,  $\Delta$ , from Index 4 ( $b_4$ ).

$J_m$  from Index 5 ( $b_5$ ).

$$\frac{J_T - J_m}{\rho^2} = J_L; \quad \frac{K}{J_m} = C; \quad \frac{J_m}{J_L}$$

$\frac{f_L}{F_T}$  from Index 6 ( $b_6$ ).

$$(f_L / F_T)(2\rho\omega_n)(J_T) = f_L; \quad f_L / J_L = B$$

$$\frac{f_L}{f_L / F_T} - \rho^2 f_L = f_m; \quad f_m / J_m = D$$

18. Have all values been cycled through?

19. Set STOPNOW after this run to stop absolutely.



20. Backlash,  $\Delta$ , = 0?

21. Print consecutive number of this parameter run and all the parameters used:

$$\begin{array}{cccccc}
 2 \rho \omega_n = A & J_m/J_L & f_L/P_T & e & \Delta & \rho \\
 J_m & J_L & J_m + \rho^2 J_L & f_m & f_L & \rho^2 \\
 K & K/J_m = C & f_m/J_m = D & f_L/J_L = B & \omega_n^2 & \rho
 \end{array}$$

22. Set program so always acts as combined system.

23. Print consecutive number of this parameter run and selected parameters for linear system:

$$2 \rho \omega_n = A \quad J_m + \rho^2 J_L \quad K \quad \omega_n^2 \quad \rho \quad \rho^2$$

24. Solve the second order equation by Runge-Kutta-Gill numerical integration every 0.01 seconds problem time when zeta is greater than 0.1, otherwise every 0.004 seconds. Initial conditions are  $\Theta_R = 1.0$ ,  $\dot{\Theta}_c = \Theta_c = 0$  and  $\ddot{\Theta}_c = 1.0$  or the previously computed point. Next point is computed by four iterations of:

$$\ddot{\Theta}_c = \omega_n^2 (\Theta_R - \Theta_c) - 2 \rho \omega_n \dot{\Theta}_c$$

25. Set EXIT from print routine.

26. Load time,  $\dot{\Theta}_c$  and  $\Theta_c$  in print buffer.

27. Go to LIMITCYC to print only the overshoot. Otherwise print the phase trajectory points for each 0.1 seconds up to a maximum of 12 cycles.

28. Store 0 for  $\dot{\Theta}_m$  and  $\Theta_m$





29. Is problem time 0.1 sec.?
30. Is problem time greater than 0.1 sec.?
31. Print the number of point computed, time,  $\dot{\Theta}_c$  and  $\Theta_c$ .
32. EXIT (automatically set for desired jump-out.)
33. Store time,  $\ddot{\Theta}_c$ ,  $\dot{\Theta}_c$  and  $\Theta_c$  for motor and load initial conditions.
34. Is slope  $N_L = N_S$ ?  

$$\frac{(\Theta_R - \Theta_c) \omega_n^2}{\dot{\Theta}_c} - 2\gamma \omega_n + \frac{f_L}{J_L} = \text{positive value?}$$
35. Is  $\dot{\Theta}_c$  negative?
36. Store  $\frac{\Theta_c - \Delta}{\rho}$  in  $\Theta_m$
37. Solve  $\ddot{\Theta}_c = -\left(\frac{f_L}{J_L}\right)(\dot{\Theta}_c)$  for  $\dot{\Theta}_c$  and  $\Theta_c$   
 by Runge-Kutta-Gill.
38. Solve  $\ddot{\Theta}_m = -\left(\frac{f_m}{J_m}\right)(\dot{\Theta}_m) + \left(\frac{K}{J_m}\right)(\Theta_R - \Theta_c)$   
 for  $\dot{\Theta}_m$  and  $\Theta_m$  by Runge-Kutta-Gill
39.  $\Theta_L - \rho \Theta_m \leq 0$ ?
40.  $\Theta_L - \rho \Theta_m - \Delta = \text{negative?}$
41. Set EXIT from print routine.
42. Set EXIT from print routine.
43. Load time,  $\dot{\Theta}_c$  and  $\Theta_c$ .
44. Load  $\dot{\Theta}_m$  and  $\Theta_m$ .
45. Print number of point computed and stored values.
46. EXIT (automatically set for desired jump-out).



47. Solve

$$\ddot{\Theta}'_c = \frac{J_m}{J_m + \rho^2 J_L} \left[ \rho \ddot{\Theta}_m (1+e) + \dot{\Theta}_c \left( \rho^2 \frac{J_L}{J_m} - e \right) \right]$$

$$\ddot{\Theta}'_m = \frac{\ddot{\Theta}' - e(\rho \ddot{\Theta}_m + \dot{\Theta}_c)}{\rho}$$

$$\ddot{\Theta}'_m = - \frac{f_m}{J_m} \dot{\Theta}'_m + \frac{K}{J_m} (\Theta_R - \Theta_c)$$

48. Set EXIT from print routine.

49. Is  $\dot{\Theta}_c$  positive?

50. Set up to count one phase trajectory when  $\dot{\Theta}_c$  is negative.

51. Is  $\Theta_c > 1.0$ ?

52. Have 12 cycles of phase trajectory been completed?

53. Arrange for no counting until  $\dot{\Theta}_c$  is positive again.

54. Is  $\rho \dot{\Theta}_m - \dot{\Theta}_c$  negative?

55. Set up  $-(\rho \dot{\Theta}_m - \dot{\Theta}_c)$ .

56. Is  $\rho \dot{\Theta}_m - \dot{\Theta}_c$  greater than preselected  $\epsilon$ ?

57. Set up combined system.

58. Is  $\dot{\Theta}_c$  positive?

59. Is  $\dot{\Theta}_c$  negative?

60. Is  $\Theta_c - 1$  positive?

61. Is  $\Theta_c - 1$  negative?

62. Is  $\Theta_c - 1$  negative?

63.  $\Theta_c - \rho \Theta_m = 0$ ?

64.  $\Theta_c - \rho \Theta_m = 0$ ?

65. Is  $\Theta_c - \rho \Theta_m$  positive?

66. Is  $\Theta_c - \rho \Theta_m$  positive?





67. Is Slope  $N_L = N_S$  ?

$$\frac{(1-\Theta_c) \omega_n^2}{\dot{\Theta}_c} - 2\rho \omega_n + \frac{f_L}{J_L} = \text{positive value?}$$

68. Modify FLOATEST to keep system combined. Takes off modification when  $\dot{\Theta}_c$  is negative.

69. Is  $\Theta_c - \rho \Theta_m$  positive?

70. Store  $\frac{\Theta_L - \Delta}{\rho}$  in  $\Theta_m$ .

71. Store  $\frac{\Theta_c}{\rho}$  in  $\Theta_m$ .

72. Is  $\Theta_c - 1$  negative?

73.  $\Theta_c - \rho \Theta_m = 0$ ?

74.  $\Theta_c - \rho \Theta_m = 0$ ?

75. Is  $\Theta_c - \rho \Theta_m$  positive?

76. Is  $\Theta_c - \rho \Theta_m$  positive?

77. Modify FLOATEST to keep system combined. Takes off modification when  $\dot{\Theta}_c$  is positive.

78. Have 1 1/2 minutes of real time elapsed since the last print-out?

79. Is  $\Theta_c < 1.0$ ?

80. Set up to print when in the fourth quadrant.

81. Check if in the fourth quadrant.

82. Is the new  $\Theta_c$  greater than the previous  $\Theta_c$ ?

83. Store the new time,  $\dot{\Theta}_c$  and  $\Theta_c$ .

84. EXIT (automatically set for desired jump-out).

85. Print the last overshoot stored in LIMITBUF (symbol 888)

86. Stop real time clock.

87. Print position in phase trajectory where it was stopped by the real time clock (symbol 999).



88. Return to beginning to start new problem if new parameters remain to be evaluated. Unconditional stop if all parameters have been evaluated.
89. Has the required number of overshoots been evaluated prior to starting the averaging routine?
90. Add the  $\Theta_c$  just evaluated to the previous sum for averaging.
91. Add one to the count prior to averaging.
92. Clear time clock.
93. Print time,  $\dot{\Theta}_c$  and  $\Theta_c$ .
94. Required number of total print-outs?
95. Clear buffers.
96. Obtain the average of  $\Theta_c$ .
97. Subtract 1.0.
98. Print the average of  $\Theta_c - 1.0$  and how many overshoots were utilized to obtain the average.
99. Is  $\Theta_c$  less than 1.005 radians?
100. Clear buffers.
101. Start real time clock.
102. EXIT (automatically set to desired jump-out).
103. Has 30 seconds of real time elapsed since the last print-out?
104. Print the position in the phase trajectory where it was stopped by the real time clock and  $\Theta_c$  being less than 1.005 radians (symbol 1005).



#### Jump Switches:

$J_1$  - For LIMITCYC, allows the maximum overshoot print-out only.

With  $J_1$  down, a phase trajectory is printed for a maximum of 12 cycles.

$J_2$  - Set the number of print-outs depending on zeta. Change the number of overshoot values used to obtain the average value.

$J_3$  - Use the real time clock for an automatic recycle to a new parameter when have:

a. 1 1/2 minutes maximum after the last print-out.

b. 30 seconds maximum and  $\theta_c$  is 1.005 radians or less.

#### Stop Switches:

$S_1$  - Stops at the end of this parameter run or stops at the end of the manual print-out.





## APPENDIX B

## COMPUTER PROGRAM

00007	74	0	00070	FAULT	ORG	00007
	75	0	40701		EXF	0 00070
					SLJ	0 FAULPRIN
40000	74	0	00100	START	ORG	40000
	75	0	40004		EXF	0 00100
40001	12	1	40623	LAZZETA	SLJ	0 NEWZETA-1
	20	0	40425		LDA	1 ZETAINDX
40002	50	1	00000		STA	0 ZETA
	75	0	40000		ENI	0 0
40003	75	0	40674	MANSTART	SLJ	0 START
	50	0	00000		SLJ	0 MANUAL
40004	12	0	40565		ENI	0 0
	20	0	40563		LDA	0 NEWSTOP
40005	12	0	40425	NEWZETA	STA	0 STOPNOW
	22	0	40564		LDA	0 ZETA
40006	32	0	40665		AJP	0 STOPINDX
	32	0	40426		FMU	0 TWO
40007	20	0	40404		FMU	0 OMEGAN
	12	0	40624		STA	0 A
40010	31	0	40425		LDA	0 ZETAINDX+1
	22	0	40433		FSB	0 ZETA
40011	22	2	40433		AJP	0 QUIKCOMP
	12	0	40402		AJP	2 QUIKCOMP
40012	20	0	40154		LDA	0 POINT01
	20	0	40173		STA	0 TABLES+1
40013	20	0	40207		STA	0 TABLE+1
	12	0	40661		STA	0 TABLEM+1
40014	20	0	40400		LDA	0 COUNT10
	50	0	00000		STA	0 TENTHSEC
40015	75	2	40437	ZZ	ENI	0 0
	50	0	00000		SLJ	2 BIGZETA
40016	12	0	40652		ENI	0 0
	20	0	40616		LDA	0 STOP20
40017	12	0	40662		STA	0 STOPZETA
	20	0	40617		LDA	0 COUNT12
40020	12	0	40672		STA	0 COUNTZET
	20	0	40620		LDA	0 EIGHT
40021	10	0	00010		STA	0 DIVIDE
	61	0	40562		ENA	0 10
40022	75	4	71000	GOAROUND	SAL	0 STOPRINT
	50	0	00000		SLJ	4 DECOF
40023	02	0	40427		ENI	0 0
	04	0	00000		02	0 FORZEROS
40024	12	0	40664		04	0 0
	20	0	40156		LDA	0 ONE
40025	10	0	00000		STA	0 UDOT
	20	0	00000		ENA	0 0
40026	20	0	40162		STA	0 0
	20	0	40161		STA	0 THETA
40027	20	0	40157		STA	0 THETADOT
	20	0	40155		STA	0 U
40030	20	0	40377		STA	0 T
	20	0	40615		STA	0 INDEX
40031	20	0	40351		STA	0 INDEXAVE
	20	0	40352		STA	0 PRINTBUF+3
40032	20	0	40353		STA	0 PRINTBUF+4
	20	0	40614		STA	0 PRINTBUF+5
40033	20	0	40607		STA	0 LIMINDEX
	20	0	40610		STA	0 LIMITBUF+2
40034	20	0	40611		STA	0 LIMITBUF+3
	20	0	40612		STA	0 LIMITBUF+4
40035	20	0	40613		STA	0 LIMITBUF+5
	12	0	40621		STA	0 LIMITBUF+6
40036	20	0	40326		LDA	0 PRINTSET
	20	0	40335		STA	0 OK2PRINT+1
40037	12	0	40622		STA	0 BOUNPRIN+4
	20	0	40544		LDA	0 NEWLIMPT
40040	12	0	40253		STA	0 LIMPRINT+1
	20	0	40071		LDA	0 FLOTDATA
40041	12	0	40254		STA	0 FLOATEST
	20	0	40072		LDA	0 FLOTDATA+1
40042	75	0	40452	NEWINPUT	STA	0 FLOATEST+1
	50	0	00000		SLJ	0 INDXVALU
					ENI	0 00000



40043	12	0	40410
	22	0	40500
40044	12	0	40513
	20	0	40071
40045	75	4	71000
	50	0	00000
40046	01	0	40404
	06	0	00001
40047	72	0	40046
	75	4	71000
40050	01	0	40412
	06	0	00000
40051	72	0	40510
	75	4	71000
40052	01	0	40420
	06	0	00000
40053	10	0	00000
	20	0	40160
40054	20	0	40163
	75	4	60200
40055	00	0	40153
	00	0	40164
40056	75	4	60201
	50	0	00000
40057	75	0	40310
	50	0	00000
40060	12	0	40155
	20	0	40174
40061	20	0	40210
	12	0	40156
40062	20	0	40175
	33	0	40411
40063	20	0	40211
	12	0	40157
40064	20	0	40176
	20	0	40200
40065	33	0	40411
	20	0	40212
40066	20	0	40214
	12	0	40162
40067	20	0	40201
	33	0	40411
40070	20	0	40215
	50	0	00000
40071	13	0	40162
	30	0	40664
40072	32	0	40424
	33	0	40161
40073	31	0	40404
	30	0	40423
40074	22	2	40053
	12	0	40161
40075	22	3	40270
	50	0	00000
40076	10	0	00000
	20	0	40177
40077	20	0	40202
	20	0	40213
40100	20	0	40216
	75	4	60200
40101	00	0	40172
	00	0	40203
40102	75	4	60201
	50	0	00000
40103	75	4	60200
	50	0	00000
40104	00	0	40206
	00	0	40217
40105	75	4	60201
	50	0	00000
40106	13	0	40215
	32	0	40411
40107	30	0	40201
	22	0	40112

COMBINED

FLOATEST

LOAD

MOTOR

CONTEST

LDA	0	DELTA
AJP	0	LINEAR
LDA	0	NOSINK
STA	0	FLOATEST
SLJ	4	DECOF
ENI	0	0
01	0	A
06	0	1
RAO	0	7-1
SLJ	4	DECOF
01	0	MOINERT
06	0	0
RAO	0	LINEAR+10
SLJ	4	DECOF
01	0	KMOTCONS
06	0	0
ENA	0	0
STA	0	QX
STA	0	QY
SLJ	4	RUNGE
0	0	TABLES
0	0	DERIVES
SLJ	4	RUNGE+1
ENI	0	0
SLJ	0	COMBPRIN
ENI	0	0
LDA	0	T
STA	0	TL
STA	0	TM
LDA	0	UDOT
STA	0	VDOT
FDV	0	RHO
STA	0	WDOT
LDA	0	U
STA	0	V
STA	0	THETADL
FDV	0	RHO
STA	0	W
STA	0	THETADM
LDA	0	THETA
STA	0	THETAL
FDV	0	RHO
STA	0	THETAM
ENI	0	0
LAC	0	THETA
FAD	0	ONE
FMU	0	OMEGANSQ
FDV	0	THETADOT
FSB	0	A
FAD	0	B
AJP	2	COMBINED
LDA	0	THETADOT
AJP	3	MODIFY
ENI	0	0
ENA	0	0
STA	0	QL
STA	0	QLL
STA	0	QM
STA	0	QMM
SLJ	4	RUNGE
0	0	TABLEL
0	0	DERIVL
SLJ	4	RUNGE+1
ENI	0	0
SLJ	4	RUNGE
ENI	0	0
0	0	TABLEM
0	0	DERIVM
SLJ	4	RUNGE+1
ENI	0	0
LAC	0	THETAM
FMU	0	RHO
FAD	0	THETAL
AJP	0	BOUNCE





40110	22	3	40112
	31	0	40410
40111	22	3	40317
	50	0	00000
40112	75	0	40331
	50	0	00000
40113	12	0	40200
	20	0	40212
40114	12	0	40417
	33	0	40405
40115	31	0	40407
	32	0	40200
40116	20	0	40200
	12	0	40664
40117	30	0	40407
	32	0	40411
40120	32	0	40214
	30	0	40200
40121	33	0	40414
	32	0	40412
40122	20	0	40200
	20	0	40176
40123	13	0	40176
	32	0	40423
40124	20	0	40175
	13	0	40214
40125	32	0	40411
	30	0	40212
40126	32	0	40407
	30	0	40200
40127	33	0	40411
	20	0	40214
40130	20	0	40212
	13	0	40212
40131	32	0	40422
	20	0	40211
40132	13	0	40201
	30	0	40664
40133	32	0	40421
	30	0	40211
40134	20	0	40211
	75	0	40332
40135	50	0	00000
	12	0	40214
40136	32	0	40411
	31	0	40200
40137	22	3	40276
	50	0	00000
40140	65	0	40403
	75	0	40301
40141	12	0	40200
	20	0	40161
40142	20	0	40157
	13	0	40157
40143	32	0	40404
	20	0	40156
40144	12	0	40201
	20	0	40162
40145	13	0	40162
	30	0	40664
40146	32	0	40424
	30	0	40156
40147	20	0	40156
	12	0	40174
40150	20	0	40155
	12	0	40200
40151	22	2	40225
	22	3	40255
40152	75	0	40273
	50	0	00000
40153	00	0	00000
	00	0	00002
40154	17	7	15075
	34	1	21727

# BOUNCE

# COMBTTEST

# TABLES

AJP	3	BOUNCE
FSB	0	DELTA
AJP	3	FLOTPRIN
ENI	0	0
SLJ	0	BOUNPRIN
ENI	0	0
LDA	0	THETADL
STA	0	W
LDA	0	RHOSQ
FDV	0	INERTTRAT
FSB	0	RESTITUT
FMU	0	THETADL
STA	0	THETADL
LDA	0	ONE
FAD	0	RESTITUT
FMU	0	RHO
FMU	0	THETADM
FAD	0	THETADL
FDV	0	TOTINERT
FMU	0	MOINERT
STA	0	THETADL
STA	0	V
LAC	0	V
FMU	0	B
STA	0	VDOT
LAC	0	THETADM
FMU	0	RHO
FAD	0	W
FMU	0	RESTITUT
FAD	0	THETADL
FDV	0	RHO
STA	0	THETADM
STA	0	W
LAC	0	W
FMU	0	D
STA	0	WDOT
LAC	0	THETAL
FAD	0	ONE
FMU	0	C
FAD	0	WDOT
STA	0	WDOT
SLJ	0	BOUNPRIN+1
ENI	0	0
LDA	0	THETADM
FMU	0	RHO
FSB	0	THETADL
AJP	3	COMPLMNT
ENI	0	00000
THS	0	DIFFERNT
SLJ	0	PREPLANS
LDA	0	THETADL
STA	0	THETADOT
STA	0	U
LAC	0	U
FMU	0	A
STA	0	UDOT
LDA	0	THETAL
STA	0	THETA
LAC	0	THETA
FAD	0	ONE
FMU	0	OMEGANSQ
FAD	0	UDOT
STA	0	UDOT
LDA	0	TL
STA	0	T
LDA	0	THETADL
AJP	2	PLUSTEST
AJP	3	MINUTEST
SLJ	0	TESTZERO
ENI	0	0
OCT	2	
DEC		.01



40155	00 0 00000	T	DEC	0
40156	00 0 00000	UDOT	DEC	1.0
40157	00 0 00000	U	DEC	0
40160	00 0 00000	QX .	DEC	0
40161	00 0 00000	THETADOT	DEC	0
40162	00 0 00000	THETA	DEC	0
40163	00 0 00000	QY	DEC	0
40164	13 0 40157	DERIVES	LAC	0 U
	32 0 40404		FMU	0 A
40165	20 0 40156		STA	0 UDOT
	13 0 40162		LAC	0 THETA
40166	30 0 40664		FAD	0 ONE
	32 0 40424		FMU	0 OMEGANSQ
40167	30 0 40156		FAD	0 UDOT
	20 0 40156		STA	0 UDOT
40170	12 0 40157		LDA	0 U
	20 0 40161		STA	0 THETADOT
40171	75 0 60202		SLJ	0 RUNGE+2
	50 0 00000		ENI	0 0
40172	00 0 00000	TABLEL	OCT	2
	00 0 00002			
40173	17 7 15075		DEC	.01
	34 1 21727			
40174	00 0 00000	TL	DEC	0
	00 0 00000			
40175	00 0 00000	VDOT	DEC	0
	00 0 00000			
40176	00 0 00000	V	DEC	0
	00 0 00000			
40177	00 0 00000	QL	DEC	0
	00 0 00000			
40200	00 0 00000	THETADL	DEC	0
	00 0 00000			
40201	00 0 00000	THETAL	DEC	0
	00 0 00000			
40202	00 0 00000	QLL	DEC	0
	00 0 00000			
40203	13 0 40176	DERIVL	LAC	0 V
	32 0 40423		FMU	0 B
40204	20 0 40175		STA	0 VDOT
	12 0 40176		LDA	0 V
40205	20 0 40200		STA	0 THETADL
	75 0 60202		SLJ	0 RUNGE+2
40206	00 0 00000	TABLEM	OCT	2
	00 0 00002			
40207	17 7 15075		DEC	.01
	34 1 21727			
40210	00 0 00000	TM	DEC	0
	00 0 00000			
40211	00 0 00000	WDOT	DEC	0
	00 0 00000			
40212	00 0 00000	W	DEC	0
	00 0 00000			
40213	00 0 00000	QM	DEC	0
	00 0 00000			
40214	00 0 00000	THETADM	DEC	0
	00 0 00000			
40215	00 0 00000	THETAM	DEC	0
	00 0 00000			
40216	00 0 00000	QMM	DEC	0
	00 0 00000			
40217	13 0 40201	DERIVM	LAC	0 THETAL
	32 0 40421		FMU	0 C
40220	20 0 40211		STA	0 WDOT
	13 0 40212		LAC	0 W
40221	32 0 40422		FMU	0 D
	30 0 40421		FAD	0 C



40222	30	0	40211	FAD	0	WDOT
	20	0	40211	STA	0	WDOT
40223	12	0	40212	LDA	0	W
	20	0	40214	STA	0	THETADM
40224	75	0	60202	SLJ	0	RUNGE+2
	50	0	00000	ENI	0	0
40225	12	0	40201	LDA	0	THETAL
	31	0	40664	FSB	0	ONE
40226	22	3	40232	AJP	3	PLUSTEST+5
	13	0	40215	LAC	0	THETAM
40227	32	0	40411	FMU	0	RHO
	30	0	40201	FAD	0	THETAL
40230	22	0	40301	AJP	0	PREPLANS
	22	2	40241	AJP	2	PLUSFORC
40231	75	0	40301	SLJ	0	PREPLANS
	50	0	00000	ENI	0	0
40232	13	0	40215	LAC	0	THETAM
	32	0	40411	FMU	0	RHO
40233	30	0	40201	FAD	0	THETAL
	22	0	40235	AJP	0	PLUSTEST+10
40234	22	2	40301	AJP	2	PREPLANS
	50	0	00000	ENI	0	0
40235	13	0	40162	LAC	0	THETA
	30	0	40664	FAD	0	ONE
40236	32	0	40424	FMU	0	OMEGANSQ
	33	0	40161	FDV	0	THETADOT
40237	31	0	40404	FSB	0	A
	30	0	40423	FAD	0	B
40240	22	2	40053	AJP	2	COMBINED
	75	0	40301	SLJ	0	PREPLANS
40241	12	0	40244	LDA	0	NUMB
	20	0	40071	STA	0	FLOATEST
40242	12	0	40245	LDA	0	NUMB+1
	20	0	40072	STA	0	FLOATEST+1
40243	75	0	40053	SLJ	0	COMBINED
	50	0	00000	ENI	0	0
40244	12	0	40161	LDA	0	THETADOT
	22	2	40053	AJP	2	COMBINED
40245	75	0	40250	SLJ	0	RESTORET
	50	0	00000	ENI	0	0
40246	12	0	40161	LDA	0	THETADOT
	22	3	40053	AJP	3	COMBINED
40247	75	0	40250	SLJ	0	RESTORET
	50	0	00000	ENI	0	0
40250	12	0	40253	LDA	0	FLOTDATA
	20	0	40071	STA	0	FLOATEST
40251	12	0	40254	LDA	0	FLOTDATA+1
	20	0	40072	STA	0	FLOATEST+1
40252	75	0	40053	SLJ	0	COMBINED
	50	0	00000	ENI	0	0
40253	13	0	40162	LAC	0	THETA
	30	0	40664	FAD	0	ONE
40254	32	0	40424	FMU	0	OMEGANSQ
	33	0	40161	FDV	0	THETADOT
40255	12	0	40201	LDA	0	THETAL
	31	0	40664	FSB	0	ONE
40256	22	2	40262	AJP	2	MINUTEST+5
	13	0	40215	LAC	0	THETAM
40257	32	0	40411	FMU	0	RHO
	30	0	40201	FAD	0	THETAL
40260	22	0	40265	AJP	0	MINUFORC
	22	2	40301	AJP	2	PREPLANS
40261	75	0	40265	SLJ	0	MINUFORC
	50	0	00000	ENI	0	0
40262	13	0	40215	LAC	0	THETAM
	32	0	40411	FMU	0	RHO
40263	30	0	40201	FAD	0	THETAL
	22	0	40301	AJP	0	PREPLANS
40264	22	2	40235	AJP	2	PLUSTEST+10
	75	0	40301	SLJ	0	PREPLANS
40265	12	0	40246	LDA	0	DUMB
	20	0	40071	STA	0	FLOATEST
40266	12	0	40247	LDA	0	DUMB+1
	20	0	40072	STA	0	FLOATEST+1





40267	75 0	40053		SLJ	0	COMBINED
	50 0	00000		ENI	0	0
40270	12 0	40162	MODIFY	LDA	0	THETA
	31 0	40410		FSB	0	DELTA
40271	33 0	40411		FDV	0	RHO
	20 0	40215		STA	0	THETAM
40272	75 0	40076		SLJ	0	LOAD
	50 0	00000		ENI	0	0
40273	12 0	40201	TESTZERO	LDA	0	THETAL
	31 0	40664		FSB	0	ONE
40274	22 2	40225		AJP	2	PLUSTEST
	22 3	40255		AJP	3	MINUTEST
40275	76 0	00000		SLS	0	0
	50 0	00000		ENI	0	0
40276	20 0	40300	COMPLMNT	STA	0	COMPLMNT+2
	13 0	40300		LAC	0	COMPLMNT+2
40277	75 0	40140		SLJ	0	COMBTST+3
	50 0	00000		ENI	0	0
40300	00 0	00000		BSS	0	1
	00 0	00000				
40301	13 0	40215	PREPLANS	LAC	0	THETAM
	32 0	40411		FMU	0	RHO
40302	30 0	40201		FAD	0	THETAL
	22 2	40305		AJP	2	PLUSCORR
40303	12 0	40201		LDA	0	THETAL
	33 0	40411		FDV	0	RHO
40304	20 0	40215		STA	0	THETAM
	75 0	40076		SLJ	0	LOAD
40305	12 0	40201	PLUSCORR	LDA	0	THETAL
	31 0	40410		FSB	0	DELTA
40306	33 0	40411		FDV	0	RHO
	20 0	40215		STA	0	THETAM
40307	75 0	40076		SLJ	0	LOAD
	50 0	00000		ENI	0	0
40310	12 0	40354	COMBPRIN	LDA	0	COMBEXIT
	20 0	40360		STA	0	EXIT
40311	12 0	40155		LDA	0	T
	20 0	40346		STA	0	PRINTBUF
40312	12 0	40157		LDA	0	U
	20 0	40347		STA	0	PRINTBUF+1
40313	12 0	40162		LDA	0	THETA
	20 0	40350		STA	0	PRINTBUF+2
40314	75 1	40522		SLJ	1	LIMITCYC
	10 0	00000		ENA	0	0
40315	20 0	40351		STA	0	PRINTBUF+3
	20 0	40352		STA	0	PRINTBUF+4
40316	75 0	40321		SLJ	0	COUNTSEC
	50 0	00000		ENI	0	0
40317	12 0	40355	FLOTPRIN	LDA	0	FLOTEXIT
	20 0	40360		STA	0	EXIT
40320	75 4	40337		SLJ	4	FLOTSTOR
	50 0	00000		ENI	0	0
40321	72 0	40377	COUNTSEC	RAO	0	INDEX
	12 0	40377		LDA	0	INDEX
40322	15 0	40400		SUB	0	TENTHSEC
	22 0	40325		AJP	0	OK2PRINT
40323	22 2	40322		AJP	2	COUNTSEC+1
	14 0	40400		ADD	0	TENTHSEC
40324	20 0	40377		STA	0	INDEX
	75 0	40360		SLJ	0	EXIT
40325	75 4	71000	OK2PRINT	SLJ	4	DECOF
	50 0	00000		ENI	0	0
40326	00 0	40346		00	0	PRINTBUF
	06 0	00001		06	0	1
40327	72 0	40326		RAO	0	/-1
	10 0	00000		ENA	0	0
40330	20 0	40377		STA	0	INDEX
	75 0	40360		SLJ	0	EXIT
40331	12 0	40356	BOUNPRIN	LDA	0	BOUNEXIT
	75 0	40333		SLJ	0	BOUNPRIN+2
40332	12 0	40357		LDA	0	BOUNEXIT+1
	50 0	00000		ENI	0	0
40333	20 0	40360		STA	0	EXIT
	75 4	40337		SLJ	4	FLOTSTOR



40334	75 4	71000	SLJ	4	DECOF
	50 0	00000	ENI	0	0
40335	00 0	40346	00	0	PRINTBUF
	06 0	00001	06	0	1
40336	75 0	40360	SLJ	0	EXIT
	50 0	00000	ENI	0	0
40337	75 0	00000	SLJ	0	0
	12 0	40174	LDA	0	TL
40340	20 0	40346	STA	0	PRINTBUF
	12 0	40176	LDA	0	V
40341	20 0	40347	STA	0	PRINTBUF+1
	12 0	40201	LDA	0	THETAL
40342	20 0	40350	STA	0	PRINTBUF+2
	75 1	40522	SLJ	1	LIMITCYC
40343	12 0	40212	LDA	0	W
	20 0	40351	STA	0	PRINTBUF+3
40344	12 0	40215	LDA	0	THETAM
	20 0	40352	STA	0	PRINTBUF+4
40345	75 0	40337	SLJ	0	FLOTSTOR
	50 0	00000	ENI	0	0
40346	00 0	00000	BSS	6	
	00 0	00000			
40354	75 0	40060	COMBEXIT	SLJ	0 COMBINED+5
	50 0	00000	ENI	0	0
40355	75 0	40076	FLOTEXIT	SLJ	0 LOAD
	50 0	00000	ENI	0	0
40356	75 0	40113	BOUNEXIT	SLJ	0 BOUNCE+1
	50 0	00000	ENI	0	0
40357	75 0	40361	SLJ	0	EXITCOUN
	50 0	00000	ENI	0	0
40360	00 0	00000	BSS	1	
	00 0	00000			
40361	75 1	40135	EXITCOUN	SLJ	1 COMBTTEST
	72 0	40377	RAO	0	INDEX
40362	72 0	40335	RAO	0	BOUNPRIN+4
	12 0	40347	LDA	0	PRINTBUF+1
40363	22 2	40372	AJP	2	TOPCYC
	12 0	40350	LDA	0	PRINTBUF+2
40364	31 0	40664	FSB	0	ONE
	22 2	40135	AJP	2	COMBTTEST
40365	72 0	40615	RAO	0	INDEXAVE
	12 0	40615	LDA	0	INDEXAVE
40366	15 0	40662	SUB	0	COUNT12
	22 0	40563	AJP	0	STOPNOW
40367	14 0	40662	ADD	0	COUNT12
	20 0	40615	STA	0	INDEXAVE
40370	12 0	40375	LDA	0	NEGAJUMP
	20 0	40364	STA	0	EXITCOUN+3
40371	75 0	40135	SLJ	0	COMBTTEST
	50 0	00000	ENI	0	00000
40372	12 0	40350	TOPCYC	LDA	0 PRINTBUF+2
	31 0	40664	FSB	0	ONE
40373	22 3	40135	AJP	3	COMBTTEST
	12 0	40376	LDA	0	NEWLOWER
40374	20 0	40364	STA	0	EXITCOUN+3
	75 0	40135	SLJ	0	COMBTTEST
40375	75 0	40135	SLJ	0	COMBTTEST
	50 0	00000	ENI	0	0
40376	31 0	40664	NEWLOWER	FSB	0 ONE
	22 2	40135	AJP	2	COMBTTEST
40377	00 0	00000	INDEX	OCT	0
	00 0	00000			
40400	00 0	00000	TENTHSEC	OCT	12
	00 0	00012			
40401	17 7	04061	POINT004	DEC	0.004
	11 5	64570			
40402	17 7	15075	POINT01	DEC	0.01
	34 1	21727			
40403	17 3	74000	DIFFERNT	OCT	1737400000000000
	00 0	00000			
40404	20 0	06314	A	DEC	.8
	63 1	46314			
40405	20 0	14000	INERTRAT	DEC	1.0
	00 0	00000			





40406	00 0	000000	FLFTPRIN	BSS	1
40407	00 0	000000	RESTITUT	DEC	0
40410	17 7	64631	DELTA	DEC	.3
40411	46 3	14631	RHO.	DEC	1.0
40412	20 0	04000	MOINERT	DEC	.5
40413	00 0	000000	JLOADVAL	BSS	1
40414	20 0	14000	TOTINERT	DEC	1.0
40415	00 0	000000	FMOTOR	BSS	1
40416	00 0	000000	FLOAD	BSS	1
40417	20 0	14000	RHOSQ	DEC	1.0
40420	20 0	14000	KMOTCONS	DEC	1.0
40421	20 0	24000	C	DEC	2.0
40422	17 7	66314	D	DEC	.4
40423	63 1	46314	B	DEC	.01
40424	17 7	15075	OMEGANSQ	DEC	1.0
40425	34 1	21727	ZETA	BSS	1
40426	20 0	14000	OMEGAN	DEC	1.0
40427	00 0	000000	FORZEROS	BSS	4
40433	12 0	40401	RUNGE	EQU	60200
40434	20 0	40154	DECOF	EQU	71000
40435	20 0	40207	QUICKCOMP	LDA	0 POINT004
40436	12 0	40654		STA	0 TABLES+1
40437	20 0	40400		STA	0 TABLEL+1
40440	20 0	40015		STA	0 TABLEM+1
40441	75 0	40000		LDA	0 STOP25
40442	50 0	00000		STA	0 TENTHSEC
40443	50 1	00000	BIGZETA	SLJ	0 ZZ
40444	50 0	00000		ENI	0 0
40445	12 0	40425		ENI	1 0
40446	31 1	40636		ENI	0 0
40447	22 2	40444		LDA	0 ZETA
40448	22 0	40444		FSB	1 POINT8
40449	54 1	00006		AJP	2 ZETAPLUS
40450	75 0	40440		AJP	0 ZETAPLUS
40451	50 1	00006		ISK	1 6
40452	50 0	00000		SLJ	0 /-2
40453	12 1	40645	ZETAPLUS	ENI	1 6
40454	20 0	40616		ENI	0 0
40455	12 1	40655		LDA	1 STOP6
40456	20 0	40617		STA	0 STOPZETA
40457	12 1	40665		LDA	1 COUNT4
40458	20 0	40620		STA	0 COUNTZET
40459	12 1	40645		LDA	1 TWO
40460	15 1	40655		STA	0 DIVIDE
40461	61 0	40562		LDA	1 STOP6
40462	50 1	00000		SUB	1 COUNT4
40463	75 0	40022		SAL	0 STOPRINT
40464	50 0	00000		ENI	1 0
40465	12 3	40706	INDXVALU	SLJ	0 GOAROUND
40466	20 0	40407		ENI	0 0
40467	12 4	40726		LDA	3 RESTVALU
40468	20 0	40410		STA	0 RESTITUT
40469	12 5	40747		LDA	4 DELTAVAL
40470	20 0	40412		STA	0 DELTA
40471	20 0	40412		LDA	5 JMOTVALU
40472	20 0	40412		STA	0 MOINERT



40455	12 0	40414	LDA	0	TOTINERT
	31 0	40412	FSB	0	MOINERT
40456	33 0	40417	FDV	0	RHOSQ
	20 0	40413	STA	0	JLOADVAL
40457	12 0	40420	LDA	0	KMOTCONS
	33 0	40412	FDV	0	MOINERT
40460	20 0	40421	STA	0	C
	12 0	40412	LDA	0	MOINERT
40461	33 0	40413	FDV	0	JLOADVAL
	20 0	40405	STA	0	INERTRAT
40462	12 6	40774	LDA	6	FLFTRATO
	20 0	40406	STA	0	FLFTPRIN
40463	32 0	40404	FMU	0	A
	32 0	40414	FMU	0	TOTINERT
40464	20 0	40416	STA	0	FLOAD
	33 0	40413	FDV	0	JLOADVAL
40465	20 0	40423	STA	0	B
	12 0	40416	LDA	0	FLOAD
40466	32 0	40417	FMU	0	RHOSQ
	20 0	40415	STA	0	FMOTOR
40467	12 0	40404	LDA	0	A
	32 0	40414	FMU	0	TOTINERT
40470	31 0	40415	FSB	0	FMOTOR
	20 0	40415	STA	0	FMOTOR
40471	33 0	40412	FDV	0	MOINERT
	20 0	40422	STA	0	D
40472	54 3	00001	ISK	3	1
	75 0	40043	SLJ	0	NEWINPUT+1
40473	54 4	00000	ISK	4	0
	75 0	40043	SLJ	0	NEWINPUT+1
40474	54 6	00005	ISK	6	5
	75 0	40043	SLJ	0	NEWINPUT+1
40475	54 5	00004	ISK	5	4
	75 0	40043	SLJ	0	NEWINPUT+1
40476	12 0	40564	LDA	0	STOPINDX
	20 0	40563	STA	0	STOPNOW
40477	75 0	40043	SLJ	0	NEWINPUT+1
	50 0	00000	ENI	0	0
40500	12 0	40512	LDA	0	NOFLOAT
	20 0	40071	STA	0	FLOATEST
40501	12 0	40404	LDA	0	A
	20 0	40514	STA	0	PRINDELT
40502	12 0	40414	LDA	0	TOTINERT
	20 0	40515	STA	0	PRINDELT+1
40503	12 0	40420	LDA	0	KMOTCONS
	20 0	40516	STA	0	PRINDELT+2
40504	12 0	40424	LDA	0	OMEGANSQ
	20 0	40517	STA	0	PRINDELT+3
40505	12 0	40411	LDA	0	RHO
	20 0	40520	STA	0	PRINDELT+4
40506	12 0	40417	LDA	0	RHOSQ
	20 0	40521	STA	0	PRINDELT+5
40507	72 0	40510	RAO	0	/+1
	75 4	71000	SLJ	4	DECOF
40510	01 0	40514	01	0	PRINDELT
	06 0	00000	06	0	0
40511	72 0	40046	RAO	0	NEWINPUT+4
	75 0	40053	SLJ	0	COMBINED
40512	75 0	40053	SLJ	0	COMBINED
	50 0	00000	ENI	0	0
40513	13 0	40162	LAC	0	THETA
	30 0	40664	FAD	0	ONE
40514	00 0	00000	BSS	6	
	00 0	00000			
40522	75 3	40523	SLJ	3	/+1
	75 0	40525	SLJ	0	/+3
40523	50 0	00000	ENI	0	0
	12 0	00000	LDA	0	0
40524	65 0	40603	THS	0	TIME90SC
	75 0	40566	SLJ	0	TIMESTOP
40525	12 0	40350	LDA	0	PRINTBUF+2
	31 0	40664	FSB	0	ONE
40526	22 3	40534	AJP	3	PRINTNOW
	50 2	77775	ENI	2	77775

LINEAR

NOFLOAT

NOSINK

PRINDELT

LIMITCYC



40527	12 0	40607	LDA	0	LIMITBUF+2
	31 0	40350	FSB	0	PRINTBUF+2
40530	22 2	40360	AJP	2	EXIT
	12 0	40346	LDA	0	PRINTBUF
40531	20 0	40605	STA	0	LIMITBUF
	12 0	40347	LDA	0	PRINTBUF+1
40532	20 0	40606	STA	0	LIMITBUF+1
	12 0	40350	LDA	0	PRINTBUF+2
40533	20 0	40607	STA	0	LIMITBUF+2
	75 0	40360	SLJ	0	EXIT
40534	54 2	77775	ISK	2	77775
	75 0	40360	SLJ	0	EXIT
40535	12 0	40615	LDA	0	INDEXAVE
	15 0	40617	SUB	0	COUNTZET
40536	22 0	40541	AJP	0	/+3
	14 0	40617	ADD	0	COUNTZET
40537	20 0	40615	STA	0	INDEXAVE
	72 0	40615	RAO	0	INDEXAVE
40540	75 0	40543	SLJ	0	LIMPRINT
	50 0	00000	ENI	0	0
40541	12 0	40607	LDA	0	LIMITBUF+2
	30 0	40613	FAD	0	LIMITBUF+6
40542	20 0	40613	STA	0	LIMITBUF+6
	50 0	00000	ENI	0	0
40543	74 0	02000	EXF	0	02000
	75 4	71000	SLJ	4	DECOF
40544	01 0	40605	01	0	LIMITBUF
	06 0	00001	06	0	1
40545	72 0	40544	RAO	0	/-1
	72 0	40614	RAO	0	LIMINDEX
40546	12 0	40614	LDA	0	LIMINDEX
	15 0	40616	SUB	0	STOPZETA
40547	22 0	40555	AJP	0	STOPAVE
	14 0	40616	ADD	0	STOPZETA
40550	20 0	40614	STA	0	LIMINDEX
	12 0	40604	LDA	0	TOOSMALL
40551	31 0	40607	FSB	0	LIMITBUF+2
	22 2	40573	AJP	2	SMALTIME
40552	10 0	00000	ENA	0	0
	20 0	40607	STA	0	LIMITBUF+2
40553	20 0	00000	STA	0	0
	74 0	01000	EXF	0	01000
40554	75 0	40360	SLJ	0	EXIT
	50 0	00000	ENI	0	0
40555	10 0	00000	ENA	0	0
	20 0	40605	STA	0	LIMITBUF
40556	20 0	40606	STA	0	LIMITBUF+1
	20 0	40607	STA	0	LIMITBUF+2
40557	12 0	40613	LDA	0	LIMITBUF+6
	33 0	40620	FDV	0	DIVIDE
40560	31 0	40664	FSB	0	ONE
	20 0	40610	STA	0	LIMITBUF+3
40561	75 4	71000	SLJ	4	DECOF
	50 0	00000	ENI	0	0
40562	01 0	40605	01	0	LIMITBUF
	06 0	00000	06	0	0
40563	76 1	40022	SLS	1	GOAROUND
	50 0	00000	ENI	0	0
40564	76 0	40000	SLS	0	START
	50 0	00000	ENI	0	0
40565	76 1	40022	SLS	1	GOAROUND
	50 0	00000	ENI	0	0
40566	50 2	00000	ENI	2	0
	75 4	71000	SLJ	4	DECOF
40567	01 0	40605	01	0	LIMITBUF
	04 0	01570	04	0	1570
40570	74 0	02000	EXF	0	02000
	75 4	71000	SLJ	4	DECOF
40571	01 0	40346	01	0	PRINTBUF
	04 0	01747	04	0	1747
40572	75 0	40563	SLJ	0	STOPNOW
	50 0	00000	ENI	0	0
40573	75 3	40574	SLJ	3	/+1
	75 0	40552	SLJ	0	LIMPRINT+7

PRINTNOW

LIMPRINT

STOPAVE

STOPPRINT

STOPNOW

STOPINDX

NEWSTOP

TIMESTOP

SMALTIME





40574	50 0 00000	ENI	0 0
	12 0 00000	LDA	0 0
40575	65 0 40602	THS	0 TIME30SC
	75 0 40577	SLJ	0 /+2
40576	75 0 40552	SLJ	0 LIMPRINT+7
	50 0 00000	ENI	0 0
40577	75 4 71000	SLJ	4 DECOF
	50 0 00000	ENI	0 0
40600	01 0 40346	01	0 PRINTBUF
	04 0 01755	04	0 1755
40601	75 0 40563	SLJ	0 STOPNOW
	50 0 00000	ENI	0 0
40602	00 0 00000	TIME30SC	OCT 3410
	00 0 03410		
40603	00 0 00000	TIME90SC	OCT 12430
	00 0 12430		
40604	20 0 14012	TOOSMALL	DEC 1.005
	17 2 70243		
40605	00 0 00000	LIMITBUF	BSS 7
	00 0 00000		
40614	00 0 00000	LIMINDEX	BSS 1
	00 0 00000		
40615	00 0 00000	INDEXAVE	BSS 1
	00 0 00000		
40616	00 0 00000	STOPZETA	BSS 1
	00 0 00000		
40617	00 0 00000	COUNTZET	BSS 1
	00 0 00000		
40620	00 0 00000	DIVIDE	BSS 1
	00 0 00000		
40621	00 0 40346	PRINTSET	00 0 PRINTBUF
	06 0 00001	06	0 1
40622	01 0 40605	NEWLIMPT	01 0 LIMITBUF
	06 0 00001	06	0 1
40623	17 7 36314	ZETAINDX	DEC 0.05
	63 1 46314		
40624	17 7 46314		DEC 0.1
	63 1 46314		
40625	17 7 56314		DEC 0.2
	63 1 46314		
40626	17 7 64631		DEC 0.3
	46 3 14631		
40627	17 7 66314		DEC 0.4
	63 1 46314		
40630	20 0 04000		DEC 0.5
	00 0 00000		
40631	20 0 04631		DEC 0.6
	46 3 14631		
40632	20 0 05463		DEC 0.7
	14 6 31463		
40633	20 0 06314		DEC 0.8
	63 1 46314		
40634	20 0 07146		DEC 0.9
	31 4 63146		
40635	20 0 14000		DEC 1.0
	00 0 00000		
40636	20 0 06314	POINT8	DEC .8
	63 1 46314		
40637	20 0 04631	POINT6	DEC .6
	46 3 14631		
40640	20 0 04000	POINT5	DEC .5
	00 0 00000		
40641	17 7 66314	POINT4	DEC .4
	63 1 46314		
40642	17 7 64631	POINT3	DEC .3
	46 3 14631		
40643	17 7 56314	POINT2	DEC 0.2
	63 1 46314		
40644	17 7 46314	POINT1	DEC 0.1
	63 1 46314		
40645	00 0 00000	STOP6	OCT 6
	00 0 00006		
40646	00 0 00000	STOP7	OCT 7
	00 0 00007		



40647	00 0 00000	STOP8	OCT	10
40650	00 0 00010	STOP10	OCT	12
	00 0 00012			
40651	00 0 00000	STOP14	OCT	16
	00 0 00016			
40652	00 0 00000	STOP20	OCT	24
	00 0 00024			
40653	00 0 00000	STOP17	OCT	21
	00 0 00021			
40654	00 0 00000	STOP25	OCT	31
	00 0 00031			
40655	00 0 00000	COUNT4	OCT	4
	00 0 00004			
40656	00 0 00000	COUNT5	OCT	5
	00 0 00005			
40657	00 0 00000		OCT	5
	00 0 00005			
40660	00 0 00000	COUNT7	OCT	7
	00 0 00007			
40661	00 0 00000	COUNT10	OCT	12
	00 0 00012			
40662	00 0 00000	COUNT12	OCT	14
	00 0 00014			
40663	00 0 00000		OCT	14
	00 0 00014			
40664	20 0 14000	ONE	DEC	1.0
	00 0 00000			
40665	20 0 24000	TWO	DEC	2.0
	00 0 00000			
40666	20 0 24000		DEC	2.0
	00 0 00000			
40667	20 0 26000	THREE	DEC	3.0
	00 0 00000			
40670	20 0 26000		DEC	3.0
	00 0 00000			
40671	20 0 34000	FOUR	DEC	4.0
	00 0 00000			
40672	20 0 44000	EIGHT	DEC	8.0
	00 0 00000			
40673	20 0 35000	FIVE	DEC	5.0
	00 0 00000			
40674	50 1 00000	MANUAL	ENI	1 0
	75 4 71000		SLJ	4 DECOF
40675	01 0 40605		01	0 LIMITBUF
	04 0 01570		04	0 1570
40676	50 2 00000		ENI	2 0
	75 4 71000		SLJ	4 DECOF
40677	01 0 40346		01	0 PRINTBUF
	04 0 03651		04	0 3651
40700	75 0 40563		SLJ	0 STOPNOW
	50 0 00000		ENI	0 0
40701	50 1 00000	FAULPRIN	ENI	1 0
	75 4 71000		SLJ	4 DECOF
40702	01 0 40605		01	0 LIMITBUF
	04 0 01570		04	0 1570
40703	50 2 00000		ENI	2 0
	75 4 71000		SLJ	4 DECOF
40704	01 0 40346		01	0 PRINTBUF
	04 0 01232		04	0 1232
40705	74 0 42003		EXF	0 42003
	76 0 40000		SLS	0 START
40706	20 0 14000	RESTVALU	DEC	1.0
	00 0 00000			
40707	00 0 00000		DEC	0
	00 0 00000			
40710	20 0 04631		DEC	0.6
	46 3 14631			
40711	20 0 06314		DEC	0.8
	63 1 46314			
40712	00 0 00000		BSS	14
	00 0 00000			
40726	17 7 64631	DELTAVAL	DEC	.3
	46 3 14631			





40727	17 7 46314	DEC	.1
	63 1 46314		
40730	17 7 27534	DEC	.03
	12 1 72702		
40731	17 7 15075	DEC	0.01
	34 1 21727		
40732	17 7 05075	DEC	0.005
	34 1 21727		
40733	00 0 00000	BSS	14
	00 0 00000		
40747	17 7 46314	JMOTVALU DEC	.1
	63 1 46314		
40750	17 7 56314	DEC	.2
	63 1 46314		
40751	20 0 04000	DEC	.5
	00 0 00000		
40752	20 0 06314	DEC	.8
	63 1 46314		
40753	20 0 07146	DEC	.9
	31 4 63146		
40754	00 0 00000	BSS	20
	00 0 00000		
40774	00 0 00000	FLFTRATO DEC	0
	00 0 00000		
40775	17 7 56314	DEC	.2
	63 1 46314		
40776	17 7 66314	DEC	.4
	63 1 46314		
40777	20 0 04631	DEC	.6
	46 3 14631		
41000	20 0 06314	DEC	.8
	63 1 46314		
41001	20 0 14000	DEC	1.0
	00 0 00000		
41002	17 7 35075	DEC	0.04
	34 1 21727		
41003	17 7 46314	DEC	0.1
	63 1 46314		
41004	20 0 07146	DEC	0.9
	31 4 63146		
41005	00 0 00000	BSS	20
	00 0 00000		
		END	













2	2507999999	J <sub>m</sub> /J <sub>L</sub> 1111111	f <sub>L</sub> /F <sub>T</sub> 59999999	e 99999999	Δ 29999999	p 99999999
	J <sub>m</sub> 89999999	J <sub>m</sub> 89999999	J <sub>m</sub> 89999999	f <sub>m</sub> 32000000	f <sub>L</sub> 47999999	p <sup>2</sup> 99999999
	K 99999999	K/J <sub>m</sub> 99999999	1 f <sub>m</sub> /J <sub>m</sub> 32000000	1 f <sub>L</sub> /J <sub>L</sub> 53333333	ω <sub>m</sub> <sup>2</sup> 99999999	f 39999999
number 1	t 35400000	1 θ <sub>c</sub> 17098208	1 θ <sub>c</sub> 13104190	1		
of	11580000	2 17034145	1 10721242	1		
maximum 2	23279999	2 18292628	2 10323347	1		
3	38859999	2 35712402	3 10200613	1		
4	58729999	2 72447348	4 10138780	1		
5	83939998	2 11243587	4 10098946	1		
6	11619999	3 10685365	5 10071240	1		
7	15810000	3 47854719	7 10051391	1		
8	21077001	3 29068282	8 10037079	1		
9	215160011794	3 -167815371770	- 2	999996862854		
1005						

1005 indicates θ<sub>c</sub> max. less than 1.005 and 30 sec. of real time has elapsed since the last maximum was recorded (low velocity).

The time, velocity, and position of the last computed point is printed.

## APPENDIX D 2

TYPICAL PRINT OUT ILLUSTRATING NO LIMIT CYCLE  
(Numbers indicated in tenths followed by power of 10)









OC 2461  
17 FEB 69

DISPLAY  
17085

50890

TA7  
.U64  
no.19

Thaler  
Backlash in second  
order feedback control  
systems.

OC 2461  
17 FEB 69

DISPLAY  
17085

TA7  
.U64  
no.19

Thaler

Backlash in second  
order feedback control  
systems.

50890

genTA 7.U64 no.19

Backlash in second order feedback contro



3 2768 001 61444 9

DUDLEY KNOX LIBRARY